The Journal of Antibiotics (2009) 62, 233–237
© 2009 Japan Antibiotics Research Association All rights reserved 0021-8820/09 $32.00
www.nature.com/ja

ORIGINAL ARTICLE

Isolation, structure elucidation and antibacterial activities of streptothricin acids

Zhiqin Ji[1], Mingan Wang[2], Shaopeng Wei[1], Jiwen Zhang[1] and Wenjun Wu[1]

Five streptothricin acids (compounds 1–5) were isolated by ion-exchange resin chromatography and preparative RP-HPLC from the fermentation broth of *Streptomyces qinlingensis*. Their structures were elucidated mainly by analyses of the IR, HR-EIS-MS and NMR spectral data. They were deduced as two known compounds, streptothricin F acid (1) and streptothricin D acid (2), and three new compounds, 12-carbamoylstreptothricin E acid (3), 12-carbamoylstreptothricin D acid (4) and N-acetyl-streptothricin D acid (5), respectively. The antibacterial activities of 1–5 against *Escherichia coli*, *Bacillus subtilis*, *Staphylococcus aureus*, *Bacillus cereus* and *Pseudomonas aeruginosa* were assayed by micro-broth dilution. Comparison of the MICs with streptothricin F and D showed that the antimicrobial activities of 1–5 were decreased significantly but varied with the structures.
The Journal of Antibiotics (2009) **62,** 233–237; doi:10.1038/ja.2009.16; published online 20 March 2009

Keywords: antibacterial activity; streptothricin acid; structural elucidation

Streptothricin antibiotic is a type of broad-spectrum antibiotics. As streptothricin F was isolated from *Streptomyces lavendulae* in 1942,[1] dozens of streptothricins (STs) have been isolated from natural resources. Although they were shown to possess strong antimicrobial activity against many species of fungi and bacteria, their application in the therapeutic area has been hampered because of the nephrotoxicity.[2–5] Hamano *et al.*[6] isolated a novel ST-resistance gene (sttH) and showed that the hydrolysis of the amide bond of streptolidine lactam could be catalyzed by the enzyme *in vitro*. With the breaking of the amide bond, the antimicrobial activity of streptothricin D (ST-D) was altered from broad-spectrum to bacteria-specific, and its toxicity against eukaryotic cells was also reduced at the same time. These results suggest that ST-D acid is a potential candidate for clinical development or use as a new lead compound for drug discovery. Attempts at preparing ST acids were made from STs chemically, but only ST-F acid, which bears one β-lysine, was readily obtained, whereas others that bear more β-lysine residues were not prepared successfully.[7,8] In addition, only the bio-activities of ST-F and ST-D acids have been investigated.[6]

In the process of screening for new antibiotics, *S. qinlingensis*, a ST producer, was isolated from soil samples. ST-F, ST-D and two other novel compounds, 12-carbamoyl-ST-F and 12-carbamoyl-ST-D, have been isolated from its fermentation broth in our laboratory.[9] In subsequent research, a facile LC-MS/MS method based on RP-HPLC coupled with electrospray ionization tandem mass spectrometry was used for the analysis of STs in the fermentation broth of *S. qinlingensis*.[10] A total of 19 ST-like compounds were identified or tentatively characterized on the basis of their mass spectral data; among them, 12 were ST acids. Here, we report the isolation, structure elucidation and antibacterial activities of five ST acids that were isolated by ion-exchange resin chromatography and preparative RP-HPLC from the fermentation broth of *S. qinlingensis*. These compounds were identified as two known compounds, ST-F acid (**1**) and ST-D acid (**2**), and three new compounds, 12-carbamoylstreptothricin E acid (**3**), 12-carbamoylstreptothricin D acid (**4**) and N-acetylstreptothricin D acid (**5**). The antibacterial activities of **1–5** against *Escherichia coli*, *Bacillus subtilis*, *Staphylococcus aureus*, *Bacillus cereus* and *Pseudomonas aeruginosa* were assayed by means of micro-broth dilution. The results indicated that **1–5** exhibited less antibacterial activities when compared with that of ST-D, but the extent of decrease varied with the structures.

RESULTS AND DISCUSSION

Physicochemical properties of 3–5

Compound **3**: colorless amorphous powder, m.p. 132–134 °C (dec), $[\alpha]_D^{25}$ −14.0 (c 0.1, MeOH). IR ν_{max} cm^{-1}: 3382, 1651, 1555, 1492, 1388, 1070 cm^{-1}. ^1H and ^{13}C NMR: see Tables 1 and 2. High-resolution electrospray ionization mass spectometry (HR-ESI-MS) (*m/z*): 649.3630 $[M+H]^+$, calcd for $C_{25}H_{49}N_{10}O_{10}$, 649.3628.

Compound **4**: colorless amorphous powder, m.p. 150–152 °C (dec), $[\alpha]_D^{25}$ +8 (c 0.1, MeOH). IR ν_{max} cm^{-1}: 3396, 1655, 1558, 1492, 1390, 1067 cm^{-1}; ^1H and ^{13}C NMR: see Tables 1 and 2. HR-ESI-MS (*m/z*): 777.4576 $[M+H]^+$, calcd for $C_{31}H_{62}N_{12}O_{11}$, 777.4577.

Compound **5**: colorless amorphous powder, m.p. 172–174 °C (dec), $[\alpha]_D^{25}$ +4.2 (c 0.1, MeOH). IR ν_{max} cm^{-1}: 3418, 1652, 1554, 1445, 1388, 1071 cm^{-1}; ^1H and ^{13}C NMR: see Tables 1 and 2. HR-ESI-MS (*m/z*): 819.4683 $[M+H]^+$, calcd for $C_{33}H_{62}N_{12}O_{12}$, 819.4683.

[1]Institute of Pesticide Science, Northwest Agricultural and Forestry University, Shaanxi, China and [2]Department of Applied Chemistry, China Agricultural University, Beijing, China
Correspondence: Professor W Wu, Institute of Pesticide Science, Northwest Agricultural & Forestry University, Yangling, Shaanxi 712100, China.
E-mail: wenjun_wu@263.net
Received 7 January 2009; revised 11 February 2009; accepted 17 February 2009; published online 20 March 2009

Table 1 ^{1}H NMR data of compounds 1–5 (500 MHz, in D_2O)

Position	***1***	***2***	***3***	***4***	***5***
2	4.58 (d, *J*=5)	4.69 (d, *J*=5)	4.63 (d, *J*=5)	4.61 (d, *J*=5)	4.71 (d, *J*=5)
3	4.27 (m)	4.34 (m)	4.30 (m)	4.30 (m)	4.36 (m)
4	4.14 (m)	4.14 (m)	4.15 (m)	4.14 (m)	4.15 (m)
5	3.28 (dd, *J*=5, 14)	3.25 (dd, *J*=5, 14)	3.28 (m)	3.29 (dd, *J*=3, 14)	3.29 (m)
5	3.12 (dd, *J*=10, 14)	3.13 (dd, *J*=11, 14)	3.13 (m)	3.13 (dd, *J*=11, 14)	3.13 (m)
7	5.14 (d, *J*=10)	5.14 (d, *J*=10)	5.09 (d, *J*=10)	5.14 (d, *J*=10)	5.12 (d, *J*=10)
8	4.25 (dd, *J*=3, 10)	4.26 (dd, *J*=3, 10)	4.31 (dd, *J*=3, 10)	4.26 (dd, *J*=3, 10)	4.26 (dd, *J*=3, 10)
9	4.18 (t, *J*=3)	4.15 (t, *J*=3)	4.10 (t, *J*=3)	4.18 (t, *J*=3)	4.08 (t, *J*=3)
10	4.79	4.79	3.88 (d, *J*=4)	3.88 (d, *J*=4)	4.79
11	4.33 (t, *J*=6)	4.33 (t, *J*=6)	4.33 (t, *J*=6)	4.33 (t, *J*=6)	4.32 (t, *J*=6)
12	3.74 (d, *J*=6)	3.74 (d, *J*=6)	4.23 (d, *J*=5)	4.23 (d, *J*=5)	3.72 (d, *J*=6)
12	3.74 (d, *J*=6)	3.74 (d, *J*=6)	4.26 (d, *J*=7)	4.26 (d, *J*=7)	3.72 (d, *J*=6)
15	2.81 (dd, *J*=5, 17)	2.79 (dd, *J*=5, 17)	2.78 (dd, *J*=5, 17)	2.80 (dd, *J*=5, 17)	2.54 (dd, *J*=5, 17)
15	2.71 (dd, *J*=8, 17)	2.65 (dd, *J*=8, 17)	2.65 (dd, *J*=8, 17)	2.71 (dd, *J*=8, 17)	2.43 (dd, *J*=8, 17)
16	3.71 (m)	3.66 (m)	3.68 (m)	3.68 (m)	4.14 (m)
17	1.79 (m)	1.81 (m)	1.74 (m)	1.72 (m)	1.54 (m)
18	1.79 (m)	1.70 (m)	1.68 (m)	1.70 (m)	1.54 (m)
19	3.05 (m)	3.12 (m)	3.24 (m)	3.07 (m)	3.19 (m)
21		2.72 (dd, *J*=5, 17)	2.75 (dd, *J*=5, 17)	2.75 (dd, *J*=5, 17)	2.75 (dd, *J*=5, 17)
21		2.63 (dd, *J*=8, 17)	2.62 (dd, *J*=8, 17)	2.62 (dd, *J*=8, 17)	2.65 (dd, *J*=8, 17)
22		3.66 (m)	3.68 (m)	3.66 (m)	3.64 (m)
23		1.71 (m)	1.82 (m)	1.75 (m)	1.70 (m)
24		1.68 (m)	1.63 (m)	1.66 (m)	1.65 (m)
25		3.24 (m)	3.07 (m)	3.23 (m)	3.24 (m)
27		2.70 (dd, *J*=5, 17)		2.72 (dd, *J*=5, 17)	2.72 (dd, *J*=5, 17)
27		2.60 (dd, *J*=8, 17)		2.62 (dd, *J*=8, 17)	2.62 (dd, *J*=8, 17)
28		3.67 (m)		3.69 (m)	3.67 (m)
29		1.78 (m)		1.81 (m)	1.82 (m)
30		1.64 (m)		1.62 (m)	1.82 (m)
31		3.26 (m)		3.24 (m)	3.07 (m)
N-acetyl					1.99 (s)

Structure elucidation

Two known compounds (**1**, **2**) and three novel compounds (**3**–**5**) were obtained from the fermentation broth of *S. qinlingensis* finally. Compounds **1** and **2** were identified as ST-F acid and ST-D acid on the basis of the M.P., IR, MS and NMR data.[7,8]

Compound **3** was obtained as a colorless amorphous powder. The molecular formula $C_{25}H_{48}N_{10}O_{10}$ was determined by HR-ESI-MS at *m/z* 649.3630 $[M+H]^+$ (calcd for $C_{25}H_{49}N_{10}O_{10}$, 649.3628). The IR spectra showed the characteristic absorption bands at 1654 and 1556 cm^{-1}, which revealed the existence of a peptide bond. The NMR spectral data (Tables 1 and 2) suggested the presence of two amido groups, one carboxylic acid group, one carbamoyl group and one guanidino group. The spectral characteristics were very similar to those of STs. By comparing the ^{1}H and ^{13}C NMR data of **3** with those of ST-D acid (**2**), we found that the chemical shift of C-4, C-5 in the ^{13}C NMR spectra and the chemical shift of H-4 and H-5 in the ^{1}H NMR spectra were not different. Compound **3** was assumed to be the ST acid type compound. The hypothesis is also proved by the results of ESI-MS/MS; *m/z* 171, which was assigned to streptolidine, was a characteristic ion peak of STs, whereas the corresponding ion was observed at *m/z* 189 in the spectrum of **3**. This indicated that streptolidine lactam was converted into acid for compound **3**. The differences between the ^{1}H and ^{13}C NMR data of **3** and **2** were also observed; we found a chemical shift of C-9 downfield 2.6 p.p.m., C-10 upfield 2.2 p.p.m., C-11 upfield 1.1 p.p.m. and C-12 downfield 3.6 p.p.m. in the ^{13}C NMR spectrum, as well as a chemical shift of H-10 upfield 0.9 p.p.m. and H-12 downfield 0.5 p.p.m. in the ^{1}H NMR spectrum. These differences may be attributed to the variety of the substitution position of the carbamoyl group attached to D-gulosamine in which the substitution position of carbamoyl was transferred from C-10 to C-12. This presumption was confirmed by the heteronuclear multiple-bond correlation (HMBC) experiment. In the HMBC spectra of **2**, the protons of H-9, H-10 and H-11 were correlated with the carbonyl of the carbamoyl group. However, the carbonyl of the carbamoyl group was correlated with the protons of H-10, H-11 and H-12 in the HMBC spectra of **3**. Thus, the carbamoyl group of **3** was substituted at C-12, and the compound was identified as 12-carbamoylstreptothricin E acid. To our best knowledge, only four 12-carbamoylstreptothricins, 12-carbamoylstreptothricin F, D, C and B, have been reported; so compound **3** is a novel 12-carbamoylstreptothricin antibiotic (Figure 1).[9,11]

Compound **4** was obtained as a colorless amorphous powder. The molecular formula $C_{31}H_{60}N_{12}O_{11}$ was determined by HR-ESI-MS at *m/z* 777.4576 $[M+H]^+$ (calcd for $C_{31}H_{61}N_{12}O_{11}$, 777.4577). The IR spectra showed the characteristic absorption bands at 1654 and 1556 cm^{-1}, which revealed the existence of a peptide bond. The NMR spectral data (Tables 1 and 2) suggested the presence of three amido groups, one carboxylic acid group, one carbamoyl group and one guanidino group. By comparing the ^{1}H and ^{13}C NMR data of **4** with those of **2** and **3**, we found that the chemical shift of C-4, C-5,

Table 2 ^{13}C NMR data of compounds 1–5 (125 MHz, in D_2O)

Position	*1*	*2*	*3*	*4*	*5*
1	173.53	173.45	172.05	174.26	173.10
2	56.74	56.73	57.05	57.18	56.83
3	61.33	61.31	61.54	61.55	61.27
4	67.97	67.96	67.96	67.98	67.96
5	40.59	40.61	40.61	40.61	41.32
6	158.46	157.84	158.26	158.35	158.46
7	79.04	79.09	79.14	79.14	79.13
8	48.95	48.92	48.68	48.92	48.93
9	66.42	66.46	69.03	67.98	66.74
10	69.98	69.99	67.76	67.76	69.97
11	73.37	73.38	72.27	72.28	73.32
12	60.19	60.21	63.79	63.79	60.26
13	157.85	158.45	158.99	158.99	157.82
14	171.97	172.11	171.82	172.08	173.82
15	36.26	36.80	36.61	36.58	41.32
16	48.25	48.67	48.46	48.43	47.17
17	28.97	29.46	29.41	29.37	31.37
18	22.85	24.28	24.27	24.25	24.85
19	38.89	38.76	38.77	38.79	38.96
20		171.82	171.62	171.62	171.62
21		36.59	36.82	36.58	36.58
22		48.66	48.49	48.43	48.46
23		29.38	29.07	29.06	29.42
24		22.88	22.89	24.25	24.30
25		38.76	38.91	38.79	36.77
26		171.61		171.62	171.62
27		36.56		36.58	36.85
28		48.45		48.43	48.70
29		29.06		29.06	29.07
30		22.89		22.90	22.90
31		38.89		38.88	39.00
N-acetyl					173.10, 22.10

C-10, C-12 in the ^{13}C NMR spectra, and the chemical shift of H-4, H-5, H-10, H-12 in the ^{1}H NMR spectra were similar; so **4** also belongs to 12-carbamoylstreptothricin acid. The molecular weight of **4** is 128 Da higher than that of **3**, which corresponds to a molecule of β-lysine. On the basis of the ^{1}H and ^{13}C NMR data and HMBC spectra, **4** was identified as 12-carbamoylstreptothricin D acid.

Compound **5** was obtained as a colorless amorphous powder. The molecular formula $C_{33}H_{62}N_{12}O_{12}$ was determined by HR-ESI-MS at *m/z* 819.4683 $[M+H]^+$ (calcd for $C_{33}H_{63}N_{12}O_{12}$, 819.4683). The IR spectra showed the characteristic absorption bands at 1651 and 1554 cm^{-1}, which revealed the existence of a peptide bond. The NMR spectral data (Tables 1 and 2) suggested the presence of four amido groups, one carboxylic acid group, one carbamoyl group and one guanidino group. By comparing the ^{1}H and ^{13}C NMR data of **5** with those of **2–4**, we found that the chemical shift of C-4, C-5 in the ^{13}C NMR spectrum, and H-4, H-5 in the ^{1}H NMR spectrum were similar to **3**; the chemical shift of C-10, C-12 in the ^{13}C NMR spectrum, and H-10, H-12 in the ^{1}H NMR spectrum were similar to **2**; so **5** belongs to ST acid. The ^{1}H NMR spectrum of **5** showed a singlet (3H) at δ 1.99 in addition to all the signals observed in that of **2**, and the signal of the methyl group was observed at δ 22.10 in the ^{13}C NMR spectrum of **5**. In the HMBC spectrum of **5**, we could find that the methyl group is attached to a carbon (δ 173.10) of carbonyl group, which was absent in the ^{13}C NMR spectrum of **2**. The protons of H-15 and H-16 were correlated with the carbonyl group at δ 173.10, indicating that the acetyl group was attached to the amino group of C-16. Thus, **5** was identified as N-acetylstreptothricin D acid.

Streptothricin F acid is the most investigated compound of ST acids, and was first prepared from ST-F by partial hydrolysis, whereas the other ST acids bearing more β-lysine residues were not readily obtained chemically.[7,8] The results may be attributed to that, although STs possess easily hydrolyzable bonds, such as ester and amido bonds, but the hydrolysis is strongly influenced by the number of β-lysine. In 2006, Hamano *et al.*[6] isolated a novel ST-resistance gene (sttH) from *S. albulus*, which could catalyze the transformation of ST-D and ST-F from lactam to acid *in vitro*. The results of HPLC-MS/MS analysis also indicated the distribution of ST acids in the metabolites of *S. qinlingensis*. We therefore hypothesized that a similar resistance gene may exist in this actinomycete, the research of which is under way in our laboratory.

Antibacterial assay

Antimicrobial activities of compounds **1–5** against *B. subtilis*, *S. aureus*, *E. coli*, *B. cereus* and *P. aeruginosa* were determined by the micro-broth dilution method, and the results are showed in Table 3. In a comparison of the MICs of STs F and D with those of **1–5**, the antimicrobial activities of **1–5** were decreased significantly, but the extents varied with the structures. The structural activity relationship of STs has been described in previous research, but that of ST acids was not investigated thoroughly.[12–15] To our best knowledge, only the antibacterial activities of ST acids F and D were reported up to now. ST-D acid exhibited higher activity against *B. subtilis* and *S. aureus* than did ST-F acid, and this indicates that the number of β-lysine plays an important role in the antibacterial activity for this type of ST acid antibiotics. The activity of **4** was slightly lower than that of **2**, and the only difference between them is the substituted position of the carbamoyl group in the D-gulosamine moiety, which implies that their activities were also influenced by the substituted position of the carbamoyl group. It is noticeable that acetylation of β-lysine almost resulted in the loss of activity, and this phenomenon was identical with that of classical ST antibiotics.[12,13]

METHODS

Microorganism and fermentation

The producing strain *S. qinlingensis* was isolated from a soil sample collected in Qinling Mountain, Shannxi Province, China, and identified by its morphology, physiology, biochemistry and 16S rRNA gene sequence. The voucher specimen of this streptomycete was deposited at the China General Microbiological Culture Collection Center as CGMCC1381, and the 16S rDNA sequence was registered in GenBank with the accession no: AM167521 in the National Center for Biological Information.

The spores of *S. qinlingensis* grown on Gause's No. 1 agar were used to inoculate into a 250 ml flask containing 50 ml of a sterile seed medium consisting of glucose 0.8%, soluble starch 0.8%, beef extract 0.6%, peptone 1.0%, and NaCl 0.5%, pH 7.2. The flask was shaken on a shaker at 210 r.p.m. for 24 h at 28 °C. Ten milliliters of the seed culture were transferred to 250 ml flasks containing 50 ml of a sterile producing medium consisting of glucose 3.0%, millet steep liquor 1.0%, peptone 1.5%, NaCl 0.5%, and $CaCO_3$ 0.5%, pH 7.2. Fermentation was carried out at 210 r.p.m. for 96 h at 28 °C on a rotary shaker.

Isolation and purification

Ten liters of harvest fermentation broth were adjusted to pH 3.5 with oxalic acid and stirred for 30 min. The acidic broth was filtered, adjusted to pH 8.0, and passed through a column of HD-2 (Na^+, 2 l; Shanghai Huazhen Sci. & Tch. Co., Shanghai, China). Active principle adsorbed on the column was eluted

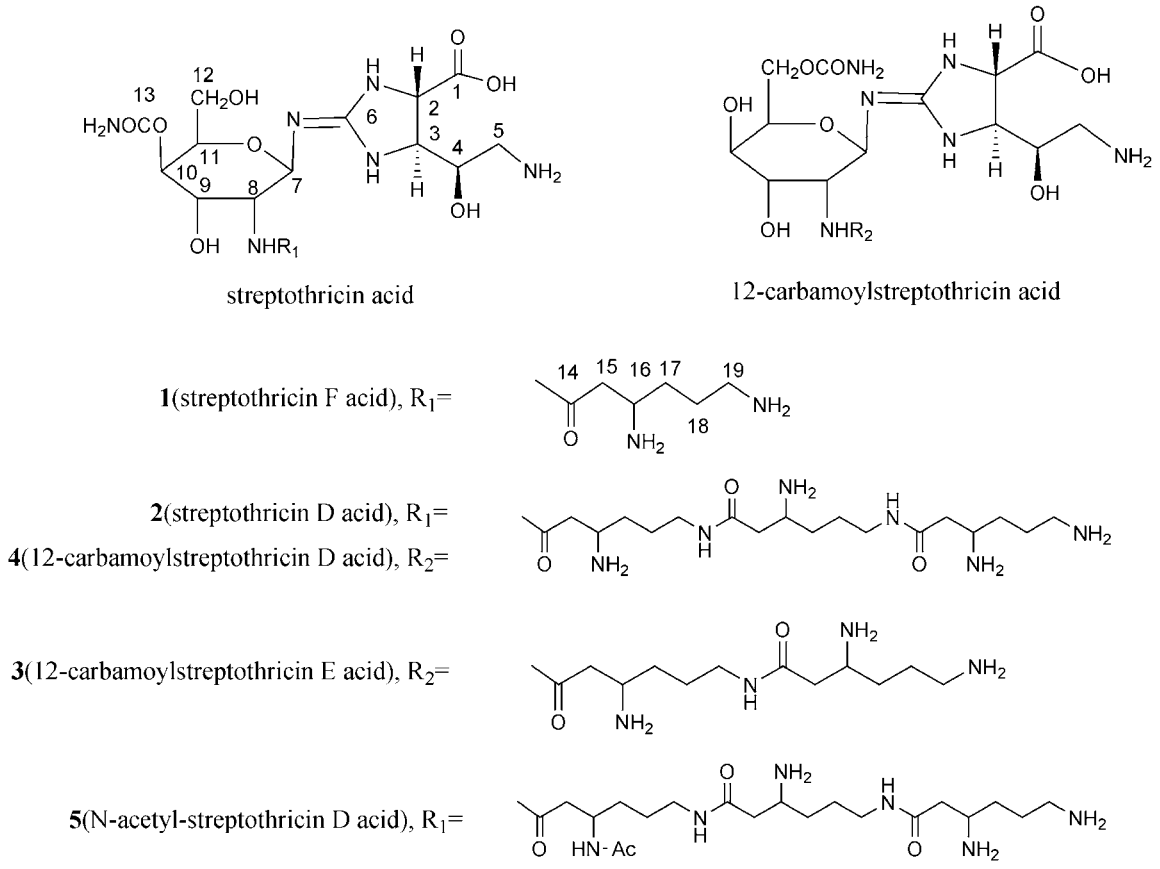

Figure 1 Structures of compounds **1–5**.

Table 3 Antibacterial *in vitro* activities of 1–5 by micro-broth dilution

	MIC (μg·ml^{-1})				
Compounds	*B. subtilis (1.0088)*	*S. aureus (1.0089)*	*E. coli (1.1636)*	*B. cereus (1.1846)*	*P. aeruginosa (1.2031)*
Streptothricin F	6.3	12.5	3.1	25.0	50.0
Streptothricin D	3.1	6.3	3.1	25.0	50.0
1	25.0	50.0	50.0	>100.0	>100.0
2	12.5	25.0	12.5	25.0	50.0
3	25.0	>100.0	25.0	50.0	>100.0
4	25.0	50	12.5	50.0	>100.0
5	50.0	>100.0	50.0	>100.0	>100.0

with 0.5 M HCl (8 l). The eluent was adjusted to pH 7.0 with $NaHCO_3$ and concentrated *in vacuo* to a small volume (about 300 ml). The concentrated solution was diluted with MeOH (3:l) to precipitate sodium chloride. The MeOH was removed on a rotary evaporator, and the aqueous solution was applied on a column of CM-Sephadex C-25 (0.5 l, Na^+). The column was eluted with a linear gradient of water and 1.0 M NaCl solution (1 l each). The eluents were collected in 50 ml fractions and analyzed by HPLC-MS/MS. The analyses were performed on a Finnigan LCQ Advantage MAX LC/MS (Thermo Finnigan, San Jose, CA, USA) equipped with a Waters (Waters, Milford, MA, USA) Atlantis dC18 column (4.6×250 mm, 5 μm), and a water/TFA/acetonitrile gradient was used as mobile phase. The gradient started with 5% acetonitrile in 0.1% aqueous TFA for 10 min. The percent of acetonitrile was increased to 20% in the next 10 min. The flow rate of the mobile phase was 0.8 ml min^{-1} and the injection volume of sample was 10 μl. The eluate from the HPLC was introduced into a splitter to provide a 0.1 ml min^{-1} flow into the mass spectrometer. An electrospray ionization (ESI) interface with positive-ion mode was used. The ESI conditions were as follows: source voltage 4.5 kV, capillary temperature 300 °C, sheath gas flow 75, auxiliary gas flow 10, capillary voltage 10 V. A data-dependent acquisition was used in the LC-MS/MS experiments. The collision energy for MS/MS was adjusted to 35% and the isolation width of precursor ions was 3.0 mass units. The results showed that ST acids were distributed in fractions 25–28 and 72–77, and these fractions were combined with fractions A and B, respectively. The two fractions were further desalted by chromatography on active carbon columns and concentrated under reduced pressure to a small volume (about 10 ml). The concentrated fractions were further separated on a Shimadzu (Tokyo, Japan) 6AD HPLC apparatus equipped with a column of Hypersil ODS-BP (20×250 mm, 10 μm, flow rate 3.5 ml min^{-1}), monitored by a Shodex (Kawasaki, Japan) RI-101 detector. Fraction A was eluted with 6.0% MeOH containing 2.0% TFA; fraction B was eluted with 8.0% MeOH containing 6.0% TFA. Five fractions were collected according to the peaks in the HPLC profiles, and each fraction was lyophilized, redissolved in water and passed through a column packed with 717 anion ion exchange resin (Cl^-, 50 ml; Shanghai Huazhen Sci. & Tch. Co.) to exchange TFA for chloride. The solutions were lyophilized to yield five compounds, with **1** (45 mg), **2** (83 mg) and **3** (51 mg) being from fraction A, and **4** (32 mg) and **5** (36 mg) being from fraction B, respectively.

Structure elucidation

The structures of these compounds were elucidated on the basis of extensive 1D and 2D NMR experiments and high-resolution mass spectrometry, and confirmed by comparison of their ESI-MS/MS data with those of LC-MS/MS. Melting points were measured on an X4 apparatus and uncorrected. IR spectra

were determined on an IR-450 instrument (KBr plate). ^{1}H, ^{13}C NMR, DEPT, COSY, heteronuclear single quantum coherence and HMBC spectra were taken on a Bruker Avance 500 MHz (500 MHz for ^{1}H and 125 MHz for ^{13}C, respectively) spectrometer (Bruker Biospin GmbH, Rheinstetten, Germany) in D_2O solution with TMS as an internal standard. The ESI-MS/MS and HR-ESI-MS spectra were obtained on a Finnigan LCQ LC-MS^n (Thermo Finnigan) and a Bruker APEX II mass spectrometer (Bruker Biospin GmbH) using glycerol as the matrix. Optical rotation was measured in methanol solution on a Perkin-Elmer 341 Polarimeter (Perkin Elmer, Fremont, CA, USA).

Antibacterial assay

Minimum inhibitory concentration of compounds **1–5** against *B. subtilis*, *S. aureus*, *E. coli*, *B. cereus* and *P. aeruginosa* were tested by the micro-broth dilution method.[16] The inoculum was prepared by suspending several colonies from an overnight culture of tested bacteria from 5% sheep blood agar medium in Mueller-Hinton broth, and adjusting to a 0.5 McFarland standard (approximately 1.5×10^8 cells ml^{-1}). A further dilution of 1:200 was made by placing 0.25 ml of the adjusted suspension into 49.75 ml of Mueller-Hinton broth. Stock solutions of tested compounds and streptomycin (positive control) in sterile water were prepared at a concentration of 1000 μg ml^{-1} and used immediately or stored in working samples at −20 °C until used. Doubling dilutions of the tested compounds were prepared in Mueller-Hinton broth. All antimicrobial solutions were prepared in large volumes (50 ml); 0.1 ml samples of the antibiotic solutions and 0.1 ml inoculated suspension of the test bacterium were delivered to wells of a 96-well plate. The final concentration of inoculum in each well was 3.7×10^5 cells ml^{-1}. Minimum inhibitory concentration end points were read after 18 h of incubation at 35 °C, and were defined as the lowest concentration of antibiotics that resulted in no bacterial growth as indicated by the ODs at 650 nm. The blank control tube contained only bacteria. Three replications were carried out for each sample.

ACKNOWLEDGEMENTS

This work was supported by the National Key Project for Basic Research of China (No. 2003CB114404) and the Hi-Tech Research and Development Project of China (No. 2002AA2455121). We thank Xi'an Modern Chemistry Research Institute for NMR analysis.

1 Waksman, S. A. & Woodruff, H. B. Streptothricin, a new selective bacteriostatic and bactericidal agent particularly against Gram-negative bacteria. *Proc. Soc. Exptl. Biol. Med.* **49,** 207–209 (1942).
2 Khokhlov, A. S. Achievements in the study of streptothricin antibiotics. *Antibiotiki.* **28,** 613–622 (1983).
3 Kim, B. T. *et al.* N-methylstreptothricin D, a new streptothricin-group antibiotic from a *Streptomyces* spp. *J. Antibiot.* **47,** 1333–1336 (1994).
4 Ando, T. *et al.* New streptothricin-group antibiotics, AN-201 I, II and III. *J. Antibiot.* **40,** 1140–1145 (1987).
5 Goo, Y. M. *et al.* A new streptothricin family antibiotic producing *Streptomyces* spp. SNUS 8810-111: characterization of the producing organisms, fermentation, isolation, and structure elucidation of antibiotics. *Arch. Pharm. Res.* **19,** 153–159 (1996).
6 Hamano, Y., Matsuura, N. & Kitamura, M. A novel enzyme conferring streptothricin resistance alters the toxicity of streptothricin D from broad-spectrum to bacteria-specific. *J. Biol. Chem.* **281,** 16842–16848 (2006).
7 Inamori, Y., Tominaga, H., Okuno, M., Sato, H. & Tsujibo, H. Antimicrobial activity on plant-pathogenic microorganisms and phytogrowth-inhibitory activity of streptothricin antibiotics, racemomycin-A and -C. *Chem. Pharm. Bull.* **36,** 1577–1580 (1988).
8 Taniyama, H., Sawada, Y. & Kitagawa, T. Studies on the inactivation and regeneration of streptothricin. *J. Antibiot.* **24,** 662–666 (1971).
9 Ji, Z. Q., Wang, M. A., Zhang, J. W., Wei, S. P. & Wu, W. J. Two new members of streptothricin class antibiotics from *Streptomyces qinlingensis* sp. nov. *J. Antibiot.* **60,** 739–744 (2007).
10 Ji, Z. Q., Zhang, J. W., Wei, S. P., Wu, W. J. & Wang, M. A. Identification of streptothricin class antibiotics in the early-stage of antibiotics screening by electrospray ionization mass spectrometry. *J. Antibiot.* **81,** 660–667 (2008).
11 Hisamoto, M. *et al.* A-53930A and B, novel N-type Ca^{2+} channel Blockers. *J. Antibiot.* **51,** 607–617 (1998).
12 Sawada, Y., Sakamoto, H. & Taniyama, H. Studies on chemical modification of streptothricin-group antibiotics. III. Pritial N-acetylation of racemomycins and their biological activity. *Yakugaku Zasshi.* **94,** 176–180 (1974).
13 Sawada, Y. & Taniyama, H. Studies on chemical modification of streptothricin-group antibiotics. IV. Preparation of β-N-acetyl-racemomycin-A and its antimicrobial activity. *Yakugaku Zasshi.* **94,** 264–266 (1974).
14 Kusumoto, S., Kambayashi, S., Imaoka, S., Shima, K. & Shiba, T. Total chemical structure of streptothricin. *J. Antibiot.* **35,** 925–927 (1982).
15 Hamano, Y., Maruyama, C. & Kimoto, H. Construction of a knockout mutant of the streptothricin-resistance gene in *Streptomyces albulus* by electroporation. *Actinomycetologica.* **20,** 35–41 (2006).
16 Martha, M. T., David, F. W. & Melvin, I. M. Antimicrobial susceptibility testing of *Streptococcus pneumoniae* by micro-broth dilution. *Antimicrob. Agents. Chemother.* **18,** 579–581 (1980).

The Journal of Antibiotics (2009) 62, 239–242
© 2009 Japan Antibiotics Research Association All rights reserved 0021-8820/09 $32.00
www.nature.com/ja

ORIGINAL ARTICLE

Pentanol derivatives from basidiomycete *Catathelasma imperiale* and their 11β-hydroxysteroid dehydrogenases inhibitory activity

Ling Zhang[1,3], Yu Shen[2], Hua-Jie Zhu[1], Fei Wang[1,4], Ying Leng[2] and Ji-Kai Liu[1]

Five new secondary metabolites derived from pentanol, namely catathelasmols A–E (1–5), were isolated from the fruiting bodies of the basidiomycete *Catathelasma imperiale*. Their structures were elucidated on the basis of spectroscopic analysis, and the absolute configurations were determined by computational chemistry. Compounds 3, 4 and 5 showed inhibitory activities against two isozymes of 11β-hydroxysteroid dehydrogenases (11β-HSD1 and 11β-HSD2), with IC_{50} values of 28.7–62.3 μg ml^{-1} (human 11β-HSD1), 30.4–149.2 μg ml^{-1} (mouse 11β-HSD1), 5.1–177 μg ml^{-1} (human 11β-HSD2) and 32.3–129.1 μg ml^{-1} (mouse 11β-HSD2), which catalyze the interconversion of cortisol and cortisone.
The Journal of Antibiotics (2009) **62,** 239–242; doi:10.1038/ja.2009.17; published online 27 March 2009

Keywords: basidiomycete; catathelasmols A–E; *Catathelasma imperiale*; pentanol derivatives; 11β-hydroxysteroid dehydrogenases

INTRODUCTION

Catathelasma imperiale (Fr.) Sing. (Tricholomataceae) is a conifer-loving basidiomycete defined by its large size, white spore print, sticky brownish cap, mealy odor and double ring. This mushroom is mainly distributed in the southwest of China. Only a few ergosterols have been reported from the chemical investigation of this fungus.[1] As a part of our efforts to discover the structurally diverse and biologically active secondary metabolites from higher fungi,[2–5] the investigation of the fruiting bodies of *C. imperiale* has led to the isolation of five new compounds, catathelasmols A–E (**1–5**). Herein, details of the isolation and structural elucidation of **1–5** are described, including assignment of the absolute configurations by computational chemistry. Among them, compounds **3–5** showed inhibitory activities against two isozymes of 11β-hydroxysteroid dehydrogenases (11β-HSD1 and 11β-HSD2), which catalyze the interconversion of cortisol and cortisone. Although these secondary metabolites are structurally simple, there are very few reports on these types of natural products.

MATERIALS AND METHODS

General

Optical rotations were obtained on a Horiba SEPA-300 polarimeter (Horiba, Tokyo, Japan). IR spectra were taken on a Bruker Tensor 27 FT-IR spectrometer (Bruker GmbH, Ettlingen, Germany) with KBr pellets. NMR spectra were recorded with a Bruker DRX-500 instrument (Bruker GmbH) in $CDCl_3$ (δ_H=7.26 p.p.m., δ_C=77.00 p.p.m.) at room temperature. EI-MS, electrospray ionization mass spectrum (ESI-MS) and high resolution electrospray ionization mass spectrum (HR-ESI-MS) were measured on Finnigan-MAT 90 (Finnigan, Somerset, NJ, USA) and API QSTAR Pulsar i (MDS Sciex, Concord, ON, Canada) mass spectrometers, respectively. Silica gel (200–300 mesh; Qingdao Marine Chemical Inc., Qingdao, China) and Sephadex LH-20 (Amersham Biosciences, Uppsala, Sweden) were used for column chromatography. Fractions were monitored by TLC and spots were visualized by heating silica gel plates sprayed with vanillin-H_2SO_4 in ethanol.

Fungus material

The fresh fruiting bodies of *C. imperiale* were purchased at a market in Nanhua County of Yunnan Province, China, in August 2005 and were identified by Professor Mu Zang. The voucher specimen (HFG 05112) was deposited in the herbarium of Kunming Institute of Botany, Chinese Academy of Sciences.

Extraction and isolation

The dry fruiting bodies of *C. imperiale* (700 g) were extracted thrice with EtOAc (total 9 l) at room temperature for 3 days each time. The extract was filtered and concentrated under reduced pressure to give a residue (18.8 g), which was subjected to silica gel column chromatography eluted with $CHCl_3$/MeOH (from 100:0 to 0:100). The fraction (6.6 g) eluted with pure $CHCl_3$ was subjected to further silica gel column chromatography using a gradient of petroleum ether:acetone (150:1; 50:1; 20:1) followed by pure MeOH to give subfractions A–D. Subfraction A (300 mg) (petroleum ether:acetone 150:1, v/v) was further isolated over a silica gel column eluted with petroleum ether:

[1]State Key Laboratory of Phytochemistry and Plant Resources in West China, Kunming Institute of Botany, Chinese Academy of Sciences, Kunming, China; [2]Shanghai Institute of Materia Medica, Chinese Academy of Sciences, Shanghai, China; [3]Graduate University of Chinese Academy of Sciences, Beijing, China and [4]BioBioPha Co., Ltd, Kunming, China
Correspondence: Professor Dr J-K Liu, State Key Laboratory of Phytochemistry and Plant Resources in West China, Kunming Institute of Botany, Chinese Academy of Sciences, Kunming 650204, China.
E-mail: jkliu@mail.kib.ac.cn or Dr Y Leng, Shanghai Institute of Materia Medica, Chinese Academy of Sciences, Shanghai 201203, China.
E-mail: yleng@mail.shcnc.ac.cn
Received 22 October 2008; revised 12 February 2009; accepted 17 February 2009; published online 27 March 2009

acetone (150:1) to give a residue (160 mg) mainly containing **1** and **2**, which was repeatedly subjected to silica gel column chromatography to yield **1** (40.0 mg) and **2** (1.7 mg). Subfraction B (180 mg) (petroleum ether:acetone 50:1, v/v), containing mainly **3** and **4**, was further isolated on a silica gel column eluted with $CHCl_3$ to yield **3** (14.6 mg) and **4** (74.1 mg). Subfraction D (121 mg) eluted with MeOH was purified by Sephadex LH-20 ($CHCl_3$/MeOH 1:1, v/v) and silica gel column chromatography using $CHCl_3$/MeOH (150:1, v/v) as the eluent, to yield **5** (61.4 mg).

Computational methods

The stable geometries of **1** with low energy were investigated using HyperChem 7.0 (HyperCube, Gainesville, FL, USA). These low-energy conformations were then optimized at the B3LYP/6-31G (d) level again. The B3LYP/6-31G (d)-optimized structures were then used for optical rotation calculations at the B3LYP/aug-cc-pVDZ//6-31+G (d). The calculated optical rotation for (*R*) configuration was +14.5°. This value is very close to the experimental magnitude of +10.6°. Thus, the absolute configuration of (+)-**1** was assigned as (*R*). Compound **5** has a linear structure and it is difficult to use the above method to compute its optical rotation to determine the absolute configuration. Our recent matrix method was used in the study. The value of the determinant (det(*D*)) for (*R*)-**5** was −2.50. According to the principle of matrix prediction, the det(*D*) and k_0 value were needed to use both. As the optical rotation was −10.4 (*c* 0.40, $CHCl_3$), the calculated k_0 value for this chiral secondary alcohol was 4.2, which is located in the window of coefficients of chiral secondary alcohols in chloroform. Thus, compound **5** was assigned (*R*) configuration.

Physicochemical properties

Catathelasmol A (**1**): amorphous powder; $[\alpha]_D^{26}$ +10.6 (*c* 0.30, $CHCl_3$); IR (KBr): 3450, 1175, 1115, 1058, 1033 cm^{-1}; ^{1}H- and ^{13}C-NMR: see Table 1; ESI-MS (pos.): 101 $[M–H_2O+H]^+$, 83 $[M–2H_2O+H]^+$; HR-ESI-MS (pos.): 101.0600 ($[M–H_2O+H]^+$, calcd. 101.0602).

Catathelasmol B (**2**): colorless oil; $[\alpha]_D^{26}$ +8.9 (*c* 0.30, $CHCl_3$); IR (KBr): 3441, 1191, 1167, 1104, 1062, 1034 cm^{-1}; ^{1}H- and ^{13}C-NMR: see Table 1; ESI-MS (pos.): 218 $[M]^+$, 201 $[M–H_2O+H]^+$, 183 $[M–2H_2O+H]^+$; HR-ESI-MS (pos.): 201.1125 ($[M–H_2O+H]^+$, calcd. 201.1126).

Catathelasmol C (**3**): colorless oil; IR (KBr): 1736, 1661, 1371, 1236, 1191 cm^{-1}. ^{1}H- and ^{13}C-NMR: see Table 2; ESI-MS (pos.): 225 $[M+Na]^+$; HR-ESI-MS (pos.): 225.0739 ($[M+Na]^+$, calcd. 225.0738).

Catathelasmol D (**4**): colorless oil; IR (KBr): 3441, 2966, 1738, 1369, 1248, 1045 cm^{-1}; ^{1}H- and ^{13}C-NMR: see Table 2; EI-MS: 160 (M^+, 2), 129 (42), 112 (17), 100 (14), 87 (100); HR-FAB-MS (pos.): 161.0838 ($[M+H]^+$, calcd. 161.0814).

Catathelasmol E (**5**): colorless oil; $[\alpha]_D^{26}$ –10.4 (*c* 0.40, $CHCl_3$); IR (KBr): 3458, 1740, 1450, 1247 cm^{-1}. ^{1}H- and ^{13}C-NMR: see Table 2; ESI-MS (pos.): 227 $[M+Na]^+$; HR-ESI-MS (pos.): 227.0889 ($[M+Na]^+$, calcd. 227.0895).

Biological testing

The inhibitory activities of the compounds on human or mouse 11β-HSD1 and 11β-HSD2 enzymatic activities were determined by the scintillation proximity assay using microsomes containing 11β-HSD1 or 11β-HSD2, according to our earlier studies.[6] Briefly, the full-length cDNAs of human or murine 11β-HSD1 and 11β-HSD2 were isolated from the cDNA libraries provided by the NIH Mammalian Gene Collection and cloned into pcDNA3 expression vector. HEK-293 cells were transfected with the pcDNA3-derived expression plasmid and selected by cultivation in the presence of 700 μg ml^{-1} of G418. The microsomal fraction overexpressing 11β-HSD1 or 11β-HSD2 was prepared from the HEK-293 cells stably transfected with either 11β-HSD1 or 11β-HSD2 and was used as the enzyme source for scintillation proximity assay. Microsomes containing human or mouse 11β-HSD1 were incubated with NADPH and [^{3}H]cortisone. Then the product, [^{3}H]cortisol, was specifically captured by a monoclonal antibody coupled to protein A-coated scintillation proximity assay beads. The 11β-HSD2 screening was performed by incubating 11β-HSD2 microsomes with [^{3}H]cortisol and NAD^+ and monitoring substrate disappearance. IC_{50} values were calculated by using Prism Version 4 (GraphPad Software, San Diego, CA, USA).

RESULTS AND DISCUSSION

Catathelasmol A (**1**), obtained as an amorphous powder, has a molecular formula of $C_5H_{10}O_3$ based on the positive-ion HR-ESI-MS, showing a quasi-molecular ion peak at *m/z* 101. 0600 (calcd. for $[C_5H_{10}O_3–H_2O+H]^+$, 101.0602) and requiring only one degree of unsaturation. The IR spectrum showed the presence of one or more hydroxyl groups (3450 cm^{-1}). The ^{13}C-NMR spectrum (Table 1) exhibited five signals: one quaternary carbon bearing two oxygens at δ 102.7, two oxymethylenes at δ 68.0 (t), 65.2 (t) and two up-field methylenes at δ 33.8 (t), 23.5 (t). It was obvious that only one degree of unsaturation was attributed to a ring. The ^{1}H-NMR spectrum (Table 1) showed eight protons: two oxygenated methylenes at δ 3.45 (1H, d, *J*=11.5 Hz), 4.14 (1H, d, *J*=11.5 Hz), 3.97 (2H, t, *J*=6.9 Hz), and up-field resonances at δ 1.61 (1H, m), 1.94 (1H, m), 1.88 (1H, m), 2.05 (1H, m). The above NMR data suggested that **1** possessed a tetrahydrofuran moiety connected with a hydroxyl and a hydroxymethyl group. The heteronuclear multi-bond correlations (HMBC) (Figure 1) from H-6 to C-2 and C-3, and from H-5 to C-2 and C-3 were observed; consequently, the hydroxyl and hydroxymethyl groups were doubtless both emplaced at C-2. The absolute configuration of (+)-**1** was assigned as (*R*) using the B3LYP/aug-cc-pVDZ//6-31+G(d) methods[7–9] based on the comparison of experimental optical rotation (+10.6°) and calculated optical rotation (+14.5°). Therefore, the structure of **1** was determined as (*R*)-(+)-2-(hydroxymethyl)-tetrahydrofuran-2-ol and named catathelasmol A, as shown in Figure 2.

Catathelasmol B (**2**), a colorless oil, was obtained as a minor constituent with a molecular formula of $C_{10}H_{18}O_5$, based on the positive-ion HR-ESI-MS: 201.1125 (calcd. for $[C_{10}H_{18}O_5–H_2O+H]^+$, 201.1126). In the NMR spectra (Table 1) of **2**, signals for the number of protons and carbon that were observed were only half of the number that would correspond to the molecular formula. This indicated that **2** is a symmetrical structure. The NMR data were considerably in accordance with those of **1**, but their TLC behavior was discriminable, which suggested that **2** was unambiguously a dimer of **1**, and there were just two possible condensed positions: C-2 or C-6 hydroxyl. There was no reaction and no corresponding product obtained in acetylation, which suggested that there was no free

Table 1 NMR spectral data for compounds 1 and 2 in $CDCl_3$

No.	***1***		***2***	
	δ_C	δ_H	δ_C	δ_H
2	102.7 (s)		103.8 (s)	
3	33.8 (t)	1.61, 1.94 (each 1H, m)	33.7 (t)	1.77, 2.11 (each 1H, m)
4	23.5 (t)	1.88, 2.05 (each 1H, m)	24.1 (t)	1.89, 2.03 (each 1H, m)
5	68.0 (t)	3.97 (2H, 6.9)	67.9 (t)	3.94, 4.00 (each 1H, m)
6	65.2 (t)	3.45 (1H, d, 11.5), 4.14 (1H, d, 11.5)	66.3 (t)	3.55 (1H, d, 11.8), 3.94 (1H, d, 11.8)

Table 2 NMR spectral data for compounds 3–5 in $CDCl_3$

No.	3		4		5	
	δ_C	δ_H	δ_C	δ_H	δ_C	δ_H
1	67.9 (t)	4.65 (2H, s)	63.1 (t)	4.26 (2H, s)	68.6 (t)	3.95 (1H, dd, 11.3, 7.2), 4.11 (1H, dd, 11.3, 7.2)
2	202.9 (s)		208.9 (s)		69.3 (d)	3.84 (1H, m)
3	35.1 (t)	2.50 (2H, t, 7.2)	34.4 (t)	2.52 (2H, t, 7.2)	29.6 (t)	1.71, 1.80 (each 1H, m)
4	22.2 (t)	1.95 (2H, m)	22.3 (t)	1.97 (2H, m)	24.6 (t)	1.52 (2H, m)
5	66.3 (t)	4.06 (2H, t, 6.3)	67.8 (t)	4.08 (2H, t, 6.3)	64.2 (t)	4.08 (2H, t, 6.5)
a_1	170.2 (s)				171.3 (s)	
a_2	20.4 (q)	2.16 (3H, s)			20.9 (q)	2.08 (3H, s)
b_1	171.0 (s)		170.9 (s)		171.3 (s)	
b_2	20.9 (q)	2.04 (3H, s)	20.5 (q)	2.04 (3H, s)	21.0 (q)	2.03 (3H, s)

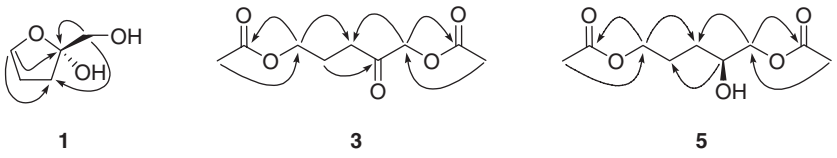

1 **3** **5**

Figure 1 Key HMBC correlations of compounds **1**, **3** and **5.**

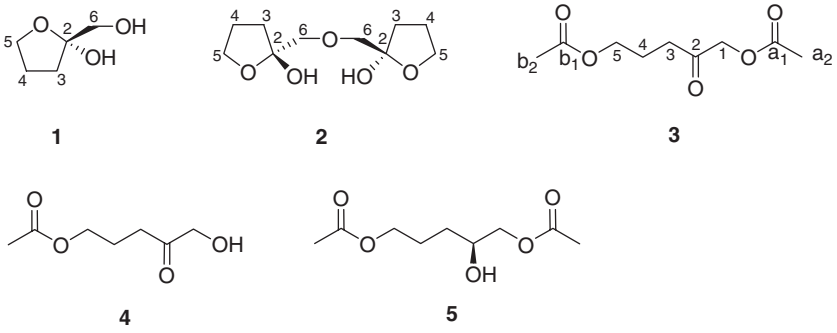

1 **2** **3**

4 **5**

Figure 2 Structures of compounds **1**–**5.**

primary hydroxyl group in the structure of **2**, but that **2** was formed from two molecules of **1** through the intermolecular dehydration at C-6 hydroxyl. Thus, the structure of **2** was proposed as (2*R*,2′*R*)-2,2′-oxybis(methylene)bis(tetrahydrofuran-2-ol), as shown in Figure 2.

Catathelasmol C (**3**) was isolated as a colorless oil possessing the molecular formula $C_9H_{14}O_5$, based on the positive-ion HR-ESI-MS: 225.0739 (calcd. for $C_9H_{14}O_5Na$, 225.0738). The IR spectrum showed the absorption bands of ester carbonyl (1736 cm^1) and keto carbonyl (1661 cm^{-1}) groups. The ^{13}C-NMR spectrum (Table 2) exhibited nine carbon resonances, including one keto carbonyl at δ 202.9 (s), two oxymethylenes at δ 67.9 (t), 66.3 (t), two up-field methylene carbons at δ 35.1 (t), 22.2 (t), as well as characteristic signals at δ 170.2 (s), 20.4 (q); 171.0 (s), 20.9 (q) contributed to two acetoxyls. The ^1H-NMR spectrum (Table 2) of **3** showed signals for two oxygenated methylenes at δ 4.65 (2H, s), 4.06 (2H, t, J=6.3 Hz), two up-field methylenes at δ 2.50 (2H, t, J=7.2 Hz), 1.95 (2H, m) together with two acetoxyl methyl singlets at δ 2.16 (3H, s), 2.04 (3H, s). The above NMR character allowed us to conclude that **3** was a diacetylated pentanediol containing a keto group. By analysis of the HMBC spectrum (Figure 1), the position of the ketone was determined at C-2, in which the correlations from H-1 to C-3 and C-a_1, from H-5 to C-3 and C-b_1 and from H-4 to C-2 were observed. Therefore, the structure of **3** was elucidated as 2-oxopentane-1,5-diyl diacetate named catathelasmol C, which was a new natural product.[10]

Catathelasmol D (**4**), also obtained as a colorless oil, has a molecular formula of $C_7H_{12}O_4$, based on the EI-MS showing a molecular ion peak at *m/z* 160, in combination with the ^{13}C-NMR (DEPT) spectrum. The NMR data (Table 2) of **4** were similar to those of **3**, but there was only one set of acetoxyl signals: δ 170.9 (s), 20.5 (q). Considering that the signal at δ 4.26 (2H, s, H-1) in **4** evidently shifted up-field (δ=0.39 p.p.m.) compared with that of **3**, the acetoxyl group must be connected at C-5 in **4**. Thus, the structure of **4** was determined as 5-hydroxy-4-oxopentyl acetate and named catathelasmol D, which was also a new natural product,[11] as shown in Figure 2.

Catathelasmol E (**5**), a colorless oil, was assigned the molecular formula $C_9H_{16}O_5$ by the positive-ion HR-ESI-MS: 227.0889 (calcd. for $C_9H_{16}O_5Na$, 227.0895). The NMR data of **5** were similar to those of **3**, and comparison of ^{13}C-NMR data showed that instead of a ketone, one oxymethine carbon at δ 69.3 (d) newly appeared in **5**. The obvious differences in the ^1H-NMR spectra were as follows: (a) the oxymethylene singlet in **3** was observed separately from each other at δ 3.95 (1H, dd, J=11.3, 7.2 Hz) and 4.11 (1H, dd, J=11.3, 7.2 Hz),

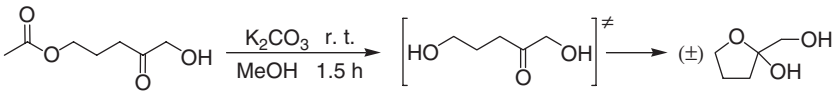

4 1

Figure 3 Chemical transformation from **4** to **1.**

respectively in **5**; and (b) an oxygen-bearing methine proton at δ 3.84 (1H, m) was newly detected in **5**. The above NMR character indicated that the keto group in **3** was hydrogenated in **5**. Initially, the modified Mosher's method[12,13] was applied to determine the absolute configuration of the hydroxyl at C-2, but failed. Alternatively, we resorted to the computational method to establish the absolute configuration. The absolute configuration of **5** was assigned as (*R*) using matrix model.[14] The det(*D*) value for this chiral alcohol was −2.50 and the calculated k_0 value was 4.2, which is located in the window of coefficients of chiral secondary alcohols in chloroform. Accordingly, the structure of **5** was established as 2-hydroxypentane-1,5-diyl diacetate, shown in Figure 2, and was named catathelasmol E.

It was not until quite recently that such simple pentanol derivatives were found, which suggested that this type of metabolites were distributed in a narrow range, so we believe that they may possess an important chemotaxonomic significance. Besides, the realization of the chemical transformation from **4** to **1** validated the structural correctness (Figure 3).

*Chemical transformation from **4** to **1**:*[15] A solution of **4** (50 mg) in MeOH (5.0 ml) was treated with K_2CO_3 (97.4 mg) at room temperature. After stirring for 1.5 h, saturated aqueous ammonium chloride was added and extracted with ethyl acetate, and the organic layer was washed with water and brine, dried over sodium sulfate, and evaporated to a residue that was purified by a silica gel column using pure $CHCl_3$ to yield **1** (12 mg). The determined optical rotation was expectedly zero. Thus, the cyclization of **4** to **1** obtained in the experiments must involve the enzyme catalysis.

Glucocorticoid hormones play important roles in many biological and physiological processes, including regulation of energy metabolism, inflammatory, immune and stress responses, and cardiovascular homeostasis. The action of glucocorticoid on target tissue is not dependent inevitably on the circulating levels, but is regulated in a tissue-specific manner by the enzymes of 11β-hydroxysteroid dehydrogenases (11β-HSD1 and 11β-HSD2), which catalyze the interconversion of active 11-hydroxy-glucocorticoids (cortisol in humans and corticosterone in rodents) and their respective inert 11-keto forms (cortisone in humans and 11-dehydrocorticosterone in rodents).[16] 11β-HSD1 is highly expressed in the liver, gonad, adipose tissue and brain, in which it acts as a reductase regenerating the active glucocorticoids from its inactive forms, thus amplifying local glucocorticoid action.[17] 11β-HSD2 is predominantly expressed in aldosterone target cells, such as the kidney and colon, in which it catalyzes the inactivation of glucocorticoids, thereby preventing the excessive activation of the mineralocorticoid receptor and sequelae, including sodium retention, hypokalemia and hypertension.

We tested the inhibitory effect of the compounds on both human and mouse 11β-HSD1 and 11β-HSD2. Compound **3** showed inhibitory activities against 11β-HSD1 (human IC_{50}=28.7 μg ml^{-1}; mouse IC_{50}=30.4 μg ml^{-1}) and 11β-HSD2 (human IC_{50}=5.1 μg ml^{-1}; mouse IC_{50}=32.3 μg ml^{-1}). Compound **4** showed inhibitory activities against 11β-HSD1 (human IC_{50}=47.4 μg ml^{-1}; mouse IC_{50}=149.2 μg ml^{-1}) and 11β-HSD2 (human IC_{50}=38.9 μg ml^{-1}; mouse IC_{50}=129.1 μg ml^{-1}). Compound **5** showed inhibitory activities against human 11β-HSD1 (IC_{50}=62.3 μg ml^{-1}) and 11β-HSD2 (IC_{50}=177.0 μg ml^{-1}). Therefore, compounds **3–5** showed inhibitory activities against 11β-HSD1 and 11β-HSD2 and provide the possibility for modulating local cortisone/cortisol availability *in vivo*.

ACKNOWLEDGEMENTS

This project was supported by National Basic Research Program of China (973 Program, 2009CB522300), National Natural Science Foundation of China (30830113) and Chinese Academy of Sciences (KSCX1-YW-R-24; KSCX2-YW-G-025).

1 Yang, S. P., Xu, J. & Yue, J. M. Sterols from the fungus *Catathelasma imperiale*. *Chin. J. Chem.* **21,** 1390–1394 (2003).
2 Liu, J. K. N-containing compounds of macromycetes. *Chem. Rev.* **105,** 2723–2744 (2005).
3 Liu, J. K. Natural terphenyls: developments since 1877. *Chem. Rev.* **106,** 2209–2223 (2006).
4 Zhou, Z. Y. *et al.* Gallicynoic acids A–I, acetylenic acids from the Basidiomycete *Coriolopsis gallica*. *J. Nat. Prod.* **71,** 223–226 (2008).
5 Zhang, L., Wang, F., Dong, Z. J., Steglich, W. & Liu, J. K. A new butenolide-type fungal pigment from the mushroom *Pulveroboletus ravenelii*. *Heterocycles* **68,** 1455–1458 (2006).
6 Yang, H. Y., Dou, W., Lou, J., Leng, Y. & Shen, J. H. Discovery of novel inhibitors of 11beta-hydroxysteroid dehydrogenase type 1 by docking and pharmacophore modeling. *Bioorg. Med. Chem. Lett.* **18,** 1340–1345 (2008).
7 Liu, D. Z. *et al.* Vibralactone: a lipase inhibitor with an unusual fused beta-lactone produced by cultures of the basidiomycete *Boreostereum vibrans*. *Org. Lett.* **8,** 5749–5752 (2006).
8 Amos, R. D. Electric and magnetic properties of CO, HF, HCl, and CH_3F. *Chem. Phys. Lett.* **87,** 23–26 (1982).
9 Polavarapu, P. L. Ab initio molecular optical rotations and absolute configurations. *Mol. Phys.* **91,** 551–554 (1997).
10 Kuschinsky, G., Lange, G., Scholtissek, C. h. & Turba, F. Reaction mechanism of digitalis constituents. *Biochem. Z.* **327,** 314–330 (1955).
11 Bonini, C., Chiummiento, L., Funicello, M., Lupattelli, P. & Pullez, M. New functionalized hydroxymethyl ketones from the mild and chemoselective $KMnO_4$ oxidation of chiral terminal olefins. *Eur. J. Org. Chem.* 80–83 (2006).
12 Dale, J. A. & Mosher, H. S. Nuclear magnetic resonance enantiomer regents. Configurational correlations via nuclear magnetic resonance chemical shifts of diastereomeric mandelate, *O*-methylmandelate, and α-methoxy-α-trifluoromethylphenylacetate (MTPA) esters. *J. Am. Chem. Soc.* **95,** 512–519 (1973).
13 Ohtani, I., Kusumi, T., Kashman, Y. & Kakisawa, H. High-field FT NMR application of Mosher's method. The absolute configurations of marine terpenoids. *J. Am. Chem. Soc.* **113,** 4092–4096 (1991).
14 Zhu, H. J., Ren, J. & Pittman, C. U. Matrix model to predict specific optical rotations of acyclic chiral molecules. *Tetrahedron* **63,** 2292–2314 (2007).
15 Yiotakis, A., Magriotisb, P. A. & Vassiliou, S. A simple synthesis of the metabotropic receptor ligand (2*S*)-α-(hydroxymethyl)-glutamic acid and its Fmoc protected derivatives. *Tetrahedron: Asymmetry* **18,** 873–877 (2007).
16 Stewart, P. M. & Draper, N. 11β-hydroxysteroid dehydrogenase and the pre-receptor regulation of corticosteroid hormone action. *J. Endocrinol.* **186,** 251–271 (2005).
17 Seckl, J. R. & Walker, B. R. Minireview: 11beta-hydroxysteroid dehydrogenase type 1-a tissue-specific amplifier of glucocorticoid action. *Endocrinology* **142,** 1371–1376 (2001).

The Journal of Antibiotics (2009) 62, 243–246
© 2009 Japan Antibiotics Research Association All rights reserved 0021-8820/09 $32.00
www.nature.com/ja

ORIGINAL ARTICLE

New atpenins, NBRI23477 A and B, inhibit the growth of human prostate cancer cells

Manabu Kawada[1], Isao Momose[1], Tetsuya Someno[1], Goh Tsujiuchi[2] and Daishiro Ikeda[1]

The growth and metastasis of prostate cancer are regulated by prostate stroma through the tumor–stromal cell interactions. Small molecules that modulate the tumor–stromal cell interactions will be new anticancer drugs. In the course of our screening of the modulators, we isolated two new atpenins, NBRI23477 A (4) and B (5), from the fermentation broth of *Penicillium atramentosum* PF1420. Compounds 4 and 5 as well as atpenin A4 (1), A5 (2) and B (3) inhibited the growth of human prostate cancer DU-145 cells in the coculture with human prostate stromal cells more strongly than that of DU-145 cells alone.
The Journal of Antibiotics (2009) **62,** 243–246; doi:10.1038/ja.2009.20; published online 13 March 2009

Keywords: antitumor drug; atpenin; prostate cancer; prostate stroma

INTRODUCTION

The growth and metastasis of prostate cancer are regulated by prostate stroma.[1,2] We have reported earlier that prostate stromal cell (PrSC) promotes the growth of human prostate cancer cells through the secretion of insulin-like growth factor-I.[3,4] There is a possibility that small molecules could inhibit cancer cell growth by modulating tumor–stromal cell interactions. We developed the *in vitro* coculture system of human prostate cancer cells and PrSC, in which the growth of prostate cancer cell is increased by the coculture with PrSC.[3,5] Using the assay method, we have been searching for the modulators of the tumor–stromal cell interactions. In the course of our screening of the modulators, we isolated new atpenins, NBRI23477 A (**4**) and B (**5**), along with the known compounds, atpenin A4 (**1**), A5 (**2**) and B (**3**).[6,7] Here we describe the isolation, structure determination and biological activity of **4** and **5**. We also report the activity of **1**, **2** and **3** on our assay.

MATERIALS AND METHODS

Reagents

Rhodanile blue was purchased from Aldrich (Milwaukee, WI, USA). Insulin and hydrocortisone were obtained from Sigma (St Louis, MO, USA). Transferrin was obtained from Wako Pure Chemical Industries (Tokyo, Japan). The recombinant human basic fibroblast growth factor was purchased from Pepro Tech (London, UK).

Cells

The human prostate cancer DU-145 cells were obtained from American Type Culture Collection (Manassas, VA, USA) and maintained in Dulbecco's modified Eagle's medium supplemented with 10% fetal bovine serum (ICN Biomedicals, Aurora, OH, USA), 100 U ml^{-1} penicillin G and 100 μg ml^{-1} streptomycin at 37 °C with 5% CO_2. The human normal PrSCs were obtained from Bio Whittaker (Walkersville, MD, USA) and maintained in Dulbecco's modified Eagle's medium supplemented with 10% fetal bovine serum, 100 U ml^{-1} penicillin G, 100 μg ml^{-1} streptomycin, ITH (5 μg ml^{-1} insulin, 5 μg ml^{-1} transferrin and 1.4 μM hydrocortisone) and 5 ng ml^{-1} human basic fibroblast growth factor at 37 °C with 5% CO_2.

Coculture experiment

A microplate assay method for the selective measurement of epithelial tumor cells in coculture with stromal cells using rhodanile blue dye was performed as described before.[5] PrSCs were first inoculated into 96-well plates at 5000 cells per well in 100 μl of Dulbecco's modified Eagle's medium supplemented with ITH and 0.1% fetal bovine serum in the presence of various concentrations of the test compounds. After 2 days, 10 μl of DU-145 cell suspension (5000 cells) in serum-free Dulbecco's modified Eagle's medium was inoculated onto a monolayer of PrSC, and the cells were further cultured for 3 days. For monoculture of DU-145 cells, the assay medium alone was first incubated in the presence of test compounds for 2 days at 37 °C. Then, DU-145 cells were inoculated as described above and cultured for further 3 days.

Analytical measurement

Melting points were obtained on a Yanagimoto micro melting point apparatus (Yanagimoto, Kyoto, Japan). Optical rotations were measured on a JASCO P-1030 polarimeter (JASCO, Tokyo, Japan). UV spectra were recorded on a Hitachi 228 A spectrometer (Hitachi, Tokyo, Japan). ^{1}H- and ^{13}C-NMR spectra were measured on a JEOL JNM A400 spectrometer (JEOL, Tokyo, Japan) using TMS as an internal standard. High resolution electrospray ionization mass spectrometry (HR-ESI-MS) spectra were measured with a JEOL JMS-T100LC spectrometer (JEOL).

Fermentation of fungal strain PF1420

Penicillium atramentosum PF1420 was isolated from a soil sample collected in Iwamizawa, Hokkaido, Japan. A slant culture of *P. atramentosum* PF1420 was used to inoculate 100-ml Erlenmeyer flasks. Each contained 20 ml of a seed

[1]Microbial Chemistry Research Center, Numazu Bio-Medical Research Institute, Shizuoka, Japan and [2]Bioscience Labs, Meiji Seika Kaisha LTD, Kanagawa, Japan
Correspondence: Dr M Kawada, Microbial Chemistry Research Center, Numazu Bio-Medical Research Institute, 18–24 Miyamoto, Numazu-shi, Shizuoka 410-0301, Japan.
E-mail: kawadam@bikaken.or.jp
Received 4 November 2008; revised 12 February 2009; accepted 23 February 2009; published online 13 March 2009

medium consisting of 2.0% soluble starch, 1.0% glucose, 0.2% soybean meal, 0.6% wheat germ, 0.5% polypeptone, 0.3% yeast extract and 0.2% $CaCO_3$ in deionized water adjusted to pH 7.2 with NaOH solution before sterilization. The flasks were incubated at 25 °C for 72 h on a rotary shaker at 220 r.p.m. Portions of 1.0 ml of this seed culture were transferred into six 500-ml Erlenmeyer flasks, each of which contained 100 ml of a seed medium. The flasks were incubated at 25 °C for 48 h on a rotary shaker at 220 r.p.m. Portions of 150 ml of this seed culture were transferred into four stainless vats, each of which contained 2.5% soybean meal and water-absorbed rice (4 kg) as solid production medium. The stainless vats were thoroughly stirred and then statically cultured at 25 °C for 14 days. After incubation, 16-kg portion of the obtained culture was extracted with 32 l of 67% aqueous acetone.

RESULTS

Isolation procedure for atpenins

The 16-kg culture broth of *P. atramentosum* PF1420 was extracted with 32 l of 67% aqueous acetone. The filtrate of the extracts was concentrated *in vacuo* to remove acetone. The aqueous solution (5 l, pH 7) was applied on an HP-20 column. After washing the column with H_2O and 50% MeOH, active ingredients were eluted with 100% MeOH. The eluate was concentrated *in vacuo,* dissolved in 600 ml H_2O and then extracted with EtOAc. The organic layer was dried over Na_2SO_4 and concentrated *in vacuo* to afford 9.92 g of dried material. The materials were applied on a silica gel column (450 g, Wakogel C-200, 75–150 μm; Wako, Osaka, Japan) prepared with $CHCl_3$, and eluted with $CHCl_3$ and $CHCl_3$-MeOH. The fractions eluted with $CHCl_3$-MeOH (25:1) were concentrated *in vacuo* to give 4.13 g of viscous material. The viscous material was applied on gel filtration chromatography of Sephadex LH-20 (MeOH). The fractions containing atpenins were concentrated *in vacuo* to give 2.76 g of crude material. The crude material was purified by a reversed-phase HPLC column (Inertsil ODS-3, 20×250 mm, 6.0 ml min^{-1}) with 50% CH_3CN to afford crude atpenins, 46.4 mg of **1**, 119.8 mg of **2**, 111.1 mg of **3** and **4**, and 14.5 mg of **5**. The crude sample of **5** was applied on a Sephadex LH-20 column (MeOH) to afford pure 8.0 mg of **5**. The crude mixture of **3** and **4** was further purified by a reversed-phase HPLC column (Inertsil ODS-3, 10×250 mm, 3.0 ml min^{-1}) with 75% CH_3CN and 0.1% TFA, and then the fractions containing

Table 2 The ^{13}C- and ^{1}H-NMR assignments of 4 and 5 in pyridine-d_5

	4		*5*	
Position	*^{13}C p.p.m. (mult.)*	*^{1}H p.p.m. (mult., J(Hz))*	*^{13}C p.p.m. (mult.)*	*^{1}H p.p.m. (mult., J(Hz))*
2[a]	162.7 (s)		162.8 (s)	
3	100.6 (s)		101.0 (s)	
4[a]	165.9 (s)		165.8 (s)	
5	125.0 (s)		124.9 (s)	
5-OCH_3	60.7 (q)	3.84 (s)	60.7 (q)	3.83 (s)
6	160.2 (s)		160.1 (s)	
6-OCH_3	54.4 (q)	3.90 (s)	54.4 (q)	3.89 (s)
1′	210.6 (s)		211.3 (s)	
2′	42.2 (d)	4.36 (m)	42.2 (d)	4.42 (m)
2′-CH_3	16.4 (q)	1.35 (d, 6.4)	18.1 (q)	1.33 (d, 6.8)
3′	36.8 (t)	2.06–2.13 (m)	41.0 (t)	1.42 (m)
				2.10 (m)
4′	48.0 (d)	2.40 (m)	36.6 (d)	2.33 (m)
4′-CH_3	15.8 (q)	1.34 (d, 6.4)	20.5 (q)	1.07 (d, 6.8)
5′	97.9 (s)		145.2 (d)	5.79 (ddd, 7.6, 10.4, 17.2)
6′	35.7 (q)	2.14 (s)	114.4 (t)	4.95 (dd, 1.2, 10.4)
				4.99 (dd, 1.2, 17.2)

[a]Assignments may be interchanged.
Chemical shifts in p.p.m. from TMS as an internal standard.
The ^{13}C- and ^{1}H-NMR were measured at 100 and 400 MHz, respectively.

Table 1 Physicochemical properties of 4 and 5

	4	*5*
Appearance	White powder	Hygroscopic solid
Melting point	130–132 °C	—
Molecular formula	$C_{15}H_{21}NO_5Cl_2$	$C_{15}H_{21}NO_5$
HR-ESI-MS (m/z)		
Found	364.0713 $(M-H)^-$	294.1361 $(M-H)^-$
Calcd.	364.0719 for $C_{15}H_{20}NO_5Cl_2$	294.1342 for $C_{15}H_{20}NO_5$
UVλ_{max} (nm) (MeOH)	236, 273, 329	235, 271, 331
$[\alpha]_D^{20}$ (*c* 0.2, EtOH)	−37°	−39°
IRυ_{max} (KBr) (cm^{-1})	2935, 1651, 1597, 1448, 1325, 1198, 1163, 995	2931, 1651, 1597, 1452, 1325, 1196, 1163, 995

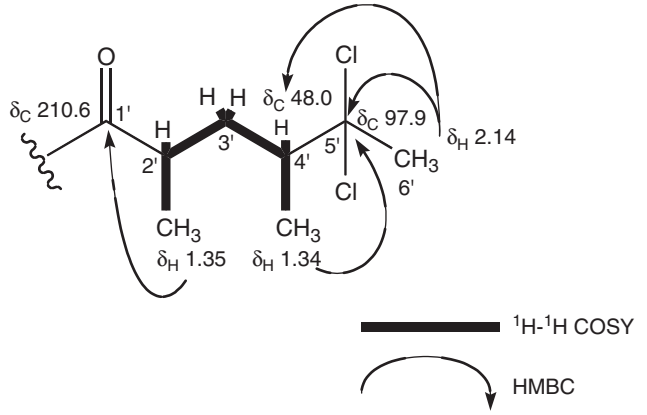

Figure 2 Partial structure of **4**.

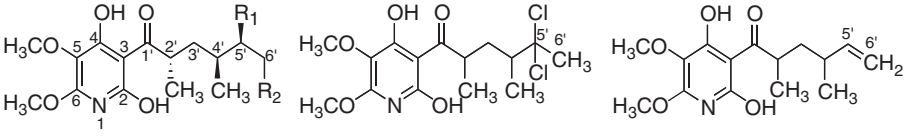

Atpenin A4 (**1**): R_1=Cl, R_2=H
Atpenin A5 (**2**): R_1=Cl, R_2=Cl
Atpenin B (**3**): R_1=H, R_2=H

NBRI23477 A (**4**)

NBRI23477 B (**5**)

Figure 1 Structures of **1**–**5**.

3 and **4** were applied on a Sephadex LH-20 column (MeOH) to afford pure 72.4 mg of **3** and 4.5 mg of **4**, respectively. The crude mixture of **1** and **2** was further purified by a reversed-phase HPLC column (Inertsil ODS-3, 10×250 mm, 3.0 ml min^{-1}) with 60% CH_3CN and 0.1% TFA, and then the fractions containing **1** and **2** were applied on a Sephadex LH-20 column (MeOH) to afford pure 15.5 mg of **1** and 26.1 mg of **2**, respectively. Separation by analytical HPLC (Inertsil ODS-3, 3 µm, 4.6×150 mm, 1.0 ml min^{-1}) with 75% CH_3CN and 0.1% TFA gave the following retention times (in minutes): 4.38 (**1**), 4.40 (**2**), 5.29 (**3**), 4.95 (**4**) and 4.28 (**5**).

Physicochemical properties

The physicochemical properties of **4** and **5** are summarized in Table 1. They are soluble in MeOH and DMSO. The molecular formulae of **4** and **5** were determined to be $C_{15}H_{21}NO_5Cl_2$ and $C_{15}H_{21}NO_5$, respectively, by HR-ESI-MS. The general features of their UV and NMR spectra resembled each other, indicating structural similarities of these compounds. Compounds **1**–**3** were identified by NMR spectra as atpenin A4 (**1**), A5 (**2**) and B (**3**), respectively (Figure 1).[6,7]

Structure determination of NBRI23477 A (4)

The ^1H- and ^{13}C-NMR data of **4** (Table 2) were similar to those of **2**.[8] However, the signals of 5′-methine and 6′-methylene of **2** were not observed in the ^{13}C-NMR spectrum of **4**, but a quaternary carbon (δ 97.9) and a methyl carbon (δ 35.7) appeared in **4**. The partial structure of **4** was established by analyses of ^1H-^1H correlation spectroscopy (COSY) and heteronuclear multiple bond connectivity (HMBC) spectra (Figure 2). ^1H-^1H COSY spectrum revealed the following fragment: -$CH(CH_3)$-CH_2-$CH(CH_3)$-. In the HMBC spectrum, singlet methyl protons (6′-H, δ 2.14) correlated to a quaternary carbon (C-5′, δ 97.9) and a methine carbon (C-4′, δ 48.0). Methyl protons (δ 1.35) connecting to C-2′ methine correlated to a carbonyl carbon (C-1′, δ 210.6). Therefore, the total structure of **4** was found to be a new family of atpenin (Figure 1).

Structure determination of NBRI23477 B (5)

The ^{13}C- and ^1H-NMR data of **5** (Table 2) were similar to those of **3**.[6,7] However, the signals of 5′-methylene and 6′-methyl of **3** were not observed in the ^{13}C-NMR spectrum of **5**. On the other hand, an olefine carbon (δ 145.2) and a terminal olefine carbon (δ 114.4) were observed in **5**. The partial structure of **5** was established by analyses of the ^1H-^1H COSY and HMBC spectra (Figure 3). ^1H-^1H COSY

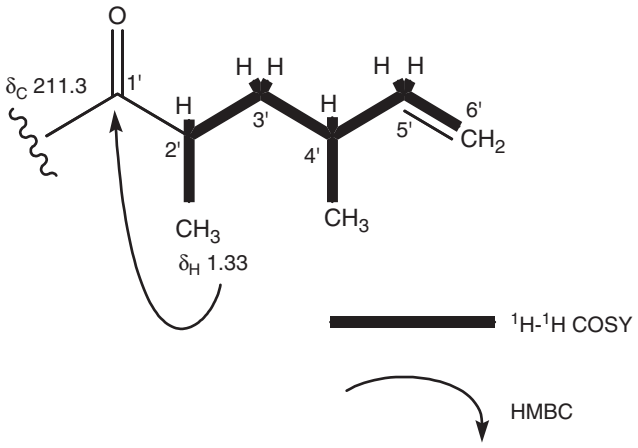

Figure 3 Partial structure of **5**.

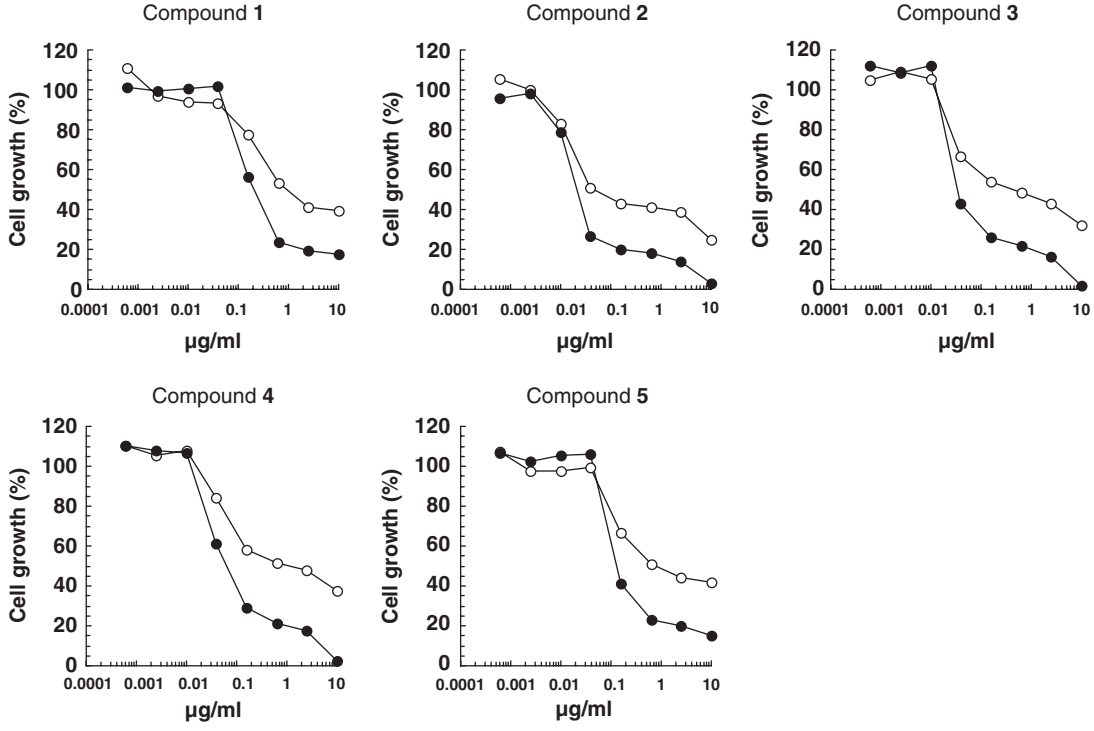

Figure 4 Effects of **1**–**5** on coculture of DU-145 cells and PrSC. The growth of DU-145 cells cocultured with PrSC (●) or that of DU-145 cells alone (○) in the presence of the indicated concentrations of **1**–**5** was determined using rhodanile blue method. Values are means of duplicate determinations. Each s.e. is less than 10%.

spectrum revealed the following fragment: -CH(CH_3)-CH_2-CH(CH_3)-CH=CH_2. In the HMBC spectrum, a methyl proton (δ 1.33) connecting to C-2′ methine correlated to a carbonyl carbon (C-1′, δ 211.3). Therefore, the total structure of **5** was found to be a new family of atpenin (Figure 1).

Biological activities

The effects of **1–5** on coculture of human prostate cancer DU-145 cells with PrSC were determined using rhodanile blue staining method.[5] In the coculture, the growth of DU-145 cells is increased by PrSC.[3,5] As shown in Figure 4, all compounds showed selective growth inhibitory activities and inhibited the growth of DU-145 cells in coculture with PrSC more strongly than that of DU-145 cells alone. The IC_{50} values of **1–5** against the growth of DU-145 cells in coculture were 0.21, 0.021, 0.034, 0.064 and 0.13 μg ml^{-1}, respectively, whereas those of **1–5** against the growth of DU-145 cells alone were 0.85, 0.048, 0.54, 0.95 and 0.71 μg ml^{-1}, respectively. All compounds did not show apparent cytotoxicity against stromal cells under microscopic observation (data not shown).

DISCUSSION

In this study, we have also obtained three structurally related compounds in addition to **1–5**. The HR-ESI-MS spectra revealed that the molecular formulae of these compounds were $C_{15}H_{22}NO_6Cl$, $C_{15}H_{23}NO_6$ and $C_{15}H_{20}NO_5Cl_3$, respectively. Among them, a compound having the molecular formula of $C_{15}H_{20}NO_5Cl_3$ may be identical to reported WF-16775 A2,[8] but we could not elucidate the structures of additional three compounds further due to their trace amounts. Ōmura *et al.*[6] reported that there were atpenins A1, A2 and A3 along with A4, A5 and B, but they did not obtain A1, A2 and A3 in pure form and did not show any structural information. We cannot exclude the possibility that **4** and **5** would be identical to one of them. However, we have actually presented here two new structures of atpenins.

Atpenins A4, A5 and B were originally isolated as antifungal antibiotics.[6,7] Thereafter, atpenin B was found to decrease the cellular adenosine 5′-triphosphate.[9] Furthermore, it is reported that atpenins specifically inhibit mitochondrial complex II (succinate–ubiquinone oxidoreductase).[10] Mitochondria is now considered as a rational target for cancer therapy.[11] Although there is a possibility that atpenins modulate tumor–stromal cell interactions by inhibiting mitochondrial functions, the elucidation of the precise mechanism of action needs to be studied further. We are now studying the effects of atpenins on tumor growth *in vivo* using mouse xenograft models.

ACKNOWLEDGEMENTS

We thank Dr R Sawa (Microbial Chemistry Research Center) for analysis of HR-ESI-MS spectra, and Ms K Adachi and Ms E Satoh for their technical assistance. This work was supported in part by a grant-in-aid from the Ministry of Education, Culture, Sports, Science and Technology of Japan.

1 Grossfeld, G. D., Hayward, S. W., Tlsty, T. D. & Cunha, G. R. The role of stroma in prostatic carcinogenesis. *Endocr. Relat. Cancer* **5,** 253–270 (1998).
2 Tuxhorn, J. A., Ayala, G. E. & Rowley, D. R. Reactive stroma in prostate cancer progression. *J. Urol.* **166,** 2472–2483 (2001).
3 Kawada, M., Inoue, H., Masuda, T. & Ikeda, D. Insulin-like growth factor I secreted from prostate stromal cells mediates tumor–stromal cell interactions of prostate cancer. *Cancer Res.* **66,** 4419–4425 (2006).
4 Kawada, M., Inoue, H., Arakawa, M. & Ikeda, D. Transforming growth factor-β1 modulates tumor–stromal cell interactions of prostate cancer through insulin-like growth factor-I. *Anticancer Res.* **28,** 721–730 (2008).
5 Kawada, M. *et al.* A microplate assay for selective measurement of growth of epithelial tumor cells in direct coculture with stromal cells. *Anticancer Res.* **24,** 1561–1568 (2004).
6 Ōmura, S. *et al.* Atpenins, new antifungal antibiotics produced by *Penicillium* sp. Production, isolation, physico-chemical and biological properties. *J. Antibiot.* **41,** 1769–1773 (1988).
7 Kumagai, H., Nishida, H., Imamura, N., Tomoda, H. & Ōmura, S. Structures of atpenins A4, A5 and B, new antifungal antibiotics produced by *Penicillium* sp. *J. Antibiot.* **43,** 1553–1558 (1990).
8 Otsuka, T., Takase, S., Terano, H. & Okuhara, M. New angiogenesis inhibitors, WF-16755A1 and A2. *J. Antibiot.* **45,** 1970–1973 (1992).
9 Oshino, K., Kumagai, H., Tomoda, H. & Ōmura, S. Mechanism of action of atpenin B on Raji cells. *J. Antibiot.* **43,** 1064–1068 (1990).
10 Miyadera, H. *et al.* Atpenins, potent and specific inhibitors of mitochondrial complex II (succinate–ubiquinone oxidoreductase). *Proc. Natl Acad. Sci. USA* **100,** 473–477 (2003).
11 Kim, J. & Dang, C. Cancer's molecular sweet tooth and the Warburg effect. *Cancer Res.* **66,** 8927–8930 (2006).

The Journal of Antibiotics (2009) 62, 251–257
© 2009 Japan Antibiotics Research Association All rights reserved 0021-8820/09 $32.00
www.nature.com/ja

ORIGINAL ARTICLE

Role of the AraC–XylS family regulator YdeO in multi-drug resistance of *Escherichia coli*

Kunihiko Nishino[1,3], Yasuko Senda[2,4], Mitsuko Hayashi-Nishino[2] and Akihito Yamaguchi[2,4]

Multi-drug efflux pumps contribute to the resistance of *Escherichia coli* to many antibiotics and biocides. In this study, we report that the AraC–XylS family regulator YdeO increases the multi-drug resistance of *E. coli* through activation of the MdtEF efflux pump. Screening of random fragments of genomic DNA for their ability to increase β-lactam resistance led to the isolation of a plasmid containing *ydeO*, which codes for the regulator of acid resistance. When overexpressed, *ydeO* significantly increased the resistance of the *E. coli* strain to oxacillin, cloxacillin, nafcillin, erythromycin, rhodamine 6G and sodium dodecyl sulfate. The increase in drug resistance caused by *ydeO* overexpression was completely suppressed by deleting the multifunctional outer membrane channel gene *tolC*. TolC interacts with different drug efflux pumps. Quantitative real-time PCR showed that YdeO activated only *mdtEF* expression and none of the other drug efflux pumps in *E. coli*. Deletion of *mdtEF* completely suppressed the YdeO-mediated multi-drug resistance. YdeO enhances the MdtEF-dependent drug efflux activity in *E. coli*. Our results indicate that the YdeO regulator, in addition to its role in acid resistance, increases the multi-drug resistance of *E. coli* by activating the MdtEF multi-drug efflux pump.
The Journal of Antibiotics (2009) **62,** 251–257; doi:10.1038/ja.2009.23; published online 27 March 2009

Keywords: drug efflux pump; *Escherichia coli*; MdtEF; multidrug resistance; YdeO

INTRODUCTION

Multi-drug efflux pumps cause serious problems in cancer chemotherapy and in the treatment of bacterial infections. Bacterial drug resistance is often associated with multi-drug efflux pumps that decrease drug accumulation in the cell.[1,2] Bacterial multi-drug efflux pumps are classified into five families on the basis of sequence similarity: major facilitator, resistance-nodulation-cell division (RND), small multi-drug resistance, multidrug and toxic compound extrusion, and ATP-binding cassette.[3–5] Of these, RND family efflux pumps play major roles in both intrinsic and elevated resistance of Gram-negative bacteria to a wide range of compounds, including β-lactams.[1,6–12] RND efflux pumps require two other proteins to function: a membrane fusion protein and an outer membrane protein. Many drug efflux pumps in *Escherichia coli* need TolC to function.[12–15] TolC is responsible for resistance to various antibiotics, including β-lactams,[12] quinolones[16] and macrolides.[17] Bacterial genome sequencing enables us to trace drug-resistance genes.[18–20] There are many putative and proven drug efflux pumps in the *E. coli* genome, and we have identified earlier 20 functional drug efflux pumps.[9,20] As many such efflux pumps have overlapping substrate spectra,[9] it is intriguing that bacteria, with their economically organized genomes, harbor such large sets of multi-drug efflux genes.

The key to understanding how bacteria utilize these multiple efflux pumps lies in the regulation of pump expression. The currently available data show that multi-drug efflux pumps are often expressed under precise and elaborate transcriptional control.[21–24] Expression of *acrAB*, which encodes the major AcrAB efflux pump, is subject to multiple levels of regulation. In *E. coli*, it is modulated locally by the repressor AcrR[25] and AcrS.[26] At a more global level, it is modulated by stress conditions and by global regulators, such as MarA, SoxS and Rob.[27,28] These examples illustrate the complexity and diversity of the mechanisms regulating bacterial multi-drug efflux pumps.

Stomach acid ($pH \leqslant 2$) kills most bacteria;[29] however, *E. coli* survives this acidity.[30,31] The acid resistance appears to contribute to the low infectious dose of pathogenic *E. coli*, and aids in the gastric passage of commensal strains.[32,33] One of the most efficient acid resistance systems in *E. coli*, the Gad system, is based on the coordinated action of two isoforms of glutamate decarboxylase (GadA and GadB) and of a specific glutamate/γ-aminobutyrate (GABA) antiporter (GadC).[34,35] The *gadA/BC* genes, activated in response to acid stress, are subject to complex circuits of regulation involving the AraC–XylS family regulator YdeO.[36] In this study, we demonstrate that YdeO contributes to the multi-drug resistance as well as the acid resistance of *E. coli*. The results suggest a role of YdeO in the multi-drug resistance of *E. coli*.

[1]Laboratory of Microbiology and Infectious Diseases, Division of Special Projects, Institute of Scientific and Industrial Research, Osaka University, Osaka, Japan; [2]Department of Cell Membrane Biology, Institute of Scientific and Industrial Research, Osaka University, Osaka, Japan; [3]PRESTO, Japan Science and Technology Agency, Tokyo, Japan and [4]Laboratory of Cell Biology, Graduate School of Pharmaceutical Sciences, Osaka University, Osaka, Japan
Correspondence: Dr K Nishino, Laboratory of Microbiology and Infectious Diseases, Division of Special Projects, Institute of Scientific and Industrial Research, Osaka University, 8-1 Mihogaoka, Ibaraki, Osaka 567-0047, Japan.
E-mail: nishino@sanken.osaka-u.ac.jp
This study was supported by the 19th Yasushi Ueda Prize, which was awarded to K.N. in 2008. This paper is dedicated to the memory of Professor Yasushi Ueda.
Received 10 December 2008; revised 4 February 2009; accepted 24 February 2009; published online 27 March 2009

MATERIALS AND METHODS

Bacterial strains, plasmids and growth conditions

The bacterial strains and plasmids used in this study are listed in Table 1. The *E. coli* strains were derived from the wild-type strain MG1655.[37] Phage P1-mediated transductions were performed as described earlier.[38] Bacterial strains were grown at 37 °C in Luria–Bertani (LB) broth.[39] Cells were collected for total RNA extraction when the cultures reached an optical density of 0.6 at 600 nm.

Screening for positive regulators of multi-drug resistance

DNA manipulation generally followed standard practice.[39] A genomic library was developed by partial *Sau*3AI digestion of the chromosomal DNA as follows. Chromosomal DNA prepared from an overnight culture of the wild-type strain MG1655[37] was digested with *Sau*3AI (1 U μl^{-1}) for 15, 20, 30 and 40 min. The digested DNA was separated on a 0.8% agarose gel, and fragments approximately 0.5–3 kb in size were purified and ligated into the *Bam*HI site of vector pHSG398 (Takara Bio Inc., Otsu, Japan). The ligation products were transformed into *E. coli* DH5α[39] to select chloramphenicol-resistant transformants. Plasmid DNA was prepared from a pool of 16,000 transformants and used to transform the *acrB* deletion strain NKE96. Cells were plated on LB agar medium[39] containing 15 $\mu g\,ml^{-1}$ chloramphenicol and inhibitory concentrations of various drugs.

Plasmid construction

The *ydeO* gene was amplified from MG1655 genomic DNA using the primers *ydeO*-F_*Bam*HI and *ydeO*-R_*Sal*I listed in Table 2, which introduced *Bam*HI and *Sal*I sites at the ends of the amplified fragment. This PCR product was cloned between the *Bam*HI and *Sal*I sites of the vector pHSG398 (Takara Bio Inc.) to produce the plasmid p*ydeO*.

Construction of gene deletion mutants

Gene deletion was performed according to the method of Datsenko and Wanner, with recombination between short homologous DNA regions catalyzed by phage λ Red recombinase.[40] A curable expression plasmid encoding Red recombinase (pKD46) was introduced into the MG1655 strain. The chloramphenicol resistance gene *cat* or the kanamycin resistance gene *kan*, flanked by Flp recognition target sites, was amplified by PCR using the primers listed in Table 2. The plasmid pKD3 or pKD4 was used as a template. This PCR product was used to transform the MG1655 strain expressing Red recombinase, and recombinant clones were isolated as chloramphenicol- or kanamycin-resistant colonies. The pKD46 vector was eliminated by incubating at a non-permissive temperature (37 °C), as confirmed by the loss of ampicillin resistance. The chromosomal structure of the mutated loci was verified by PCR, as described earlier,[40] and by Southern hybridization using probes specific for (i) the antibiotic resistance genes used during the construction of chromosomal deletions and (ii) sequences flanking the inactivated loci. The deletions were then transferred to the wild-type MG1655 strain by P1 transduction. The *cat* and *kan* genes were eliminated using the plasmid pCP20, as described earlier.[40]

Determination of the MICs for toxic compounds

The antibacterial activities of different agents were determined on Luria agar (1% tryptone, 0.5% yeast extract and 0.5% NaCl) plates containing various concentrations of the compounds (Sigma-Aldrich, St Louis, MO, USA) listed in Table 3. The agar plates were prepared by the two-fold agar dilution technique, as described earlier.[41] The MIC was defined as the lowest concentration of a compound that inhibited cell growth. To determine the MICs, bacteria were grown in LB broth at 37 °C overnight and diluted in the same medium. Then, the organisms were tested at a final inoculum size of 10^4 cfu μl^{-1} using a multipoint inoculator (Sakuma Seisakusyo, Tokyo, Japan), and were incubated at 37 °C for 20 h.

RNA extraction

Total RNA was isolated from bacterial cultures using the RNeasy Protect Bacteria Mini Kit (Qiagen, Hilden, Germany) and RNase-Free DNase (Qiagen), as described earlier.[42] The total RNA was isolated from exponential-phase cultures of *ΔacrB*/vector (NKE154) and *ΔacrB*/p*ydeO* (NKE169). The absence of genomic DNA from the DNase-treated RNA samples was confirmed by both non-denaturing agarose electrophoresis gels and PCR with primers against target genomic DNA. The RNA concentration was then determined spectrophotometrically.[39]

Determination of specific transcript levels by quantitative real-time PCR following reverse transcription (RT)

Bulk cDNA samples were synthesized from total RNA using TaqMan Reverse Transcription Reagents (Applied Biosystems, Carlsbad, CA, USA) and random hexamers, as described earlier.[43,44] The specific primer pairs listed in Table 2 were designed using ABI PRISM Primer Express software (Applied Biosystems). *rrsA* of 16S rRNA was chosen as the normalizing gene.[45] Real-time PCR was

Table 1 *E. coli* strains and plasmids used in this study

Strains or plasmids	*Original names*	*Characteristics*	*Sources or references*
Strains as in text			
WT	MG1655	Wild type	37
Δ*acrB*	NKE 96	Δ*acrB*	Present study
Δ*acrB*/vector	NKE 154	Δ*acrB*/pHSG398	Present study
Δ*acrB*/p*ydeO*	NKE 169	Δ*acrB*/p*ydeO*	Present study
Δ*acrB tolC*	NKE 128	Δ*acrB* Δ*tolC*	Present study
Δ*acrB tolC*/vector	NKE 160	Δ*acrB* Δ*tolC*/pHSG398	Present study
Δ*acrB tolC*/p*ydeO*	NKE 174	Δ*acrB* Δ*tolC*/p*ydeO*	Present study
Δ*acrB mdtEF*	NKE 139	Δ*acrB* Δ*mdtEF*::Km^R	Present study
Δ*acrB mdtEF*/vector	NKE 176	Δ*acrB* Δ*mdtEF*::Km^R/pHSG398	Present study
Δ*acrB mdtEF*/p*ydeO*	NKE 180	Δ*acrB* Δ*mdtEF*::Km^R/p*ydeO*	Present study
Plasmids			
pKD46		Red recombinase expression plasmid, Ap^R	40
pKD3		$rep_{R6K\gamma[ori]}Ap^RFRT\ Cm^RFRT$	40
pKD4		$rep_{R6K\gamma[ori]}Ap^RFRT\ Km^RFRT$	40
pCP20		$rep_{pSC101}{}^{ts}\ Ap^R\ Cm^R$ *cI857*λP_R*flp*	40
pHSG398		$rep_{pMB1}\ Cm^R$	Takara Bio Inc.
p*ydeO*		*ydeO* gene cloned into pHSG398, Cm^R	Present study

Table 2 Primers used in the present study

Primers	*Sequences (5′–3′)*
For gene deletion	
tolC-P1	ACTGGTGCCGGGCTATCAGGCGCATAACCATCAGCAATAGGTGTAGGCTGGAGCTGCTTC
tolC-P2	TTACAGTTTGATCGCGCTAAATACTGCTTCACCACAAGGACATATGAATATCCTCCTTAG
acrB-P1	AAAAAGGCCGCTTACGCGGCCTTAGTGATTACACGTTGTAGTGTAGGCTGGAGCTGCTTC
acrB-P2	GAACAGTCCAAGTCTTAACTTAAACAGGAGCCGTTAAGACCATATGAATATCCTCCTTAG
mdtE-P1	TTAAAGAACCGTTATTTCTCAAGAATTTTCAGGGACTAAAGTGTAGGCTGGAGCTGCTTC
mdtF-P2	AGGCTGAACCTTCATGTTCAACCTTACTCTCATTTACACGCATATGAATATCCTCCTTAG
For gene cloning	
ydeO-F_BamHI	CGCGGATCCAAACAAACAGCAAATTATAAA
ydeO-R_SalI	CGCGTCGACTTTCAATAAATATATCGCCTA
For quantitative PCR	
rrsA-F	CGGTGGAGCATGTGGTTTAA
rrsA-R	GAAAACTTCCGTGGATGTCAAGA
acrA-F	GTCTATCACCCTACGCGCTATCTT
acrA-R	GCGCGCACGAACATACC
acrD-F	GTACCCTGGCGATTTTTTCATT
acrD-R	CGGTCACTCGCACATTCG
acrE-F	CGTGATTGCCGCAAAAGC
acrE-R	TTGGCGCAGTGACTTTGGTA
bcr-F	TGTTTTTCTGTTCGTGATGACCAT
bcr-R	GGAACATATTTAACGCGCCAAT
cusB-F	CGCTTACCGTGGGCGATA
cusB-R	TTCCACCCAGTCAGGAATGG
emrA-F	GCGAATATTGAGGTGCAGAAAA
emrA-R	GGCACACGGCGGTTGTA
emrD-F	GTGGATCCCCGACTGGTTT
emrD-R	CCCGGCACCGAAAAAGA
emrE-F	GGTATTGTCCTGATTAGCTTACTGTCAT
emrE-R	GCACAAATCAACATCATGCCTATAA
emrK-F	GCGCTTAAACGTACGGATATTAAGA
emrK-R	ACTGTTTCGCCGACCTGAAC
fsr-F	TGGTGTTGGCGCAAATCA
fsr-R	TCGTCGCTTTGGGTTTTCC
macA-F	CGGTGATTGCCGCACAA
macA-R	TTACCAGCATGGCGCTCAT
mdfA-F	CTTGCTGTTAGCGCGTCTGA
mdfA-R	GCCAGCCGCCCATAATAAT
mdtA-F	CGCCGTAGAACAGGCAGTTC
mdtA-R	TGCGCACCGTAACGGTATTA
mdtE-F	CCCCCGGTTCGGTCAA
mdtE-R	GGACGTATCTCGGCAACTTCAT
mdtF-F	TTACCGTCAGCGCTACCTATCC
mdtF-R	GCCATCAAGCCCATTCATATTT
mdtG-F	CGGTATTGTCTTCAGCATTACATTTT
mdtG-R	GGCGAGTCCACCCCAAA
mdtH-F	TTTTCACCCTGATTTGTCTGTTTTAT
mdtH-R	CAGCGAAGCACTTAAGGTTTCA
mdtJ-F	TGATGAAAATTGCCGGGTTAA
mdtJ-R	CGCTTTACGGGTACCTGATTTTA
mdtK-F	CCGGTTATCGCGCAATTAAAT
mdtK-R	GAAACCTTGTCGCACCTGATG
mdtL-F	TATCCCGCCGGGATTGATAT
mdtL-R	CGCTTCGCTGGCATTGA
mdtM-F	CGTGATTTTAATGCCGATGTCA
mdtM-R	GCCATACCGCCAGCAAGAT
tolC-F	CCGGGATTTCTGACACCTCTT
tolC-R	TTTGTTCTGGCCCATATTGCT

Table 3 Susceptibility of *E. coli* strains to β-lactams and toxic compounds

	MIC (μg/ml)					
Strains	*OXA*	*MCIPC*	*NAF*	*ERM*	*R6G*	*SDS*
WT	256	>512	512	128	>512	>512
Δ*acrB*	0.5	1	2	4	2	64
Δ*acrB*/vector	0.5	1	2	4	2	64
Δ*acrB*/p*ydeO*	**16**	**64**	**32**	**64**	**256**	**>512**
Δ*acrB tolC*	0.5	0.25	1	2	2	16
Δ*acrB tolC*/vector	0.5	0.25	1	2	2	16
Δ*acrB tolC*/p*ydeO*	0.5	0.25	1	2	2	16
Δ*acrB mdtEF*	0.5	1	2	4	2	64
Δ*acrB mdtEF*/vector	0.5	1	2	4	2	64
Δ*acrB mdtEF*/p*ydeO*	0.5	1	2	4	2	64

Abbreviations: ERM, erythromycin; MCIPC, cloxacillin; NAF, nafcillin; OXA, oxacillin; R6G, rhodamine 6G; SDS, sodium dodecyl sulfate.
Values in bold face are larger than those of a corresponding parental strain haboring the pHSG398 vector. MIC determinations were repeated at least three times.

performed with each specific primer pair using SYBR Green PCR Master Mix (Applied Biosystems). The reactions were run on an ABI PRISM 7000 Sequence Detection System (Applied Biosystems); the fluorescence signal due to SYBR Green intercalation was monitored to quantify the double-stranded DNA product formed in each PCR cycle. The expression levels of drug efflux pump genes and *tolC* in *ΔacrB*/p*ydeO* (NKE169) were compared with those in *ΔacrB*/vector (NKE154).

Acid resistance assay

A single colony of an *E. coli* strain harboring plasmid was inoculated into 1 ml of LB broth containing chloramphenicol and grown overnight at 37 °C. The LB broth (20 ml) was inoculated with 0.1 ml of the overnight culture and grown at 37 °C. When the cultures reached a cell density of 2×10^8 cfu ml^{-1}, 50 μl of the culture was transferred to 2 ml of phosphate-buffered saline (PBS; pH 7.2) and to 2 ml of warmed LB broth (pH 2.5, adjusted with HCl). The cfu ml^{-1} in PBS was determined by plating serial dilutions in PBS buffer (pH 7.2) on LB agar and using these as initial cell populations. The LB broth (pH 2.5) inoculated with *E. coli* was incubated at 37 °C for 1 h, and the cfu ml^{-1} in the LB broth (pH 2.5) was determined as described above and used as the final cell population. The percentage acid survival was then calculated as the number of cfu ml^{-1} remaining after acid treatment divided by the initial cfu ml^{-1} at time zero. Each experiment was performed in triplicate. The percentage survival values were converted to logarithmic values ($\log_{10} x$, where x equals the percentage survival) for the calculation of geometric means and standard errors (s.e.).

Drug efflux assay

The drug efflux activities of *E. coli* cells were measured using cells preloaded with rhodamine 6G. The exponential cultures of *E. coli* cells were harvested and washed twice with 100 mM potassium phosphate buffer (pH 7.5) containing 5 mM $MgSO_4$. For maximal accumulation of the fluorophore, the cells (optical density of 1.0 at 600 nm) were incubated with 1 μM rhodamine 6G and 40 μM carbonyl cyanide *m*-chlorophenylhydrazone (CCCP) at 37 °C for 1 h. The cells were then centrifuged, resuspended in the same medium with the addition of 25 mM glucose as an energy source, and subjected to fluorescence measurement. The fluorescence of the compound was continuously monitored using a Hitachi model F-2000 fluorescence spectrophotometer (Hitachi High-Technologies Corp., Tokyo, Japan). Rhodamine 6G transport was measured with excitation at 529 nm and emission at 553 nm.

RESULTS

Overexpression of *ydeO* increases resistance to oxacillin

The expression of multi-drug efflux genes is often regulated in a complex manner, as described in the Introduction section. We therefore screened the genomic library of the *E. coli* for genes that increased multi-drug resistance levels in this organism. We screened a host strain lacking a functional *acrB* gene in order to identify regulatory elements involved in the expression of other multi-drug resistance systems. The library was developed from the chromosomal DNA of the MG1655 strain, and then, the recombinant plasmids were transformed into the Δ*acrB* strain NKE96 as described in the Materials and methods section. In one experiment, we found a 32-fold increase in oxacillin MIC against the transformant (data not shown). Introduction of the plasmid isolated from this strain into fresh Δ*acrB* cells resulted in the same oxacillin resistance phenotype: the MIC increased 32-fold over the recipient strain (data not shown).

Sequencing of the plasmid revealed an insertion containing the complete coding sequence of *ydeO* and a partial sequence of *yneN*. YdeO is the AraC–XylS family regulator that controls genes involved in acid resistance, such as glutamate decarboxylase genes (*gadA* and *gadB*) and a specific glutamate/GABA antiporter (*gadC*).[34,36] It seemed likely that overexpressed YdeO caused the transcriptional activation of genes involved in oxacillin resistance in the cells carrying this plasmid.

Full-length wild-type *ydeO* was cloned into the pHSG398 vector to obtain p*ydeO* (Table 1). Oxacillin MICs for NKE96 cells harboring p*ydeO* were 32 times higher (16 versus 0.5 μg ml^{-1}) than that for cells harboring the pHSG398 vector (Table 3), suggesting that the YdeO regulator produced by this plasmid conferred oxacillin resistance on *E. coli*. Further experiments were therefore carried out with p*ydeO*.

Overexpression of *ydeO* increases resistance to β-lactams, erythromycin, rhodamine 6G and sodium dodecyl sulfate (SDS)

Our results showed that overexpression of *ydeO* increased *E. coli* resistance to oxacillin, a β-lactam antibiotic. We therefore investigated the effect of *ydeO* overexpression on the susceptibility of *E. coli* to other β-lactams. p*ydeO* also increased the resistance of Δ*acrB* cells to cloxacillin and nafcillin (Table 3). Various other drugs were tested, including common substrates of multi-drug efflux pumps, and we found that p*ydeO* increased the resistance of the Δ*acrB* strain to erythromycin, rhodamine 6G and SDS (Table 3). These results indicate that the overproduced YdeO regulator induces the multi-drug resistance of *E. coli*.

Effect of *tolC* deletion on multi-drug resistance modulated by the YdeO regulator

The results described above indicate that the expression of a multi-drug efflux pump may be induced by overexpression of *ydeO*. In order to determine whether YdeO-mediated multi-drug resistance is attributable to TolC-dependent drug efflux pump(s), we investigated the effect of *tolC* deletion on drug resistance in cells overexpressing *ydeO*. Deletion of *tolC* from the Δ*acrB* strain increased susceptibility to many antimicrobial agents and chemical compounds, including cloxacillin, nafcillin, erythromycin and SDS (Table 3), which is in good agreement with earlier reports.[12] The *tolC* deletion completely inhibited YdeO-mediated multi-drug resistance (Table 3). This result indicates that YdeO-mediated multi-drug resistance is attributable to increased expression of a TolC-dependent drug efflux pump.

Determination of the amounts of drug exporter transcripts by quantitative real-time RT-PCR (qRT-PCR)

In order to determine which drug efflux pump shows increased expression when *ydeO* is overexpressed, we used qRT-PCR to investigate changes in the amounts of drug exporter gene mRNAs. The results are shown in Figure 1. The expression levels of *mdtE* and *mdtF*

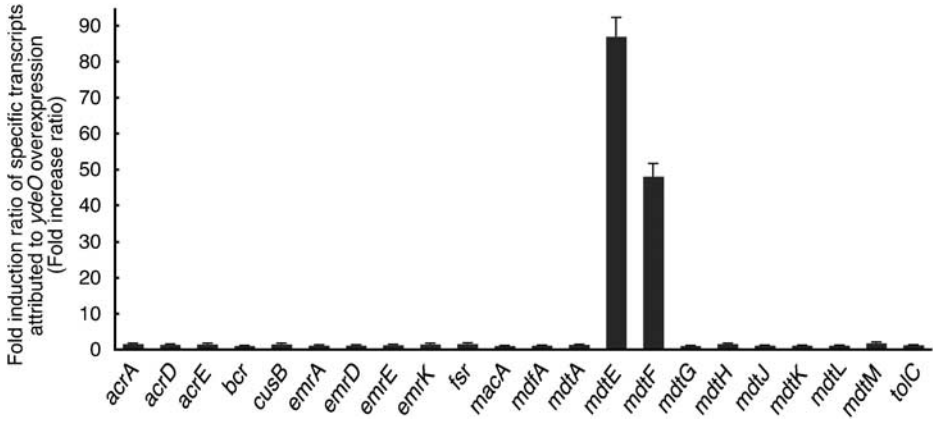

Figure 1 YdeO activates the expression of *mdtEF* multi-drug efflux genes. The amount of transcript was determined by quantitative real-time PCR as described in the Materials and methods section. The fold increase ratio was calculated by dividing the expression level of the gene in the Δ*acrB*/p*ydeO* strain by that in the Δ*acrB*/vector strain. Experiments were performed in triplicate and the data are represented as mean ± s.d.

were significantly increased (more than 10-fold in comparison with basal levels) by *ydeO* overexpression: 87- and 48-fold increases were observed for *mdtE* and *mdtF*, respectively. Overexpression of *ydeO* did not increase the expression of other drug exporter gene transcripts (Figure 1).

Effects of deletion of the MdtEF drug efflux pump on YdeO-mediated multi-drug resistance

To determine whether the multi-drug resistance mediated by *ydeO* overexpression is because of increased expression of *mdtEF*, we investigated the effects of deleting these genes on drug resistance levels in Δ*acrB*/vector and Δ*acrB*/p*ydeO* (Table 3). When *mdtEF* was deleted from the Δ*acrB* strain, there was no change in drug resistance in the resulting strains. In the Δ*mdtEF acrB* strain, overexpression of *ydeO* conferred no drug resistance (Table 3). Together, these data indicate that the multi-drug resistance conferred by the YdeO regulator is because of the increased expression of *mdtEF* multi-drug efflux genes.

Effects of YdeO and MdtEF on the acid resistance of *E. coli*

It was reported that YdeO activates the expression of genes involved in acid resistance.[36] In this study, we found that YdeO induces the expression of *mdtEF* multi-drug efflux genes. To test whether MdtEF contributes to acid resistance modulated by YdeO, we measured survival percentage of the wild-type strain and the Δ*mdtEF* mutant harboring vector (pHSG398) or p*ydeO* at pH 2.5 (Figure 2). Overexpression of *ydeO* enhances the acid resistance of both the wild-type strain and the Δ*mdtEF* mutant (Figure 2), indicating that the MdtEF multi-drug efflux pump is not essential for YdeO-induced acid resistance.

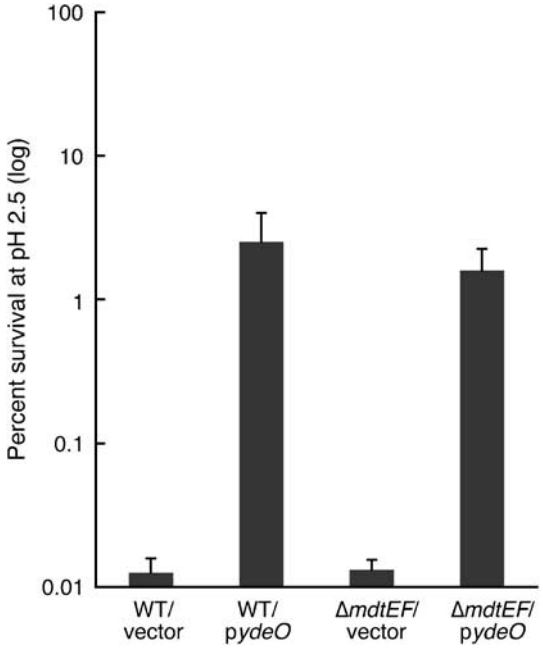

Figure 2 Effect of YdeO and MdtEF on acid resistance of *E. coli*. Acid resistance of the wild-type strain (WT) and the Δ*mdtEF* mutant harboring vector (pHSG398) or p*ydeO* were grown to mid-log phase in LB broth (pH 7.0). Cells were diluted 40-fold using LB broth (pH 2.5) and incubated for 1 h at 37 °C. Error bars represent standard errors of the mean values.

YdeO enhances the MdtEF-dependent drug efflux activity of *E. coli*

In this study, we found that YdeO activates the expression of *mdtEF* multi-drug efflux genes and drug resistance to *E. coli* cells. *E. coli* cells with a plasmid carrying the *ydeO* gene became resistant to rhodamine 6G, a toxic dye. This compound can be detected by its fluorescence. To determine whether the *ydeO*-induced drug resistance is because of efflux of this compound from the cells, we measured the efflux activity of rhodamine 6G from the cells. As shown in Figure 3, rapid efflux of rhodamine 6G from *E. coli* Δ*acrB*/p*ydeO* cells was observed as an increase in fluorescence. However, no significant efflux was observed from Δ*acrB* and Δ*acrB mdtEF*/p*ydeO* cells (Figure 3). These results indicate that the YdeO-induced multi-drug resistance is because of the enhanced drug efflux activity of *E. coli* cells, which is caused by the increased expression of *mdtEF*.

DISCUSSION

In this study, we performed a genome-wide search for a regulator of multi-drug resistance of *E. coli* by random shotgun cloning and discovered YdeO, which up-regulates *mdtEF* expression, thereby increasing the resistance to β-lactams, erythromycin, rhodamine 6G and SDS. We initially found that the plasmid carrying *ydeO* conferred oxacillin resistance on the Δ*acrB* strain. Then, we investigated the susceptibility of the *ydeO*-overexpressing Δ*acrB* strain to various drugs, including the common substrates of multi-drug efflux pumps, and found that YdeO stimulates *E. coli* resistance to oxacillin,

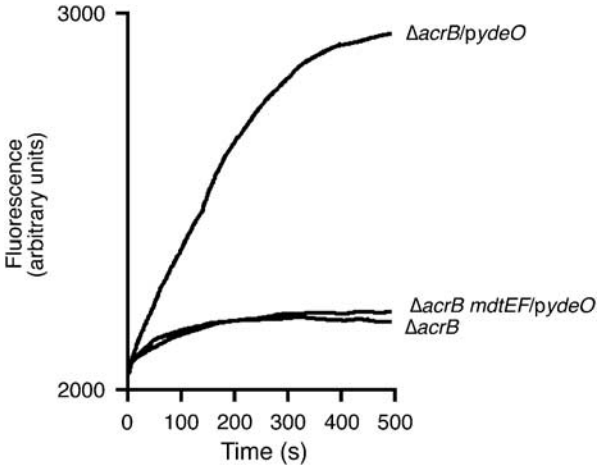

Figure 3 YdeO enhances MdtEF-dependent efflux activity in *E. coli*. Active efflux of rhodamine 6G from *E. coli* Δ*acrB* and Δ*acrB mdtEF* cells overproducing YdeO was measured as described in the Materials and methods section.

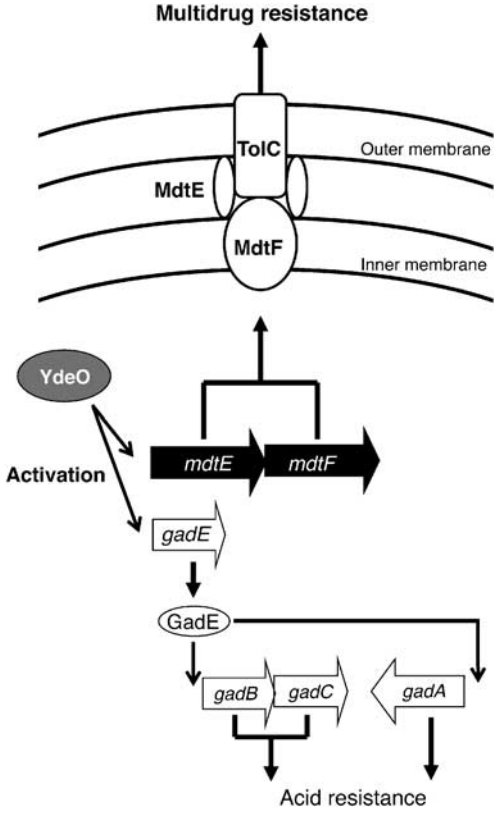

Figure 4 Model for YdeO control of multi-drug resistance and acid resistance. YdeO controls expression of *gadABCE* acid resistance genes and *mdtEF* multi-drug efflux pump genes. The results of this study show that overexpression of *ydeO* activates expression of *mdtEF* and confers multi-drug resistance on *E. coli*.

cloxacillin, nafcillin, erythromycin, rhodamine 6G and SDS (Table 3). We discovered the importance of YdeO as a drug resistance factor through induction of the multi-drug efflux gene. Earlier, we reported that the MdtEF multi-drug efflux pump requires TolC to function.[12] YdeO-mediated multi-drug resistance was completely suppressed by deleting the *tolC* or *mdtEF* gene (Table 3). Although nothing is known of the potential YdeO-binding consensus sequence, it was reported that YdeO has an ability to bind the intergenic region between *hdeD* and *gadE*, located upstream of *mdtEF*.[36] The *gadE* and *mdtEF* genes are located in tandem and they might be co-transcribed. These facts suggest that the up-regulation of *mdtEF* expression might have occurred by the YdeO-binding to the upstream region of *gadE*.

An important feature of *E. coli* pathogenesis is the organism's ability to withstand extremely acidic environments (pH 2 or lower). This acid resistance contributes to the low infectious dose of pathogenic *E. coli* species. One very efficient *E. coli* acid resistance system encompasses two isoforms of glutamate decarboxylase (*gadA* and *gadB*) and a putative glutamate/GABA antiporter (*gadC*).[34,35] It is subject to complex controls that vary with growth medium, growth phase and growth pH. Earlier work has revealed that this system is also controlled by YdeO (Figure 4).[36] The YdeO protein is involved in transcriptional activation of the *gadE* gene coding for a protein that regulates *gadABC* (Figure 4).[36,46] YdeO belongs to the AraC–XylS family of bacterial transcriptional regulators known to activate acid resistance[36,47,48] and repress virulence.[49] We investigated the contribution of the MdtEF multi-drug efflux pump in YdeO-induced acid resistance, but MdtEF is not essential for acid resistance of *E. coli*.

In addition to the roles of YdeO in acid resistance, we found that it contributes to the multi-drug resistance of *E. coli* by activating the MdtEF multi-drug efflux pump (Figure 4). The present evidence suggests that it may enhance the resistance of *E. coli* to low pH and multiple drugs in hostile environments. Further investigation of the regulation of multi-drug efflux systems in several natural environments, such as inside hosts, is required to elucidate the biological significance of their regulatory networks. Such investigations may provide further insights into the role of multi-drug efflux systems in the physiology of the cell.

ACKNOWLEDGEMENTS

We thank Barry L Wanner for providing the strains and plasmids. This research was supported by a research aid from the Japan Antibiotics Research Association (KN); the Nakajima Foundation (KN); the Kao Foundation for Arts and Sciences (KN); the Program for Promotion of Fundamental Studies in Health Sciences of the National Institute of Biomedical Innovation (AY and KN); a grant from the Ministry of Education, Culture, Sports, Science and Technology of Japan (KN); a Grant-in-Aid for Young Scientists (S) from the Japan Society for the Promotion of Science (KN); and PRESTO (KN), Japan Science and Technology Agency, Japan.

1 Nikaido, H. Multidrug efflux pumps of gram-negative bacteria. *J. Bacteriol.* **178,** 5853–5859 (1996).
2 Zgurskaya, H. I. & Nikaido, H. Multidrug resistance mechanisms: drug efflux across two membranes. *Mol. Microbiol.* **37,** 219–225 (2000).
3 Putman, M., van Veen, H. W. & Konings, W. N. Molecular properties of bacterial multidrug transporters. *Microbiol. Mol. Biol. Rev.* **64,** 672–693 (2000).
4 Brown, M. H., Paulsen, I. T. & Skurray, R. A. The multidrug efflux protein NorM is a prototype of a new family of transporters. *Mol. Microbiol.* **31,** 394–395 (1999).
5 Paulsen, I. T., Chen, J., Nelson, K. E. & Saier, M. H. Comparative genomics of microbial drug efflux systems. *J. Mol. Microbiol. Biotechnol.* **3,** 145–150 (2001).
6 Murakami, S., Nakashima, R., Yamashita, E. & Yamaguchi, A. Crystal structure of bacterial multidrug efflux transporter AcrB. *Nature* **419,** 587–593 (2002).
7 Yu, E. W., Aires, J. R. & Nikaido, H. AcrB multidrug efflux pump of *Escherichia coli*: composite substrate-binding cavity of exceptional flexibility generates its extremely wide substrate specificity. *J. Bacteriol.* **185,** 5657–5664 (2003).
8 Murakami, S., Nakashima, R., Yamashita, E., Matsumoto, T. & Yamaguchi, A. Crystal structures of a multidrug transporter reveal a functionally rotating mechanism. *Nature.* **443,** 173–179 (2006).
9 Nishino, K. & Yamaguchi, A. Analysis of a complete library of putative drug transporter genes in *Escherichia coli*. *J. Bacteriol.* **183,** 5803–5812 (2001).

10 Ma, D., Cook, D. N., Hearst, J. E. & Nikaido, H. Efflux pumps and drug resistance in gram-negative bacteria. *Trends Microbiol.* **2,** 489–493 (1994).
11 Nikaido, H. Prevention of drug access to bacterial targets: permeability barriers and active efflux. *Science.* **264,** 382–388 (1994).
12 Nishino, K., Yamada, J., Hirakawa, H., Hirata, T. & Yamaguchi, A. Roles of TolC-dependent multidrug transporters of *Escherichia coli* in resistance to β-lactams. *Antimicrob. Agents Chemother.* **47,** 3030–3033 (2003).
13 Elkins, C. A. & Nikaido, H. Substrate specificity of the RND-type multidrug efflux pumps AcrB and AcrD of *Escherichia coli* is determined predominantly by two large periplasmic loops. *J. Bacteriol.* **184,** 6490–6498 (2002).
14 Fralick, J. A. Evidence that TolC is required for functioning of the Mar/AcrAB efflux pump of *Escherichia coli*. *J. Bacteriol.* **178,** 5803–5805 (1996).
15 Nishino, K. & Yamaguchi, A. EvgA of the two-component signal transduction system modulates production of the *yhiUV* multidrug transporter in *Escherichia coli*. *J. Bacteriol.* **184,** 2319–2323 (2002).
16 Baucheron, S. *et al.* AcrAB-TolC directs efflux-mediated multidrug resistance in *Salmonella enterica* serovar Typhimurium DT104. *Antimicrob. Agents Chemother.* **48,** 3729–3735 (2004).
17 Moore, S. D. & Sauer, R. T. Revisiting the mechanism of macrolide-antibiotic resistance mediated by ribosomal protein L22. *Proc. Natl Acad. Sci. USA* **105,** 18261–18266 (2008).
18 Paulsen, I. T., Sliwinski, M. K. & Saier, M. H. Microbial genome analyses: global comparisons of transport capabilities based on phylogenies, bioenergetics and substrate specificities. *J. Mol. Biol.* **277,** 573–592 (1998).
19 Paulsen, I. T., Nguyen, L., Sliwinski, M. K., Rabus, R. & Saier, M. H. Microbial genome analyses: comparative transport capabilities in eighteen prokaryotes. *J. Mol. Biol.* **301,** 75–100 (2000).
20 Nishino, K. Bacterial multidrug exporters: insights into acquisition of multidrug resistance. *Science* (online): [http://www.sciencemag.org/feature/data/prizes/ge/2004/nishino.dtl] (2005).
21 Ahmed, M., Borsch, C. M., Taylor, S. S., Vazquez-Laslop, N. & Neyfakh, A. A. A protein that activates expression of a multidrug efflux transporter upon binding the transporter substrates. *J. Biol. Chem.* **269,** 28506–28513 (1994).
22 Brooun, A., Tomashek, J. J. & Lewis, K. Purification and ligand binding of EmrR, a regulator of a multidrug transporter. *J. Bacteriol.* **181,** 5131–5133 (1999).
23 Lomovskaya, O., Lewis, K. & Matin, A. EmrR is a negative regulator of the *Escherichia coli* multidrug resistance pump EmrAB. *J. Bacteriol.* **177,** 2328–2334 (1995).
24 Grkovic, S., Brown, M. H. & Skurray, R. A. Regulation of bacterial drug export systems. *Microbiol. Mol. Biol. Rev.* **66,** 671–701 (2002).
25 Ma, D., Alberti, M., Lynch, C., Nikaido, H. & Hearst, J. E. The local repressor AcrR plays a modulating role in the regulation of *acrAB* genes of *Escherichia coli* by global stress signals. *Mol. Microbiol.* **19,** 101–112 (1996).
26 Hirakawa, H. *et al.* AcrS/EnvR represses expression of the *acrAB* multidrug efflux genes in *Escherichia coli*. *J. Bacteriol.* **190,** 6276–6279 (2008).
27 Randall, L. P. & Woodward, M. J. The multiple antibiotic resistance (*mar*) locus and its significance. *Res. Vet. Sci.* **72,** 87–93 (2002).
28 Rosenberg, E. Y., Bertenthal, D., Nilles, M. L., Bertrand, K. P. & Nikaido, H. Bile salts and fatty acids induce the expression of *Escherichia coli* AcrAB multidrug efflux pump through their interaction with Rob regulatory protein. *Mol. Microbiol.* **48,** 1609–1619 (2003).
29 Smith, J. L. The role of gastric acid in preventing foodborne disease and how bacteria overcome acid conditions. *J. Food Prot.* **66,** 1292–1303 (2003).
30 Gorden, J. & Small, P. L. Acid resistance in enteric bacteria. *Infect. Immun.* **61,** 364–367 (1993).
31 Lin, J. *et al.* Mechanisms of acid resistance in enterohemorrhagic *Escherichia coli*. *Appl. Environ. Microbiol.* **62,** 3094–3100 (1996).
32 Giannella, R. A., Broitman, S. A. & Zamcheck, N. Influence of gastric acidity on bacterial and parasitic enteric infections. A perspective. *Ann. Intern. Med.* **78,** 271–276 (1973).
33 Price, S. B., Wright, J. C., DeGraves, F. J., Castanie-Cornet, M. P. & Foster, J. W. Acid resistance systems required for survival of *Escherichia coli* O157:H7 in the bovine gastrointestinal tract and in apple cider are different. *Appl. Environ. Microbiol.* **70,** 4792–4799 (2004).
34 Castanie-Cornet, M. P., Penfound, T. A., Smith, D., Elliott, J. F. & Foster, J. W. Control of acid resistance in *Escherichia coli*. *J. Bacteriol.* **181,** 3525–3535 (1999).
35 De Biase, D., Tramonti, A., Bossa, F. & Visca, P. The response to stationary-phase stress conditions in *Escherichia coli*: role and regulation of the glutamic acid decarboxylase system. *Mol. Microbiol.* **32,** 1198–1211 (1999).
36 Ma, Z., Masuda, N. & Foster, J. W. Characterization of EvgAS-YdeO-GadE branched regulatory circuit governing glutamate-dependent acid resistance in *Escherichia coli*. *J. Bacteriol.* **186,** 7378–7389 (2004).
37 Blattner, F. R. *et al.* The complete genome sequence of *Escherichia coli* K-12. *Science* **277,** 1453–1474 (1997).
38 Davis, R. W., Bolstein, D. & Roth, J. R. *Advanced Bacterial Genetics*, Cold Spring Harbor Laboratory Press: Cold Spring Harbor, NY, (1980).
39 Sambrook, J., Fritsch, E. F. & Maniatis, T. *Molecular Cloning: A Laboratory Manual*, 2nd edn.Cold Spring Harbor Laboratory: Cold Spring Harbor, NY, (1989).
40 Datsenko, K. A. & Wanner, B. L. One-step inactivation of chromosomal genes in *Escherichia coli* K-12 using PCR products. *Proc. Natl Acad. Sci. USA* **97,** 6640–6645 (2000).
41 Nishino, K. & Yamaguchi, A. Role of histone-like protein H-NS in multidrug resistance of *Escherichia coli*. *J. Bacteriol.* **186,** 1423–1429 (2004).
42 Nishino, K., Honda, T. & Yamaguchi, A. Genome-wide analyses of *Escherichia coli* gene expression responsive to the BaeSR two-component regulatory system. *J. Bacteriol.* **187,** 1763–1772 (2005).
43 Nishino, K. & Yamaguchi, A. Overexpression of the response regulator *evgA* of the two-component signal transduction system modulates multidrug resistance conferred by multidrug resistance transporters. *J. Bacteriol.* **183,** 1455–1458 (2001).
44 Nishino, K., Inazumi, Y. & Yamaguchi, A. Global analysis of genes regulated by EvgA of the two-component regulatory system in *Escherichia coli*. *J. Bacteriol.* **185,** 2667–2672 (2003).
45 Nishino, K., Latifi, T. & Groisman, E. A. Virulence and drug resistance roles of multidrug efflux systems of *Salmonella enterica* serovar Typhimurium. *Mol. Microbiol.* **59,** 126–141 (2006).
46 Ma, Z. *et al.* GadE (YhiE) activates glutamate decarboxylase-dependent acid resistance in Escherichia coli K-12. *Mol. Microbiol.* **49,** 1309–1320 (2003).
47 Gallegos, M. T., Schleif, R., Bairoch, A., Hofmann, K. & Ramos, J. L. Arac/XylS family of transcriptional regulators. *Microbiol. Mol. Biol. Rev.* **61,** 393–410 (1997).
48 Martin, R. G. & Rosner, J. L. The AraC transcriptional activators. *Curr. Opin. Microbiol.* **4,** 132–137 (2001).
49 Nadler, C., Shifrin, Y., Nov, S., Kobi, S. & Rosenshine, I. Characterization of enteropathogenic *Escherichia coli* mutants that fail to disrupt host cell spreading and attachment to substratum. *Infect. Immun.* **74,** 839–849 (2006).

The Journal of Antibiotics (2009) 62, 259–263
© 2009 Japan Antibiotics Research Association All rights reserved 0021-8820/09 $32.00
www.nature.com/ja

ORIGINAL ARTICLE

The novel anti-*Propionibacterium acnes* compound, Sargafuran, found in the marine brown alga *Sargassum macrocarpum*

Yuto Kamei[1], Miyuki Sueyoshi[1], Ken-ichiro Hayashi[2], Ryuta Terada[3] and Hiroshi Nozaki[2]

We screened extracts of 342 species of marine algae collected from Japanese coastlines for antibacterial activity against *Propionibacterium acnes*, and found a novel antibacterial compound, which we named Sargafuran, from the MeOH extract of the marine brown alga, *Sargassum macrocarpum*. Sargafuran has low cytotoxicity, and the MIC against *P. acnes* was 15 μg ml^{-1}, showing a broad antibacterial activity against Gram-positive bacteria. A time-kill study showed that Sargafuran was bactericidal and completely killed *P. acnes* at 4×MIC by lysing bacterial cells. These results suggest that Sargafuran might be useful as a lead compound to develop new types of anti-*P. acnes* substances and new skin care cosmetics to prevent or improve acne.
The Journal of Antibiotics (2009) **62,** 259–263; doi:10.1038/ja.2009.25; published online 27 March 2009

Keywords: anti-acne; antibacterial; marine alga; *Propionibacterium acnes*; Sargafuran; *Sargassum macrocarpum*

INTRODUCTION

Acne vulgaris is a common skin disease, affecting about 70–80% of adolescents and young adults. It is a multifactorial disease of the pilosebaceous unit.[1] *Propionibacterium acnes*, a common skin organism, is most often recognized in acne vulgaris and produces a number of virulence factors. Clindamycin and erythromycin are most commonly used as topical antibiotics against *P. acnes*.[2]

In our laboratory, we screened the biological activities of marine algae collected from the Japanese coastline and found several bioactive compounds,[3–6] including an antibacterial compound.[7] Other reports show that some distinct seaweeds contain antimicrobial substances against both Gram-positive and -negative bacteria.[8,9] Thus, marine algae are a promising bioresource to find new antibacterial compounds against *P. acnes* and to develop new natural cosmetic products to prevent acne. In this study, we screened a total of 342 species of marine algae, collected from the Japanese coastline, for activity against *P. acnes,* and found a novel anti-*P. acnes* compound from one of these algae.

MATERIALS AND METHODS

Bacterial strains and media

P. acnes (ATCC 11827) was used for the screening of antibacterial activity of marine algal extracts. This test strain was cultured with Reinforced Clostridial Medium (Sigma-Aldrich, Tokyo, Japan). Bacteria used for the antibacterial spectrum assay were methicillin-resistant *Staphylococcus aureus* (ATCC 33591), methicillin-sensitive *S. aureus* (ATCC 25923), *Bacillus subtilis* (IFO 14419), *Escherichia coli* (NBRC 12734), *Enterococcus faecium* (NBRC 3826), *Enterococcus faecalis* (NBRC 3971), *Enterococcus serolicida* (NG 8206), *Streptococcus mutans* (NBRC 13955), *Streptococcus pneumoniae* (GTC 261), *Streptococcus pyogenes* (GTC 262), *Pseudomonas aeruginosa* (IFO 13736) and *Vibrio alginolyticus* (V7) as well as two strains of *P. acnes* (ATCC 1187 and ATCC 25746). These strains were cultured with Tryptic Soy Agar medium (Difco Laboratories, Detroit, MI, USA), except for *P. acnes* and *V. alginolyticus* which was cultured in ZoBell 2216E agar medium.[10]

Marine algae collection and preparation of extracts

During the period from April 1994 to August 2003, marine algae samples were collected at 96 points from north to south along the Japanese coastline and were stored at −20 °C until needed. The marine algae extracts were prepared as described in our earlier paper.[11]

Screening assay for anti-*P. acnes* activity

Sterilized paper disks (φ8 mm; Advantec, Tokyo, Japan) permeated with 50 μl each of phosphate-buffered saline or MeOH algal extract and dried completely were placed on double-layer agar plates inoculated with 5.0×10^6 CFU ml^{-1} of *P. acnes* strain. These plates were incubated at 37 °C for 2 days under anaerobic condition. After incubation, the zones of inhibition were measured and recorded.

Isolation and purification of Sargafuran

One liter of the MeOH extract from the marine brown alga *Sargassum macrocarpum* (250 g wet weight) was partitioned with a chloroform/water (1:1) mixture. The chloroform/MeOH fraction was concentrated to dryness and redissolved in *n*-hexane/acetone (6:1), and then subjected to a silica gel-60 (Merck, Darmstadt, Germany) column chromatography under continuous elution with *n*-hexane/acetone (6:1, 5:1 and 4:1) and MeOH. The active fractions were pooled and concentrated, and then further chromatographed

[1]Coastal Bioenvironment Center, Saga University, Karatsu, Saga, Japan; [2]Department of Biochemistry, Okayama University of Science, Okayama, Japan and [3]Department of Fisheries Biology and Oceanography, Faculty of Fisheries, Kagoshima University, Shimoarata, Kagoshima, Japan
Correspondence: Dr Y Kamei, Coastal Bioenvironment Center, Saga University, 152-1 Shonan-cho, Karatsu, Saga 847-0021, Japan.
E-mail: kameiy@cc.saga-u.ac.jp
Received 12 December 2008; revised 12 February 2009; accepted 5 March 2009; published online 27 March 2009

on a second silica gel column, eluting with *n*-hexane/acetyl ethyl ester (10:1, 6:1 and 3:1) and MeOH, and on a reverse-phase Cosmosil (Nacalai Tesque Inc., Kyoto, Japan) column, eluting with 60–80% MeOH containing 0.1% trifluoroacetic acid (Sigma-Aldrich). The active fractions were finally purified with an HPLC on a reversed-phase column (Mightysil RP-8 GP, ∅ 4.6×250 mm; Kanto Chemical Co. Inc., Tokyo, Japan), eluting with a gradient of acetonitrile and water containing 0.1% trifluoroacetic acid.

Spectrometric analyses of Sargafuran

Optical rotations were measured with an SEPT-200 polarimeter (Horiba, Tokyo, Japan). UV spectra were recorded on a U-3210 spectrophotometer (Hitachi, Tokyo, Japan) and IR spectra on a model 1720 spectrometer (Perkin-Elmer, Waltham, MA, USA). NMR spectra were recorded in $CDCl_3$ on a JEOL lambda 500 NMR spectrometer (JEOL, Tokyo, Japan). Chemical shifts are shown as δ values from TMS as the internal reference. Peak multiplicities are quoted in Hz. Mass spectra were measured on a JMS-700 spectrometer (JEOL).

Antibacterial test

The MICs of Sargafuran were determined by the standard microdilution method described by the National Committee for Clinical Laboratory Standards,[12] using a Tryptic Soy Broth medium (Difco Laboratories), except for *P. acnes* and *V. alginolyticus* which was in ZoBell 2216E broth medium. The final volume of Tryptic Soy Broth, Reinforced Clostridial Medium or ZoBell broth medium containing Sargafuran was 100 µl per well to give a starting inoculum density of 5×10^5 CFU ml^{-1}.

Time-kill curve experiment

The time-kill experiment was conducted by the method described by Aeschlimann and Rybak[13] and Etenza *et al.*[14] The experiments were conducted in test tubes containing 15 ml of fresh Reinforced Clostridial Medium inoculated with an overnight culture of *P. acnes* (ATCC 11827) to give an initial bacterial density of 10^6 cells per ml. The inoculation was carried out immediately after the addition of Sargafuran or Clindamycin (Sigma-Aldrich) at the final concentrations of MIC, 2×MIC and 4×MIC and incubated at 37 °C for 2 days under anaerobic condition.

Bacteriolytic assay

The seed culture of *P. acnes* (ATCC 11827) on an RCA plate was resuspended in Reinforced Clostridial Medium and washed twice with sterile 10 mM Tris-HCl buffer (pH 7.6). The absorbance was adjusted to 0.1 at 660 nm. The bacterial cell suspension (5 ml each) was aliquoted in sterile test tubes and exposed to Sargafuran at various concentrations or to Achromopeptidase (Wako Pure Chemical Industries Ltd, Tokyo, Japan) at 134 µg ml^{-1} as a positive control. Untreated bacterial suspensions were used as negative controls. The concentration of MeOH (the solvent of Sargafuran) in each tube was less than 0.1% (v/v). The test tubes were incubated at 37 °C under anaerobic conditions. The absorbance at 660 nm was measured at 0, 0.15, 0.5, 0.45, 1, 2, 3, 4, 5, 6, 7, 8, 9, 10, 11 and 12 h after incubation, and the relative absorbance was calculated by dividing each absorbance by that of the negative control. Each treatment was conducted in duplicate.

Cytotoxicity test

The cytotoxic activity of Sargafuran was evaluated as described earlier.[15] Human normal dermal fibroblasts (Morinaga Institute of Biological Science, Yokohama, Japan) were prepared at 5×10^3 cells per 100 µl per well in a 96-well plate. Then Sargafuran, serially diluted twofold, was added to give final concentrations ranging from 3.8 to 480 µg ml^{-1}. The cells were incubated at 37 °C for 3 days. The proliferation of cells was evaluated by an 3-[4,5-dimethylthiazol-2-ly]-2,5-diphenyltetrazolium bromide (MTT) assay[16] and the growth rate relative to the control treatment was calculated.

RESULTS

Marine algae with anti-*P. acnes* activity

We found 13 species of marine algae with anti-*P. acnes* activity, based on disk diffusion assays, using the extracts from a total of 342 species of marine algae collected from the Japanese coastline. The algae are *Laurencia brongniartii, Laurencia okamurae, Osonthalia corymbifera, Rhodomela teres, Dictyopteris divaricata, Dictyopteris undulata, Ishige okamurai, Padina crassa, Sargassum fulvellum, S. macrocarpum, Sargassum siliquastrum, Sargassum yezoense* and *Zonaria diesingiana*, showing approximate MIC ranges of 62.5–1000 µg per disk against *P. acnes* (Table 1). Most of the positive marine algae were brown algae and showed a relatively high anti-*P. acnes* activity at 62.5–250 µg per disk.

Purification of the antibacterial compound, Sargafuran, from *S. macrocarpum*

As described above, several marine algae showed promising anti-*P. acnes* activity. One of those positive algae, *S. macrocarpum,* is widely distributed throughout the Japanese coastline and can be collected in large amounts during any season. Thus, we selected this algal species to proceed with the isolation and purification of the antibacterial compound against *P. acnes* from the MeOH extract. After several purification steps, starting from 250 g wet weight of *S. macrocarpum,* 3.6 mg of the antibacterial compound, which we named Sargafuran, was obtained.

Structure determination of Sargafuran

Sargafuran was isolated as a colorless oil [UV λ_{max} ($CHCl_3$) nm ($\log\varepsilon$): 241 (4.27), 263 (3.79); $[\alpha]_D$–1.26°($CHCl_3$, *c* 0.95)]. The molecular formula was determined to be $C_{27}H_{36}O_4$ (found 424.2593, calcd. 424.2614) by high resolution electron impact mass spectrometry (HR-EI-MS). The IR spectrum showed absorption bands at 1686 and 3400 cm^{-1} attributable to a carbonyl and hydroxyl group, respectively. ^{1}H- and ^{13}C-NMR spectroscopic data indicate that Sargafuran has five singlet methyl groups (C-18, C-19, C-21, C-26 and C-27), seven olefinic bonds, six aliphatic methylenes, a carbonyl group and a quaternary carbon attached to oxygen. Taken together with the presence of seven olefinic bonds and a carbonyl group, 10 units of unsaturation in Sargafuran indicate that the compound has two rings in its structure. ^{1}H-^{1}H COSY spectrum revealed the linkages among the methylenes, and olefinic protons (H-6 to H-8, H-10 to H-12 and H-14 to H-16), in addition to two sets of

Table 1 MeOH extracts from marine algae exhibited potent anti-*Propionibacterium acnes* activity

Marine algae	*Anti-P. acnes activity*[a]
Red algae	+++
Laurencia brongniartii	+++
Laurencia okamurae	++
Odonthalia corymbifera	+++
Rhodomela teres	
Brown algae	
Dictyopteris divaricata	++
Dictyopteris undulata	++
Ishige okamurai	++
Padina crassa	+++
Sargassum fulvellum	++
Sargassum macrocarpum	++
Sargassum siliquastrum	++
Sargassum yezoense	++
Zonaria diesingiana	+

[a]+++, ⩾19-mm inhibition zone; ++, 12- to 18-mm inhibition zone; +, ⩽11-mm inhibition zone; anti-*P. acnes* activities of the MeOH extracts were evaluated by the disk diffusion method.

connection between olefinic protons (H-2/H-3 and H-23/H-24). The connections in the triene chain (C-6 to C-21) were established from the HMBC correlations (H-8/C-10, 19, H-19/C-9, 10, H-10/C-9, H-11/C-9, 13, H-12/C-14, 20, H-14/C-13, 20, H-18/C-16, 17 and H-21/C-16, 17) among the olefinic methines (H-8, H-12 and H-16), methyl groups (H-18, -19 and -21) and a carbonyl carbon (C-20). The geometry of olefinic bonds was determined to be *E* (C-8/C-9) and *Z* (C-12/C-13), respectively, by NOESY correlations (H-7/H-19, H-8/H-10 and H-12/H-14). The 2-methyl furan moiety (C-22 to C-26) was revealed by the HMBC correlations (H-23/C-22, 25, H-24/C-22, 25 and H-26/C-24, 25) and the small J_{H-H} coupling value between H-23 and H-24 (J=3 Hz). Additional HMBC correlations (H-2/C-1, -4, H-3/C-1, -4 and H-27/C-1, -2, -5) indicated the presence of 1-methyl-cyclopenta-2,4-dienol moiety (C-1 to C5, and C-27). The remaining carbonyl carbon (C-20) was attributed to a carboxylic acid. The cyclopentadiene moiety was connected with C-6 of the triene chain at C-5 and with C-22 of methylfuran at C-4 on the basis of HMBC correlations (H-7/C-5, H-6/C-1, H-3/C-22 and H-23/C-4), and this was further supported by a strong fragment ion at *m/z* 175 (100%) in the EI-MS spectrum. Thus, the structure of Sargafuran was determined as shown in Figure 1. The assignments of ^{1}H- and ^{13}C-NMR signals are indicated in Table 2.

Minimum inhibitory concentration

Sargafuran showed antibacterial activity against *P. acnes* at 15 μg ml^{-1}. At the same concentration, Sargafuran also showed antibacterial activity against other Gram-positive bacteria, *S. pyogenes* and *S. pneumoniae,* and a Gram-negative bacterium, *V. alginolyticus* (Table 3). However, this compound did not inhibit the bacterial growth of the Gram-negative bacteria, *E. coli* and *P. aeruginosa,* and another Gram-positive bacterium, *S. mutans,* even at a concentration of 120 μg ml^{-1}.

Bactericidal activity of Sargafuran

The time-kill study showed that Sargafuran decreased the bacterial counts of *P. acnes* at 1/2×MIC (7.5 μg ml^{-1}) during a 16-h exposure (Figure 2). At MIC (15 μg ml^{-1}), Sargafuran completely killed the *P. acnes* strain tested within 4 h. However, Clindamycin did not show bactericidal activity against the *P. acnes* strain tested even after 72 h of incubation at 4×MIC (0.1 μg ml^{-1}). This bactericidal property of Sargafuran seems to be very promising for developing new types of antibiotics against the multi-drug-resistant *P. acnes* strains.

Bacteriolytic activity

The reduction in the absorbance of *P. acnes* cell suspensions was not observed in the presence of Sargafuran, at up to 4×MIC (60 μg ml^{-1}), until the end of the incubation period (Figure 3). In contrast, the absorbance of *P. acnes* cell suspensions treated with Achromopeptidase at 134 μg ml^{-1} as the positive control was reduced drastically in the early incubation period. These results indicated that Sargafuran did not lyse *P. acnes* cells.

Cytotoxicity

An MTT assay showed that Sargafuran was not cytotoxic to human normal dermal fibroblast cells (Figure 4). At concentrations up to

Table 2 ^{1}H- and ^{13}C-NMR data of Sargafuran

No.	*^{1}H*	*^{13}C*
1	2.13 (3H, *s*)	15.5 (CH_3)
2		144.9 (C)
3	6.47 (1H, *d*, 3.0)	117.1 (CH)
4	6.32 (1H, *d*, 3.0)	110.3 (CH)
5		148.5 (C)
6		122.9 (C)
7	6.24 (1H, *d*, 10.0)	121.3 (CH)
8	5.57 (1H, *d*, 10.0)	130.7 (CH)
9		77.8 (C)
10		126.4 (C)
11	1.67 (2H, *m*)	40.7 (CH_2)
12	2.11 (2H, *m*)	22.6 (CH_2)
13	5.13 (1H, *dd*, 6.0, 7.3)	124.9 (CH)
14		134.4 (C)
15	2.06 (2H, *t*, 7.5)	39.1 (CH_2)
16	2.58 (2H, *m*)	28.1 (CH_2)
17	5.99 (1H, *dd*, 7.5, 7.0 Hz)	145.7 (CH)
18		130.5 (C)
19	2.26 (2H, *t*, 7.5)	34.5 (CH_2)
20	2.11 (2H, *m*)	27.9 (CH_2)
21	5.09 (1H, *t*, 7.0)	123.0 (CH)
22		132.3 (C)
23	1.67 (3H, *s*)	25.7 (CH_3)
24	1.35 (3H, *s*)	25.9 (CH_3)
25	1.57 (3H, *s*)	15.8 (CH_3)
26		173.3 (C)
27	1.58 (3H, *s*)	17.7 (CH_3)

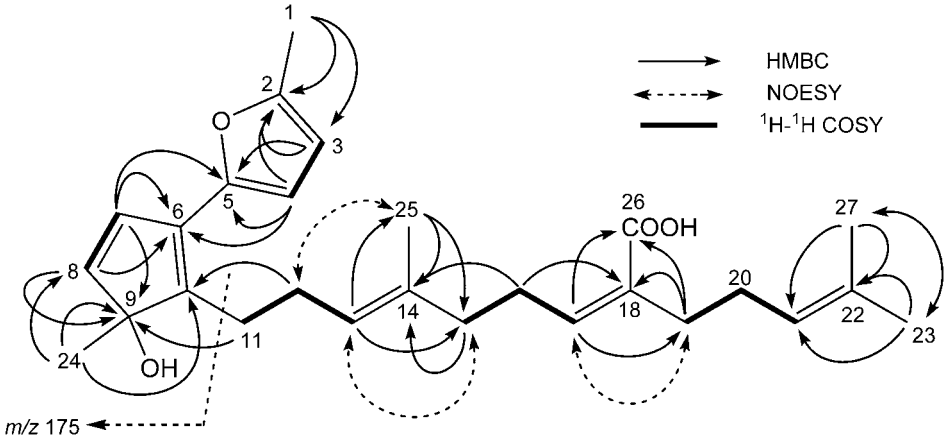

Figure 1 2D NMR correlations and mass fragmentation of Sargafuran.

Table 3 Comparative antibacterial activities of Sargafuran and Clindamycin

	MIC ($\mu g\,ml^{-1}$)	
Bacterial strain	*Sargafuran*	*Clindamycin*
Propionibacterium acnes (ATCC 11827)	15	0.03
P. acnes (ATCC 25746)	15	0.67
MSSA (ATCC 25923)	30	0.47
MRSA (ATCC 33951)	30	>120
Bacillus subtilis (IFO 14419)	30	1.88
Escherichia coli (NBRC 12734)	>120	>120
Enterococcus faecalis (NBRC 3971)	30	>120
Enterococcus faecium (NBRC 3826)	60	0.90
Enterococcus serolicida (NG 8206)	60	1.88
Streptococcus pyogenes (GTC 262)	15	7.50
Streptococcus pneumoniae (GTC 261)	15	7.50
Streptococcus mutans (NBRC 13955)	>120	3.75
Pseudomonas aeruginosa (IFO 13736)	>120	>120
Vibrio alginolyticus (V-7)	15	30

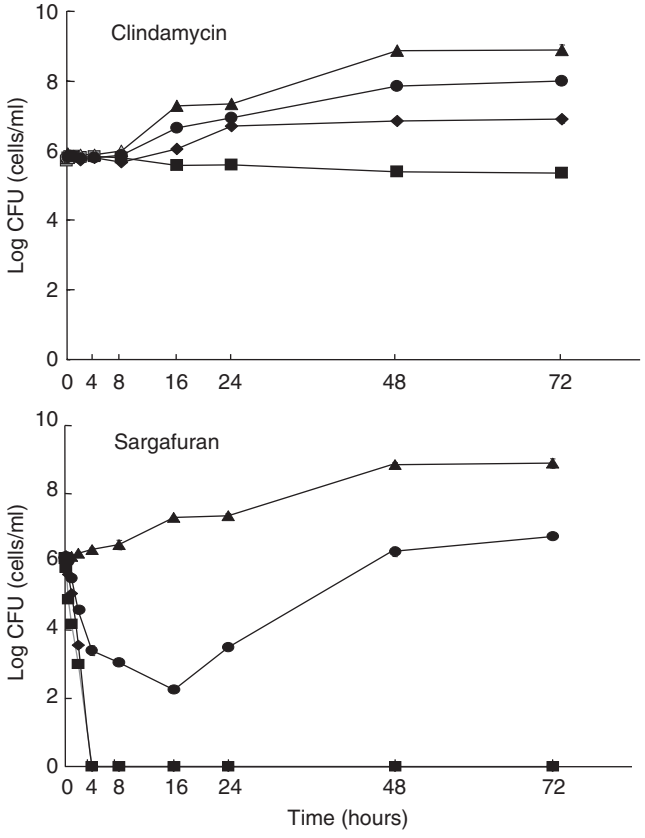

Figure 2 Comparative bactericidal activities of Sargafuran and vancomycin against *P. acnes* (ATCC 11827). ▲, Negative control (antibacterial substance not added); ●, 1/2×MIC; ◆, 1×MIC; ■, 4×MIC. The values with the standard error bars are mean values from duplicate experiments.

2× the MIC ($30\,\mu g\,ml^{-1}$), it did not significantly affect cell viability and did not reduce cell viability by 50% at any concentrations up to $480\,\mu g\,ml^{-1}$.

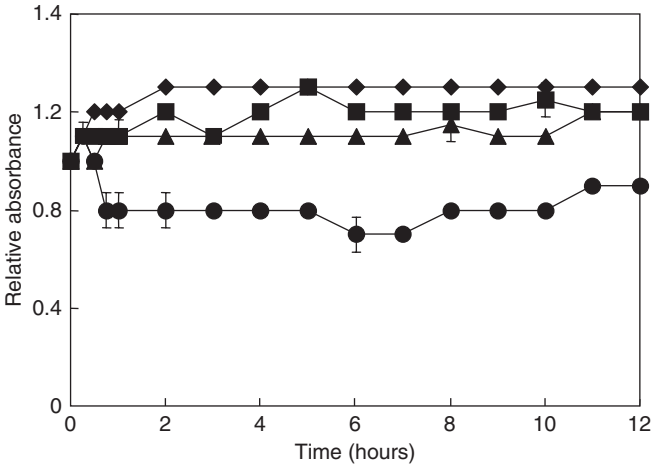

Figure 3 Bacteriolytic activity of Sargafuran against *P. acnes* (ATCC 11827). ●, Positive control ($134\,\mu g\,ml^{-1}$) Achromopeptidase; ◆, 1×MIC; ■, 2×MIC; ▲, 4×MIC. Relative absorbance was calculated by dividing the absorbance of the treated tube by that of the negative control tube. The values with the standard error bars are mean values from triplicate experiments.

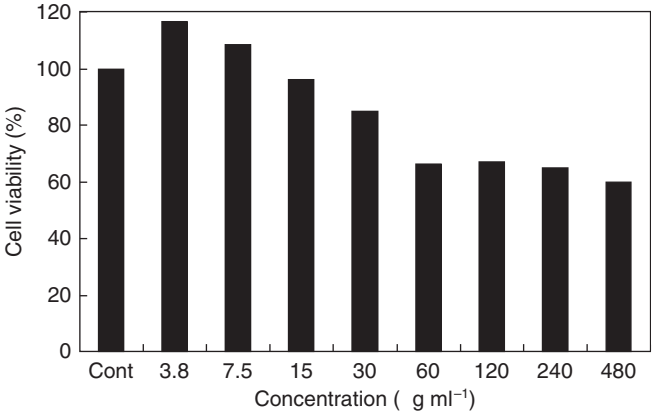

Figure 4 Cytotoxicity of Sargafuran to human normal dermal fibroblast cells.

DISCUSSION

Acne vulgaris is a multifactorial disease with an unclear etiology and pathogenesis. The factors known to cause acne vulgaris include follicular hyperkeratosis, sebum secretion, *P. acnes* and inflammation.[17] Recently, cosmetics and toiletries containing natural products, such as extracts of herbs, Chinese plant medicine and seaweed, have been prevalent in commercial markets because of consumer concerns over synthetic chemical ingredients.

This study was conducted to screen marine algae collected from the Japan coastline for antibacterial activity against *P. acnes* to develop new types of cosmetics to treat acne. We found a new anti-*P. acnes* compound, Sargafuran, from the marine brown alga, *S. macrocarpum*. We also have reported two neurostimulating substances, sargaquinoic acid and sargachromenol, from this alga[18,19] and determined their structures to be 2-methylquinone-type compounds having side chain (C-20 unit). The 2-methylquinone moiety and C-20 side chain of these compounds would be biosynthesized from sikimic acid (C-7 unit) and geranyl geranyl diphospate (C-20 unit). It is likely that the

biosynthetic pathway of Sargafuran carbon skeleton would share with the pathway of sargaquinoic acid and sargachromenol skeletons, because Sargafuran has a similar side chain and the same number of carbons. Sargafuran was stable against heating up to 60 °C, pH 4–7 and irradiation for 24 h. These properties are suitable for cosmetics or skin care products to prevent acne. Clindamycin is generally used for curing acne as a clinical treatment. However, Clindamycin was shown to be bacteriastatic even at 4×MIC, whereas Sargafuran showed bactericidal activity against *P. acnes*. This is a superior property because bactericidal activity minimizes the chance of development of resistance. Takahashi *et al.*[20] have also reported that eucalyptus leaf extracts and constituent flavonoids showed great antibacterial activity against Gram-positive bacteria, including *P. acnes*. The marine brown alga, *S. macrocarpum*, containing Sargafuran might be a good candidate from which to develop and produce the anti-acne cosmetics or skin care products in the near future.

ACKNOWLEDGEMENTS

We are grateful to T Takeda (Hokkaido Kushiro Fisheries Experimental Station, Hokkaido, Japan) for kindly donating *V. alginolyticus* strain tested in this study.

1 Krautheim, A. & Gollnick, H. P. M. Acne: topical treatment. *Clin. Dermatol.* **22,** 398–407 (2004).
2 Toyoda, M. & Morohashi, M. Pathogenesis of acne. *Med. Electron. Microsc.* **34,** 29–40 (2001).
3 Nakano, T., Noro, T. & Kamei, Y. *In vitro* promoting activity of human interferon ß production by extracts of marine algae from Japan. *Cytotechnology* **25,** 239–241 (1997).
4 Harada, H. & Kamei, Y. Dose-dependent selective cytotoxicity of the extracts from the marine green algae, *Cladophoropsis vaucheriaeformis* against mouse leukemia L1210 cell. *Biol. Pharm. Bull.* **21,** 386–389 (1998).
5 Kanegawa, K. *et al.* Telomerase inhibiting activity *in vitro* from natural resources, marine algae extracts. *Cytotechnology* **33,** 221–227 (2000).
6 Tsang, C. K., Sagara, A. & Kamei, Y. Structure–activity relationship of a neurite outgrowth-promoting substance purified from the brown alga, *Sargassum macrocarpum*, and its analogues on PC12D cells. *J. Appl. Phycol.* **13,** 349–357 (2001).
7 Horikawa, M., Noro, T. & Kamei, Y. *In vitro* anti-methicillin-resistant *Staphylococcus aureus* activity found in extracts of marine algae indigenous to the coastline of Japan. *J. Antibiot.* **52,** 186–189 (1999).
8 Vairappan, C. S., Kawamoto, T., Miwa, H. & Suzuki, M. Potent antibacterial activity of halogenated compounds against antibiotic-resistant bacteria. *Planta Med.* **70,** 1087–1090 (2004).
9 Mayer, A. M. S. & Hamann, M. T. Marine pharmacology in 2001–2002: marine compounds with antihelminthic, antibacterial, anticoagulant, antidiabetic, antifungal, anti-inflammatory, antimalarial, antiplatelet, antiprotozoal, antituberculosis, and antiviral activities; affecting the cardiovascular, immune and nervous systems and other miscellaneous mechanisms of action. *Comp. Biochem. Physiol.* **140,** 265–286 (2005).
10 Oppenheimer, C. H. & ZoBell, C. E. The growth and viability of sixty-three species of marine bacteria as influenced by hydrostatic pressure. *J. Mar. Res.* **11,** 10–18 (1952).
11 Harada, H., Noro, T. & Kamei, Y. Selective antitumor activity *in vitro* from marine algae from Japan coasts. *Biol. Pharm. Bull.* **20,** 541–546 (1997).
12 National Committee for Clinical Laboratory Standards. Method for Dilution Antimicrobial Susceptibility Test for Bacteria That Grow Aerobically 4th edn, 1–29 (NCCLS, Pennsylvania, 1997).
13 Aeschliman, J. R. & Rybak, M. J. Pharmacodynamic analysis of the activity of quinopristin–dalfopristin against vancomycin-resistant *Enterococcus faecium* with differing MBCs via time-kill-curve and postantibiotic effect methods. *Antimicrob. Agents Chemother.* **42,** 2188–2192 (1998).
14 Entenza, J. M., Marchetti, O., Glauser, M. P. & Moreillon, P. Y-688, a new quinolone active against quinolone-resistant *Staphylococcus aureus*: lack of *in vivo* efficacy in experimental endocarditis. *Antimicrob. Agents Chemother.* **42,** 1889–1894 (1998).
15 Harada, H. & Kamei, Y. Selective cytotoxicity of marine algae extracts to several human leukemic cell lines. *Cytotechnology* **25,** 213–219 (1997).
16 Mosmann, T. Rapid colorimetric assay for cellular growth and survival: application to proliferation and cytotoxicity assays. *J. Immunol. Methods* **65,** 55–63 (1983).
17 Knor, T. The pathogenesis of acne. *Acta Dermatovenerol. Croat.* **13,** 44–49 (2005).
18 Kamei, Y. & Tsang, C. K. Sargaquinoic acid promotes neurite outgrowth via protein kinase A and MAP kinases-mediated signaling pathways in PC12D cells. *Int. J. Dev. Neurosci.* **21,** 255–262 (2003).
19 Tsang, C. K., Ina, A., Goto, T. & Kamei, Y. Sargachromenol, a novel nerve growth factor-potentiating substance isolated from *Sargassum macrocarpum*, promotes neurite outgrowth and survival via distinct signaling pathways in PC12D cells. *Neuroscience* **132,** 633–643 (2005).
20 Takahashi, T., Kokubo, R. & Sakaino, M. Antimicrobial activities of eucalyptus leaf extracts and flavonoids from *Eucalyptus maculata*. *Lett. Appl. Microbiol.* **39,** 60–64 (2004).

The Journal of Antibiotics (2009) 62, 265–269
© 2009 Japan Antibiotics Research Association All rights reserved 0021-8820/09 $32.00
www.nature.com/ja

ORIGINAL ARTICLE

Discovery and antibacterial activity of glabramycin A–C from *Neosartorya glabra* by an antisense strategy

Hiranthi Jayasuriya[1], Deborah Zink[1], Angela Basilio[2], Francisca Vicente[2], Javier Collado[2], Gerald Bills[2], Mary Lee Goldman[1], Mary Motyl[1], Joann Huber[1], Gabe Dezeny[1], Kevin Byrne[1] and Sheo B Singh[1]

Treatment of drug-resistant bacteria is a significant unmet medical need. This challenge can be met only by the discovery and development of new antibiotics. Antisense technology is one of the newest discovery tools that provides enhanced sensitivity for detection of antibacterials, and has led to the discovery of a number of interesting new antibacterial natural products. Continued utilization of this technology led to the discovery of three new bicyclic lactones, glabramycins A–C, from a *Neosartorya glabra* strain. Glabramycin C showed strong antibiotic activity against *Streptococcus pneumoniae* (MIC 2 μg ml^{-1}) and modest antibiotic activity against *Staphylococcus aureus* (MIC 16 μg ml^{-1}). The isolation, structure, relative configuration and antibacterial activity, and plausible biogenesis of these compounds have been discussed.
The Journal of Antibiotics (2009) **62,** 265–269; doi:10.1038/ja.2009.26; published online 3 April 2009

Keywords: antisense; rpsD; Neosartorya; glabra; glabramycin; antibacterial; *Staphylococcus aureus*

INTRODUCTION

The discovery and development of clinically useful antibiotic classes, such as, the aminoglycosides, macrolides and tetracyclines, have clearly shown that bacterial protein synthesis is a viable target for antibacterial drug discovery.[1,2] The bacterial ribosome responsible for protein synthesis consists of a small 30S and a large 50S subunit. The ribosomal subunit (aka S4), referred to as RpsD, is a component of the 30S subunit.[3–5] The RpsD protein is encoded by the *rps*D gene, which is essential and resides in an operon containing only one other gene, *SAV1718,* which is a nonessential gene.[6,7] Therefore, this gene was selected as a drug-target for the discovery of antibacterial agents.

For antibiotic discovery targeting the *rps*D gene, we constructed a *Staphylococcus aureus* S1-782B strain expressing antisense RNA under xylose control, leading to hypersensitivity against RpsD inhibitors. To implement this approach for drug discovery, we designed a two-plate assay in which one plate was seeded with an *rps*D antisense *S. aureus* strain and the other with an *S. aureus* EP 167 (control) strain. A similar general methodology led to the discovery of platensimycin and platencin.[8–13] The screening of over 138 000 microbial extracts against *rps*D two-plate antisense whole-cell assay led to the isolation of a series of interesting new compounds exemplified by lucensimycins,[14–16] coniothyrione,[17] pleosporone,[18] phaeosphenone,[19] and okilactomycin.[20] Continued screening and follow-up of one of the active extracts produced by *Neosartorya glabra* led to the isolation of three macrolactones namely, glabramycin A–C (**1**–**3**, Figure 1). The isolation, structure elucidation, relative configuration and antibacterial activity of the glabramycins (**1**–**3**) are described.

RESULTS AND DISCUSSION

The producing organism was isolated from a soil sample collected from Candamia, Spain. The strain was identified as *Neosartorya glabra* by sequencing the large subunit of DNA of the D1D2 region and by tracing the phylogenetic relationships. The strain was grown in a submerged fermentation for 14 days and compounds were extracted with an equal volume of acetone. The extract was chromatographed on Amberchrome, a capture resin, followed by reversed-phase C_8 HPLC to give **1** (7 mg, 7 mg l^{-1}), **2** (1.9 mg, 1.9 mg l^{-1}) and **3** (1 mg, 1 mg l^{-1}), each as yellow gums.

Glabramycin A (**1**), the most abundant of the three compounds, showed a molecular formula $C_{22}H_{24}O_6$ as deduced from the HRESIFTMS data. The ^{13}C NMR spectrum and distortionless enhancement by polarization transfer (DEPT) analysis of **1** showed signals for one methyl, four methylenes, ten methines and seven quaternary carbons (Table 1). The ^{1}H NMR spectrum showed signals for four olefinic methine doublet of doublets with J=15 and 11 Hz, and two methine doublets with J=15 Hz. The COSY correlations of these six olefinic methines indicated the presence of an *E*-triene in which each end terminated with a quaternary carbon. The methine (δ_H 5.90) at one end of the triene chain showed heteronuclear multiple bond correlations (HMBCs) to a carboxyl carbon at δ_C 170.3, and a carboxylic group was thus placed at one end of the triene. The terminal methine (δ_H 6.00) at the other end of the triene chain showed HMBC correlations to two quaternary olefinic carbons resonating at δ_C 167.4 and δ_C 108.6, allowing for further extension of the triene chain.

[1]Merck Research Laboratories, Rahway, NJ, USA and [2]CIBE, Merck Sharp & Dohme de Espana, SA Josefa Valcárcel 38, Madrid, Spain
Correspondence: Dr SB Singh, Medicinal Chemistry, Merck Res Lab., 126 E Lincoln Ave., Rahway, NJ 7065, USA.
E-mail: sheo_singh@merck.com
Received 11 December 2008; revised 19 February 2009; accepted 20 February 2009; published online 3 April 2009

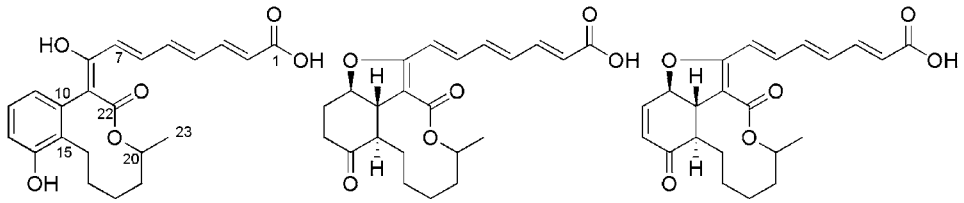

1 (Glabramycin A) **2** (Glabramycin B) **3** (Glabramycin C)

Figure 1 Structures and relative configurations of glabramycins A–C (**1**–**3**).

Table 1 ^{1}H (600 MHz) and ^{13}C (125 MHz)-NMR assignments of glabramycin A (1), B (2) and C (3)

	1		**2**		**3**	
	1	*CD_3OD*	***2***	*CD_3OD*	***3***	*$CDCl_3$*
Position	δ_C	δ_H, mult, *J* in Hz	δ_C	δ_H, mult, *J* in Hz	δ_C	δ_H, mult, *J* in Hz
1	170.3		170.1		170.8	
2	124.4	5.90, d, 15	124.5	6.00, d, 15	122.2	5.90, d, 15
3	145.6	7.30, dd, 15, 11	145.2	7.30, dd, 15, 11	145.5	7.40, dd, 15, 11
4	136.0	6.60, dd, 15, 11	136.2	6.60, dd, 15, 11	134.5	6.57, dd, 15, 11
5	140.4	6.54, dd, 15, 11	140.3	6.80, dd, 15, 11	140.0	6.75, dd, 15, 11
6	136.9	7.10, dd, 15, 11	137.3	7.00, dd, 15, 11	135.9	6.97, dd, 15, 11
7	129.1	6.0, d, 15	123.3	7.20, d, 15	122.9	7.32, d, 15
8	167.4		164.5		163.1	
9	108.6		110.9		112.0	
10	125.3		49.4	3.46, t, 9.6	44.0	3.62, dd, 10, 4.5
11	124.9	6.49, dd, 7.5, 1.0	82.0	5.00, m	77.5	5.09, dd, 8.5, 4.5
12	126.9	6.95, t, 7.5	35.9	2.20, m, 2.40, m	137.6	6.87, dd, 10.5, 4.5
13	115.9	6.73, dd, 10, 7.5	26.0	2.20, m, 2.40, m	132.5	6.23, d, 10.5
14	157.4		213.3		198.7	
15	131.8		50.6	2.60, m	48.3	2.46, m
		2.07, m		1.46, m,		2.05, m
16	27.3	2.70, m	23.7	1.62, m	22.9	1.40, m
		1.94, m		1.80, m		1.53, m
17	29.5	1.87, m	25.2	1.30, m	23.6	1.89, m
		1.34, m		1.78, m		1.65, m
18	22.6	1.53, m	24.9	1.88, m	32.4	1.76, m
		1.49, m		1.56, m		1.38, m
19	33.9	1.83, m	32.9	1.83, m	24.8	1.77, m
20	73.5	5.30, m	74.1	4.94, m	73.2	5.00, m
22	164.7		170.1		164.9	
23	18.5	1.10, d, 6.5	20.3	1.28, d, 6.5	20.6	1.30, d, 6.5

Three of the remaining olefinic methines coupled with each other, with *J*=7.5 Hz indicating the presence of a 1, 2, 3-tri-substituted phenyl group. The only non-olefinic methine proton resonating at δ_H 5.30 showed heteronuclear multiple quantum coherence (HMQC) correlation to an oxygenated carbon resonating at δ_C 73.5. The methyl group resonating at δ_H1.10 showed HMBC correlations to the methine carbon C-20 (δ_C 73.5) and to the methylene at C-19 (δ_C 33.9). This observation allowed for the placement of the methyl group on the oxygenated carbon C-20. The COSY correlations from the methyl protons, H_3-23 at δ_H 1.10 to the methylene H_2-16 at δ_H 2.07 and δ_H 2.7, established the C16-C20-C23 spin system. The HMBC correlations of the terminal methylene protons of the alkyl chain at δ_H 2.70 and δ_H 2.07 to carbons δ_C 131.8 (C-15), 125.3 (C-10) and 157.4 (C-14) established its connection to the phenyl group. The HMBC correlation of the methine proton (δ_H 5.30)to an ester carbonyl at δ_C 164.7 (C-22) allowed for the linkage of this carbonyl and the methine in the form of a lactone ring. Finally, the ester carbonyl C-22 was connected to the olefinic carbon C-9 (δ_C 108.6) to form the macrocyclic lactone, to satisfy the degrees of unsaturation and the molecular formula. This assignment was supported by the ^{13}C chemical shifts of C-8, C-9 and C-22. The substitution around the phenyl ring was confirmed by HMBC correlations of the aromatic protons and supported by HMBC correlations of the benzylic methylene protons (Figure 2).

The structures for glabramycins, B (**2**) and C (**3**), were determined by comparison of ^{13}C and ^{1}H NMR spectral data with **1** (Table 1).

Glabramycin B (**2**) exhibited a molecular formula, $C_{22}H_{26}O_6$. The ^1H NMR spectrum of **2** showed only six olefinic protons of trienoic acid moiety, indicating the presence of a saturated six-membered ring system. The COSY spectrum showed an extended spin system comprising C20(C23)-C15-C10-C14. The HMBC correlations of H-10 (δ_H 3.46), H_2-12 (δ_H 2.20, 2.40) and H_2-16 (δ_H 1.46, 1.62) to the downfield carbonyl C-14 (δ_C 213.3) allowed the placement of a carbonyl group at C-14 in the cyclohexanone ring. The ether bridge between C8 and C11 made the dihydrofuran ring that satisfied the molecular formula. The relative configurations at C-10, C-11 and C-15 were established from the magnitude of the scalar couplings. H-10 resonated as a triplet with J=9.6 Hz because of axial–axial couplings both from H-11 and H-15, thus establishing an anti relationship between these three protons and a *trans*-ring fusion.

Glabramycin C (**3**) showed a molecular formula that was isomeric to that of **1**. Comparison of the ^1H and ^{13}C NMR spectra of **3** with those of compound **2** indicated the presence of a pair of olefinic protons, δ_H 6.23 (d, J=10.5 Hz) and 6.87 (dd, J=10.5, 4.5 Hz), which were assigned to H-13 and H-12 by COSY correlations and confirmed by their HMBC correlations to an upfield shifted C-14 carbonyl (δ_C 198.7), thus assigning structure **3** for glabramycin C (Table 1).

On the basis of these data, structures **1**, **2** and **3,** with relative configurations, were assigned for glabramycins A, B and C, respectively. Biogenetically, these compounds are likely to originate from a polyketide pathway by condensation of 11 acetate units to a undecaketide, which likely undergoes cyclization, reduction and dehydration to produce compound **1**, which then produces compounds **3** and **2**.

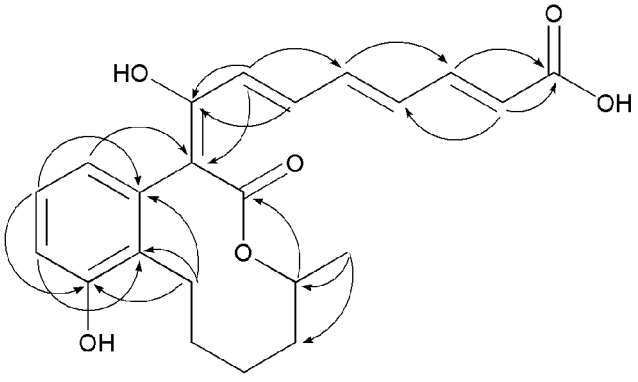

Figure 2 Heteronuclear multiple bond correlations (HMBC) of glabramycin A (**1**).

Biological activities

All three glabramycins were tested in the *S. aureus* antisense *rpsD*-sensitized two-plate differential sensitivity assay. Glabramycin C showed the most potent activity in this assay and showed a minimum detection concentration (MDC) of 62 μg ml^{-1}. At this concentration, a more than 5 mm zone differential was observed with a 10.78 mm zone of inhibition on the antisense plate vs a 5.63 mm zone of inhibition on the control plate. The size of the zone of clearance was dose dependent, and at 500 μg ml^{-1}, it produced a zone of clearance of 16.89 and 6.8 mm on the antisense and the control plate, respectively. The other two compounds were less active. Glabramycin A was approximately four-fold less active and showed intermediate activity with MDC of 250 μg ml^{-1}, producing zone sizes of 11.24 and 6.25 mm on the antisense and the control plate, respectively. The MDC of glabramycin B was greater than 500 μg ml^{-1}. Glabramycin C showed better activity against a panel of bacteria used in this assay. It inhibited *S. aureus* growth with MIC values of 16 μg ml^{-1} (Table 2). Glabramycin C exhibited a similar activity against *Bacillus subtilis,* but was less active against *Enterococcus faecalis* (MIC >32 μg ml^{-1}). The best activity was against *Streptococcus pneumoniae* regardless of the medium used, and inhibited the growth with an MIC value of 2 μg ml^{-1}. Glabramycins A and B were significantly less active, see Table 2. None of these compounds inhibited growth of Gram-negative bacteria or fungi *Candida albicans*. Mechanistically, glabramycin A, the most abundant of the three, showed 2–3-fold preferential inhibition of RNA synthesis (IC_{50} 10 μg ml^{-1}) compared with DNA and protein synthesis in a macromolecular synthesis assay (Figure 3). Inhibition of RNA synthesis, IC_{50} (10 μg ml^{-1}), of *S. aureus* is 10 times more potent than the MIC value (100 μg ml^{-1}) against the same *S. aureus* strain. Why the compounds discovered in this assay preferentially inhibit RNA synthesis rather than the expected protein synthesis is not clear and requires further investigation.

No compounds have earlier been reported from *N. glabra* strain, but a large number of biologically active compounds have been reported from genera *Neosartorya*, for example, the angiogenesis inhibitor, azaspirene.[21] It seems that the most chemically studied

Table 2 Antibacterial activities (MIC, μg ml^{-1})[a] of glabramycins A–C (1–3)

Strains[b]	*Phenotype*	*Strain #*	***1***[c]	***2***[c]	***3***[c]
S. aureus	meth^S	ATCC 29213	>64	>64	16
S. aureus	meth^S	MB2865	>64 (64)	>64	16 (8)
S. aureus (+50% human serum)	meth^S	MB2865	>64	>64	>32
S. pneumoniae[d]	pen^S, quin^S, mac^S	CL2883	>64	4	2
S. pneumoniae[e]	pen^S, quin^S, mac^S	CL2883	32	64	2
E. faecalis	van^S, mac^R	CL8516	>64	>64	>32 (32)
B. subtilis	Wt	MB964	>64	>64	16
H. influenzae	Amp^S, quin^S, mac^S	MB4572	>64	>64	>64
E. coli	Wt	MB2884	>64	>64	>32
E. coli envA/tolC	Wt	MB2884	64	>64	>32
C. albicans	Wt	MY1055	>64	>64	>32

Abbreviations: CAMHB, cation adjusted Mueller–Hinton broth; MIC, minimum inhibitory concentration; MIC80, minimum inhibitory concentration that inhibits 80% growth.
[a]MIC determined using NLSI protocols.
[b]All strains were tested in CAMHB medium, unless mentioned otherwise, under National Committee for Clinical laboratory Standards (NCCLS) guidelines.
[c]The data in parentheses are MIC80 values.
[d]CAMHB +2.5% lysed horse blood medium.
[e]Isosensitet medium.

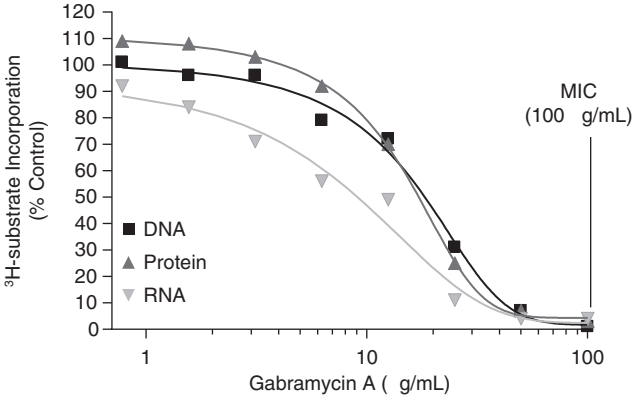

Figure 3 Macromolecular synthesis inhibition by glabramycin A (**1**) in *S. aureus*. No significant preference to inhibition of DNA, RNA and protein synthesis was observed.

species is *Neosartorya fischeri*, which is known to produce substance P inhibitors namely the fiscalins,[22] the toxin fischerin[23] and the tremorgenic mycotoxins, fumitremorgins,[23] neosartorrin,[24] and terreins.[25]

In conclusion, it is evident that the antisense screening approach provides higher sensitivity and allows the discovery of antibiotics with weaker activity, exemplified by the discovery of the three new compounds, glabramycins A–C. One of the three compounds showed moderate antibacterial activity without being a general toxin and can be exploited further. Screening using an antisense sensitized *rpsD* strains of *S. aureus* led to the isolation of a number of antibacterial agents that do not preferentially inhibit protein synthesis but often RNA synthesis. Understanding of this phenomenon requires further study.[14,15,17–19] Although lack of selectivity for protein synthesis inhibition by compounds discovered by *rpsD*-sensitized antisense screening is perplexing, it cannot be merely explained as a generalized technology artifact, because a similar screening approach using a *fabF*-sensitized strain led to the discoveries of platensimycin and platencin, highly selective fatty-acid synthesis inhibitors.[10,11]

EXPERIMENTAL SECTION

For general experimental procedure, see, for example, Zhang *et al.*[26]

Producing organism

The *N. glabra* (MF7030, F-155,700) strains were isolated from hot water-pasteurized soil collected from Candamia, near Valdefresno province of León, Spain. The ascomata, ascospores and conidial states were observed on malt yeast extract agar and were readily recognized as a species of *Neosartorya* (Ascomycota, Eurotiales).

The DNA of strain F-155,700 was extracted and used as a template for polymerase chain reaction (PCR) reactions. The D1D2 region of the large subunit of ribosomal DNA (LSU rDNA) was amplified and sequenced to aid in identification and to infer phylogenetic relationships of the strains to other fungi. The sequences were used to query GenBank for similar ribosomal sequences. The best matches with the large subunit (LSU) region and the percentage similarities were: *N. glabra* (U28456) 99%.

Inoculum was prepared by inoculating agar plugs into a 250 ml Erlenmeyer flask containing 60 ml seed medium of the following composition: g l^{-1} in distilled water (corn steep powder, 2.5; tomato paste, 40.0; oat flour; 10.0; glucose, 10.0; $FeSO_4{\cdot}7H_2O$, 0.01; $MnSO_4{\cdot}4H_2O$, 0.01; $CuCl_2{\cdot}2H_2O$, 0.0025; $CaCl_2{\cdot}2H_2O$, 0.001; H_3BO_3, 0.00056; $(NH_4)_6MoO_{24}{\cdot}4H_2O$, 0.00019; $ZnSO_4{\cdot}7H_2O$, 0.01). The pH was adjusted to 6.8 before autoclaving. The seed culture was incubated for 5 days at 22 °C on a gyratory shaker (220 rev min^{-1}) before the inoculation of the production medium. The production medium, designated asWS80, consisted of g/l in distilled water (whole wheat flour (Pillsbury), 50; xylose, 40; and fructose, 40). The 100 ml medium aliquots was dispensed in 500 ml Erlenmeyer flasks, inoculated with 1% volume of the seed culture, and were agitated for 14 days at 22 °C.

Extraction and isolation of glabramycins

One l fermentation broth (10 flasks) was extracted with one l acetone by shaking for 1 h after the harvest. The acetone extract (2 l) was evaporated under reduced pressure to less than one liter and further diluted with 500 ml water and loaded onto a 50 cc Amberchrome CG161 m (Rohm & Haas, Reading, PA, USA) column. The column was eluted with a 100 min 10–100% aqueous methanol-gradient. The activity was detected in a late eluting band. The active fraction (600 mg) was further purified by repeated reversed-phase HPLC (50% aqueous CH_3CN + 0.1% TFA on a Zorbax SB C_8, 24×250 mm, Agilent Technologies, Santa Clara, CA, USA). The identical fractions were pooled from 10 runs and lyophilized to afford glabramycin A (7 mg, 7 mg/l), glabramycin B (1.9 mg, 1.9 mg/l) and glabramycin C (1 mg, 1 mg/l) as yellow gums.

Glabramycin A (**1**): $[\alpha]^{23}_D$ +7.7 (*c* 0.44, CH_3OH), UV (CH_3OH) λ_{max} 278 (log ε 3.73), 333 (3.70), IR (ZnSe) ν_{max} 3369, 2936, 1684, 1627, 1580, 1498, 1457, 1377, 1284, 1252, 1210, 1142, 1052, 888 cm^{-1}, High Resolution Electrospray Ionization Fourier Transformation mass spectrometry (HRESIFTMS) (*m/z*) 385.1648 (calcd for $C_{22}H_{24}O_6$+H, 385.1651), for ^{1}H and ^{13}C NMR see Table 1.

Glabramycin B (**2**): $[\alpha]^{23}_D$−0.8 (*c* 0.6, CH_3OH), UV (CH_3OH) λ_{max} 269 (log ε 3.39), IR (ZnSe) ν_{max} 3445, 2966, 2933, 1722, 1693, 1661, 1465, 1375, 1239, 1190, 1128, 1013 cm^{-1}, HRESIFTMS (*m/z*) 387.1802 (calcd for $C_{22}H_{26}O_6$+H, 387.1808), for ^{1}H and ^{13}C NMR see Table 1.

Glabramycin C (**3**): $[\alpha]^{23}_D$−1.3 (*c* 0.6, CH_3OH), UV (CH_3OH) λ_{max} 277 (log ε 3.49), IR (ZnSe) ν_{max} 3445, 2965, 2933, 1735, 1657 1466, 1386, 1349, 1307, 1284, 1259, 1184, 1151, 1130, 1094, 1011 cm^{-1}, HRESIFTMS (*m/z*) 385.1647 (calcd for $C_{22}H_{22}O_6$+H, 385.1651), for ^{1}H and ^{13}C NMR see Table 1.

Two-plate differential sensitivity rpsD assay

Staphyloccus aureus cells (RN450) carrying plasmid S1-782B bearing antisense to *rps*D (AS-RNA strain) or a vector (control strain) were inoculated from a frozen vial source into a tube containing 3 ml of Miller's LB Broth (Invitrogen, Carlsbad, CA, USA) plus 34 μg ml^{-1}of chloramphenicol. Tubes were incubated at 37 °C at 220 r.p.m. for 18–20 h and kept at room temperature (23 °C) until use. Miller's LB broth was supplemented with 1.2% Select agar (Invitrogen), 0.2% glucose, 15 μg ml^{-1} chloramphenicol and 12 mM of xylose (only for the antisense strain). The OD_{600} of the culture was measured and diluted to 1/1000, and an OD 3.0 culture was inoculated. Next, 100 ml of the culture media was poured into each NUNC plate, the well-caster templates were placed into the agar and the agar was allowed to solidify. Thereafter, 20 μl of the test samples were added to the wells and the plates were incubated at 37 °C for 18 h and zones of inhibition were measured. MDC (minimum detection concentration) values were determined by two-fold serial dilution.

Antibiotic assay (MIC)

The MIC (minimum inhibitory concentration) against each of the strains was determined as described earlier and under the guidelines of the National Laboratory Standards Institute (NLSI). The Cells were inoculated at 10^5cfu ml^{-1}, followed by incubation at 37 °C with a 2-fold serial dilution of compounds in the growth medium for 20 h. MIC is defined as the lowest concentration of an antibiotic inhibiting visible growth.

Macromolecular synthesis inhibition

The assay was carried out as described earlier. Briefly, mid-log (A_{600}=0.5–0.6) *S. aureus* growths were incubated with an increasing concentration of each inhibitor at 37 °C for 20 min with 1 μCi ml^{-1} 6-[^{3}H]thymidine, 1 μCi ml^{-1} 5,6-[^{3}H]uracil or 5 μCi ml^{-1} 4,5-[^{3}H]leucine, to measure DNA, RNA and protein synthesis, respectively. The reaction was stopped by the addition of 10% trichloroacetic acid and the cells were harvested using a glass fiber filter

(Perkin-Elmer Life Sciences, Waltham, MA, USA, 1205-401). The filter was dried and counted with a scintillation fluid.

ACKNOWLEDGEMENTS

We thank John Ondeyka for some initial help.

1 Poehlsgaard, J. & Douthwaite, S. The bacterial ribosome as a target for antibiotics. *Nat. Rev. Microbiol.* **3,** 870–881 (2005).
2 Singh, S. B. & Barrett, J. F. Empirical antibacterial drug discovery-foundation in natural products. *Biochem. Pharmacol.* **71,** 1006–1015 (2006).
3 Ramakrishnan, V. Ribosome structure and the mechanism of translation. *Cell* **108,** 557–572 (2002).
4 Culver, G. M. Assembly of the 30S ribosomal subunit. *Biopolymers* **68,** 234–249 (2003).
5 Ogle, J. M., Carter, A. P. & Ramakrishnan, V. Insights into the decoding mechanism from recent ribosome structures. *Trends Biochem. Sci.* **28,** 259–266 (2003).
6 Grundy, F. J. & Henkin, T. M. The rpsD gene, encoding ribosomal protein S4, is autogenously regulated in Bacillus subtilis. *J. Bacteriol.* **173,** 4595–4602 (1991).
7 Forsyth, R. A. *et al.* A genome-wide strategy for the identification of essential genes in Staphylococcus aureus. *Mol. Microbiol.* **43,** 1387–1400 (2002).
8 Young, K. *et al.* Discovery of FabH/FabF inhibitors from natural products. *Antimicrob. Agents Chemother.* **50,** 519–526 (2006).
9 Singh, S. B., Phillips, J. W. & Wang, J. Highly sensitive target based whole cell antibacterial discovery strategy by antisense RNA silencing. *Curr. Opin. Drug Discov. Dev.* **10,** 160–166 (2007).
10 Wang, J. *et al.* Platensimycin is a selective FabF inhibitor with potent antibiotic properties. *Nature* **441,** 358–361 (2006).
11 Wang, J. *et al.* Platencin is a dual fabf and fabh inhibitor with potent *in vivo* antibiotic properties. *Proc. Natl Acad. Sci. USA* **104,** 7612–7616 (2007).
12 Singh, S. B. *et al.* Isolation, structure, and absolute stereochemistry of platensimycin, a broad spectrum antibiotic discovered using an antisense differential sensitivity strategy. *J. Am. Chem. Soc.* **128,** 11916–11920, 15547 (2006).
13 Jayasuriya, H. *et al.* Isolation and structure of platencin: a novel FabH and FabF dual inhibitor with potent broad spectrum antibiotic activity produced by Streptomyces platensis MA7339. *Angew. Chem. Int. Ed. Engl.* **46,** 4684–4688 (2007).
14 Singh, S. B. *et al.* Discovery of lucensimycins A and B from Streptomyces lucensis MA7349 using an antisense strategy. *Org. Lett.* **8,** 5449–5452 (2006).
15 Singh, S. B., Zink, DL, Herath, KB, Salazar, O & Genilloud, O Discovery and antibacterial activity of lucensimycin C from Streptomyces lucensis. *Tetrahedron Lett.* **49,** 2616–2619 (2008).
16 Singh, S. B. *et al.* Isolation, structure, and antibacterial activities of lucensimycins D-G, discovered from Streptomyces lucensis MA7349 using an antisense strategy (perpendicular). *J. Nat. Prod.* e-pub ahead of print 30 December 2008 (2008).
17 Ondeyka, J. G., *et al.* Coniothyrione, a chlorocyclopentandienylbenzopyrone as a bacterial protein synthesis inhibitor discovered by antisense technology. *J. Nat. Prod.* **70,** 668–670 (2007).
18 Zhang, C. *et al.* Isolation, structure and antibacterial activity of pleosporone from a pleosporalean ascomycete discovered by using antisense strategy. *Bioorg. Med. Chem.* **17,** 2162–2166 (2009).
19 Zhang, C. *et al.* Isolation, structure and antibacterial activity of phaeosphenone from a phaeosphaeria sp. Discovered by antisense strategy. *J. Nat. Prod.* **71,** 1304–1307 (2008).
20 Zhang, C. *et al.* Discovery of okilactomycin and congeners from Streptomyces scabrisporus by antisense differential sensitivity assay targeting ribosomal protein S4. *J. Antibiot. (Tokyo)* **62,** 55–61 (2009).
21 Asami, Y. *et al.* Azaspirene: a novel angiogenesis inhibitor containing a 1-oxa-7-azaspiro[4.4]non-2-ene-4,6-dione skeleton produced by the fungus Neosartorya sp. *Org. Lett.* **4,** 2845–2848 (2002).
22 Wong, S. M., et al Fiscalins: new substance P inhibitors produced by the fungus Neosartorya fischeri. Taxonomy, fermentation, structures, and biological properties. *J. Antibiot. (Tokyo)* **46,** 545–553 (1993).
23 Fujimoto, H., Ikeda, M., Yamamoto, K. & Yamazaki, M. Structure of fischerin, a new toxic metabolite from an ascomycete, Neosartorya fischeri var. fischeri. *Nat. Prod.* **56,** 1268–1275 (1993).
24 Proksa, B., Uhrin, D., Liptaj, T. & Sturdikova, M. Neosartorin, an ergochrome biosynthesized by Neosartorya fischeri. *Phytochemistry* **48,** 1161–1164 (1998).
25 Hong, S. B., Go, S. J., Shin, H. D., Frisvad, J. C. & Samson, R. A. Polyphasic taxonomy of Aspergillus fumigatus and related species. *Mycologia* **97,** 1316–1329 (2005).
26 Zhang, C. *et al.* Isolation, structure, and antibacterial activity of philipimycin, a thiazolyl peptide discovered from Actinoplanes philippinensis MA7347. *J. Am. Chem. Soc.* **130,** 12102–12110 (2008).
27 Kodali, S. *et al.* Determination of selectivity and efficacy of fatty acid synthesis inhibitors. *J. Biol. Chem.* **280,** 1669–1677 (2005).
28 Onishi, H. R. *et al.* Antibacterial agents that inhibit lipid A biosynthesis. *Science* **274,** 980–982 (1996).

The Journal of Antibiotics (2009) 62, 271–276
© 2009 Japan Antibiotics Research Association All rights reserved 0021-8820/09 $32.00
www.nature.com/ja

ORIGINAL ARTICLE

Prodigiosin biosynthesis gene cluster in the roseophilin producer *Streptomyces griseoviridis*

Takashi Kawasaki, Fumi Sakurai, Shun-ya Nagatsuka and Yoichi Hayakawa

***Streptomyces griseoviridis* 2464-S5 produces prodigiosin R1, a tripyrrole antibiotic, and roseophilin, a structurally related compound containing two pyrrole and one furan rings. A gene cluster for the biosynthesis of a prodigiosin was identified in *S. griseoviridis*. The cluster consisted of 24 open reading frames, including 21 genes (*rphD–rphZ*) homologous to prodigiosin biosynthesis genes in the *red* cluster in *Streptomyces coelicolor* A3(2). The expression of *rphN* in *S. coelicolor* lacking *redN* restored the production of prodigiosin.**
The Journal of Antibiotics (2009) **62,** 271–276; doi:10.1038/ja.2009.27; published online 27 March 2009

Keywords: biosynthesis gene; prodigiosin; roseophilin; *Streptomyces griseoviridis*

INTRODUCTION

Several tripyrrole antibiotics are known to belong to the prodigiosin family.[1–4] *S. griseoviridis* 2464-S5 produces prodigiosin R1[5] and roseophilin,[6] a structurally related compound containing two pyrrole and one furan rings, as shown in Figure 1. Roseophilin is considered to be biosynthesized partially with the same pathway as prodigiosin R1. Prodigiosin-family biosynthesis genes have been reported to exist in the *pig* gene clusters in *Serratia marcescens* ATCC 274 and *Serratia* sp. ATCC 39006 (which make prodigiosin itself),[7] in the *red* gene cluster in *S. coelicolor* A3(2) (which makes undecylprodiginine)[8] and in the *hap* gene cluster in *Hahella chejuensis* KCTC 2396 (which makes prodigiosin itself).[9] PCR amplification of *S. griseoviridis* genomic DNA has identified genes homologous to *redH*, *redM* and *redW,* involved in the biosynthesis of undecylprodiginine in *S. coelicolor* (Figure 2).[5] We report herein the cloning and characterization of the *rph* gene cluster for prodigiosin biosynthesis from *S. griseoviridis* 2464-S5.

RESULTS

Amplification of prodigiosin biosynthesis genes from *S. griseoviridis*

In the biosynthesis of prodigiosin, the *redN*/*pigH* gene product is involved in the formation of the central pyrrole moiety (Figure 2). As roseophilin contains a furan ring in place of the central pyrrole ring in prodigiosins, *redN*/*pigH* might be characteristic of the prodigiosin biosynthesis. A pair of primers was designed from the conserved amino acid (aa) sequences of *redN*/*pigH* in the three prodigiosin producers, *S. coelicolor* A3(2), *Serratia marcescens* ATCC 274 and *Serratia* sp. ATCC 39006.[7,8] PCR amplification of *S. griseoviridis* genomic DNA gave a *redN*/*pigH*-like gene fragment. Nucleotide sequencing and homology search showed that the fragment shared amino acid identity of 84% with RedN.

The prodigiosin biosynthesis genes, *redM* and *redW,* encode L-prolyl-AMP ligase and L-prolyl-PCP dehydrogenase, respectively (Figure 2). These two enzymes have been reported to be commonly involved in the biosynthesis of pyrrole-containing antibiotics.[10] PCR was carried out using several primers designed from the conserved amino acid sequences of L-prolyl-AMP ligase and L-prolyl-PCP dehydrogenase genes in the coumermycin A_1 producer, *Streptomyces rishiriensis* DSM 40489 (*proB* and *proA*),[11] in the pyrrolomycin producers, *Streptomyces vitaminophilum* ATCC 31673 (*pyr8* and *pyr7*) and *Streptomyces* sp. Strain UC 11065 (*dox8* and *dox7*)[12] and in the prodigiosin producer, *S. coelicolor* A3(2) (*redM* and *red W*). DNA sequencing of the PCR products identified single genes encoding L-prolyl-AMP ligase and L-prolyl-PCP dehydrogenase in *S. griseoviridis*.

Southern hybridization of genomic DNA with prodigiosin biosynthesis genes

Southern blot analysis was carried out on *S. griseoviridis* genomic DNA to identify *redH*-, *redM*-, *redN*- and *redW*-like genes. Digested genomic DNA with *Bam*HI in agarose gel was hybridized with the PCR products as probes. Each single band was detected by Southern hybridization as shown in Figure 3, suggesting that the strain contained a single set of genes for prodigiosin/roseophilin biosynthesis.

Cloning of a prodigiosin biosynthesis gene cluster from *S. griseoviridis*

A cosmid clone was selected by colony hybridization and Southern blot analysis from a cosmid library using the *redW*-like gene fragment as a probe. Nucleotide sequencing identified genes homologous to *redY, redX* and *redD,* as well as *redW,* in a *Sac*I 6.0-kbp fragment of the cosmid (Figure 4). Further Southern hybridization was carried out on

Department of Medicinal and Life Science, Faculty of Pharmaceutical Sciences, Tokyo University of Science, Yamazaki, Noda, Chiba, Japan
Correspondence: Dr Y Hayakawa, Faculty of Pharmaceutical Sciences, Tokyo University of Science, 2641 Yamazaki, Noda, Chiba 278-8510, Japan.
E-mail: hykw@rs.noda.tus.ac.jp
Received 14 November 2008; revised 27 February 2009; accepted 5 March 2009; published online 27 March 2009

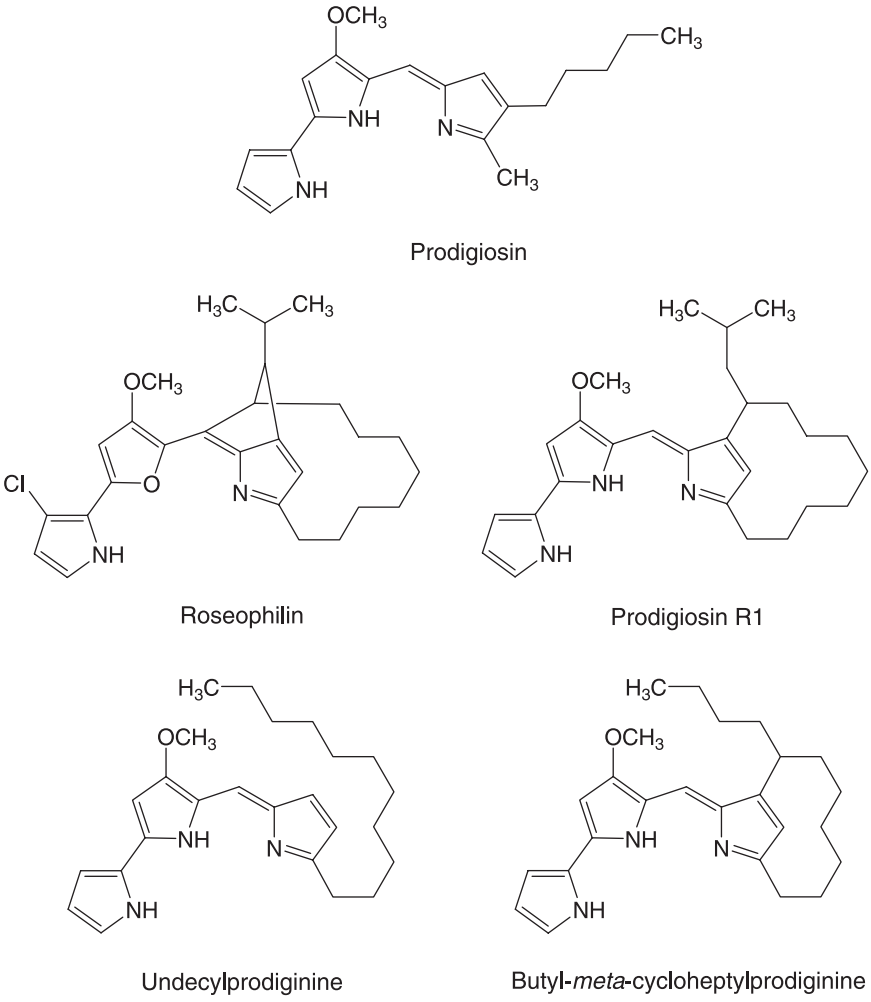

Figure 1 Structures of roseophilin and prodigiosins.

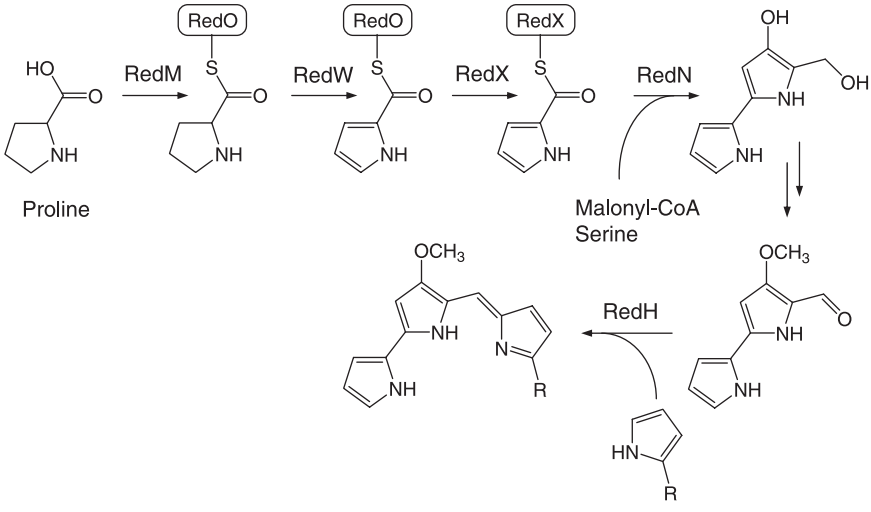

Figure 2 Proposed pathway of prodigiosin biosynthesis.

various cosmid fragments using the *redH*-, *redM*- and *redN*-like gene fragments as probes. Selected cosmid fragments were sequenced to identify a gene cluster containing 24 open reading frames (ORFs) as shown in Figure 4. Homology search showed that 21 of the 24 ORFs were homologous to the *red* genes involved in the biosynthesis of undecylprodiginine and butyl-*meta*-cycloheptylprodiginine in

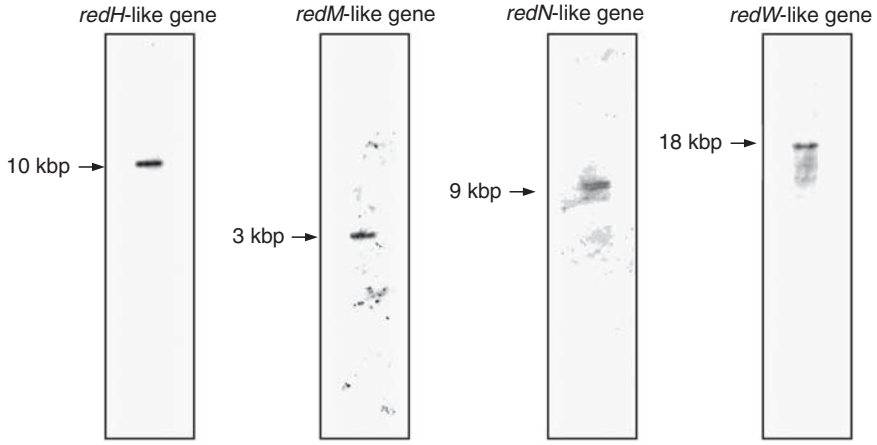

Figure 3 Southern blot analysis of *S. griseoviridis* genomic DNA.

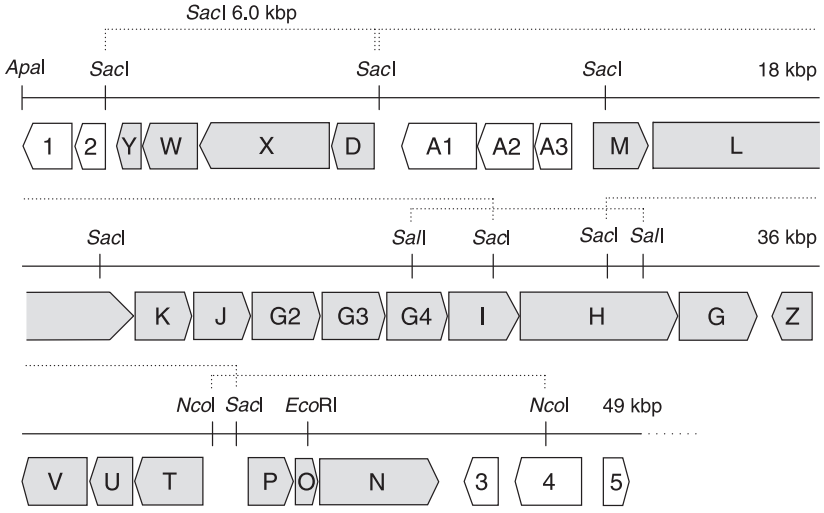

Figure 4 Prodigiosin biosynthesis gene cluster (*rph* cluster) from *S. griseoviridis*.

S. coelicolor A3(2),[8] and the corresponding genes in *S. griseoviridis* were designated as *rphD–rphZ* (Table 1). In the cluster, sequence homology of *rphA1* and *rphA2* to ABC-transporter genes assigned them to self-resistance genes. A regulatory gene, *rphA3*, was also identified from sequence homology to a transcriptional regulator gene in *Mycobacterium ulcerans* (Table 1).

Expression of *rphN* in *S. coelicolor* lacking *redN*

To establish the function of the *rph* genes, we disrupted the *redN* gene in *S. coelicolor* A3(2). The disruption plasmid, pRedN-DIS, was constructed (Figure 5) and introduced into *S. coelicolor*. Three colorless colonies were selected on R2YE plates and the *redN* gene disruption was confirmed by PCR analysis using their genomic DNAs as templates.

The *rphN* expression vector, pWHM-rphN, was constructed and introduced into *S. coelicolor* lacking *redN* (*S. coelicolor* Δ*redN*). *S. coelicolor* Δ*redN*, harboring pWHM-rphN or an empty vector (pWHM860), and the wild-type strain were cultivated and the mycelial extracts were analyzed by HPLC. The *redN* disruptant expressing *rphN* produced undecylprodiginine, a major prodigiosin from the wild type (Figure 6), thereby showing that *rphN* can act as a prodigiosin biosynthesis gene in *S. coelicolor*.

DISCUSSION

The *rph* gene cluster consisted of 21 genes homologous to prodigiosin biosynthesis genes in *S. coelicolor*, two self-resistance genes and a regulatory gene. The putative functions and locations of *orf1* (DNA helicase) and *orf3* (RNA methyltransferase) suggested that *orf1*, *orf2*, *orf3*, *orf4* and *orf5* are excluded from the biosynthesis gene cluster (Table 1 and Figure 4). The *rph* cluster did not contain genes homologous to *redC*, *redE*, *redF*, *redQ*, *redR* or *redS* in *S. coelicolor* (Figure 7). Among them, *redQ* and *redR* have been reported to be involved in the biosynthesis of an alkyl side chain and not to be essential for the biosynthesis of undecylprodiginine.[13] Although the *redF*-homologous gene, *pigN*, was involved in *O*-methylation, two *pigN* mutants reduced, but retained, prodigiosin productivity.[14] No role has been assigned to *redS* in the prodigiosin pathway and only the 146 aa *N*-terminal region of PigB (671 aa) shows sequence similarity with RedS.[7] In *Serratia* sp., PigB catalyzes the formation of 2-methyl-3-*n*-amylpyrrole (MAP), which is replaced by 2-undecylpyrrole in *S. coelicolor*.[14] No role has been assigned to *redC* or to *redE*, and no homologous genes have been found in the *pig* cluster in *Serratia* sp.[7] These findings suggest that these genes are non-essential for the biosynthesis of prodigiosins, and the *rph* gene cluster identified here contains all the genes for prodigiosin biosynthesis in

Table 1 Deduced functions of gene products in the *rph* cluster

Gene products	*Homologous protein*	*Identity (%)*
Orf1	ATP-dependent DNA helicase of *Streptomyces avermitilis*	77
Orf2	Uncharacterized protein of *S. avermitilis*	47
RphY	Hypothetical protein (RedY)	55
RphW	L-Prolyl-PCP dehydrogenase (RedW)	69
RphX	β-Ketomyristoyl-ACP synthase (RedX)	47
RphD	Transcriptional regulator (RedD)	61
RphA1	ABC-transporter of *Mycobacterium ulcerans*	46
RphA2	ABC-transporter of *M. ulcerans*	57
RphA3	Transcriptional regulator of *M. ulcerans*	40
RphM	L-Prolyl-AMP ligase (RedM)	54
RphL	Polyketide synthase (RedL)	54
RphK	Oxidoreductase (RedK)	68
RphJ	Thioesterase (RedJ)	58
RphG2	Oxygenase (RedG)	51
RphG3	Oxygenase (RedG)	39
RphG4	Oxygenase (RedG)	44
RphI	*O*-methyltransferase (RedI)	59
RphH	Pyrrole-condensing enzyme (RedH)	59
RphG	Oxygenase (RedG)	57
RphZ	Response regulator (RedZ)	50
RphV	Dehydrogenase (RedV)	42
RphU	Phosphopantetheinyl transferase (RedU)	46
RphT	Hypothetical protein (RedT)	63
RphP	3-Oxoacyl-ACP synthase (RedP)	58
RphO	Peptidyl carrier protein (RedO)	75
RphN	4-Hydroxy-2,2'-bipyrrole-4-methanol synthase (RedN)	78
Orf3	RNA methyltransferase of *Brucella abortus*	31
Orf4	Uncharacterized protein of *Streptomyces coelicolor*	54
Orf5	Integral membrane protein of *S. coelicolor*	63

S. griseoviridis. Moreover, primers designed from *redS*/*PigB* and *redF*/*pigN* did not amplify *S. griseoviridis* genomic DNA (data not shown).

The *rph* cluster included four putative oxygenase genes (*rphG*, *rphG2*, *rphG3* and *rphG4*) homologous to *redG*, which was assumed to catalyze the cyclization of an alkyl side chain for the biosynthesis of butyl-*meta*-cycloheptylprodiginine.[8] The same function is required by the high-sequence similarity of *rphG* and *redG* and their locations (Table 1 and Figure 7). The difference in the number and position of carbon–carbon bridges between prodigiosin R1 and roseophilin might be explained by the presence of multiple oxygenase genes.

The *rph* cluster did not contain biosynthesis genes characteristic of roseophilin. Such genes are involved in the furan ring formation and chlorination. The PCR and Southern hybridization analyses, however, detected single genes homologous to *redH*, *redM* and *redW*, which are considered to be common to both prodigiosin and roseophilin biosynthesis. These results suggested the existence of another gene cluster to complement the biosynthesis of roseophilin. Search for the second gene cluster for the roseophilin biosynthesis is in progress.

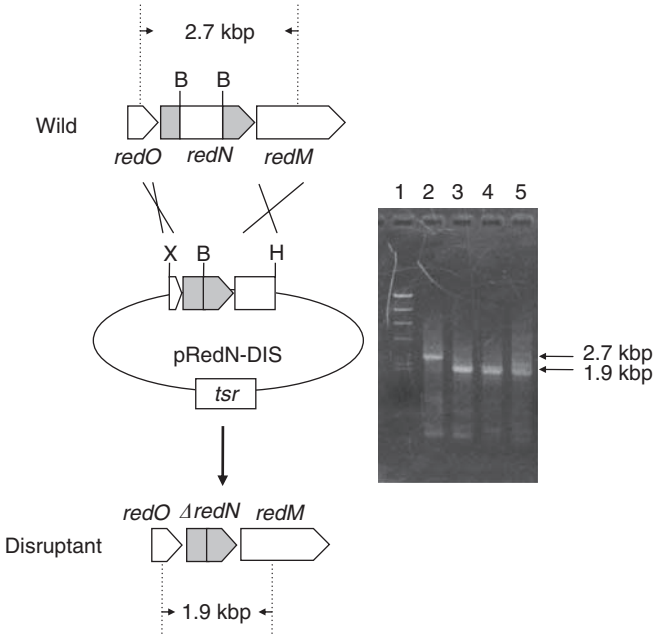

Figure 5 Disruption of the *redN* gene in *S. coelicolor*. Molecular marker (lane 1), PCR product from the wild-type strain (lane 2) and PCR products from the *redN* disruptants (lane 3–5). Amplified fragments are shown schematically. Arrows indicate primers used for PCR analysis. B: *Bgl*II site. X: *Xba*I site. H: *Hind*III site.

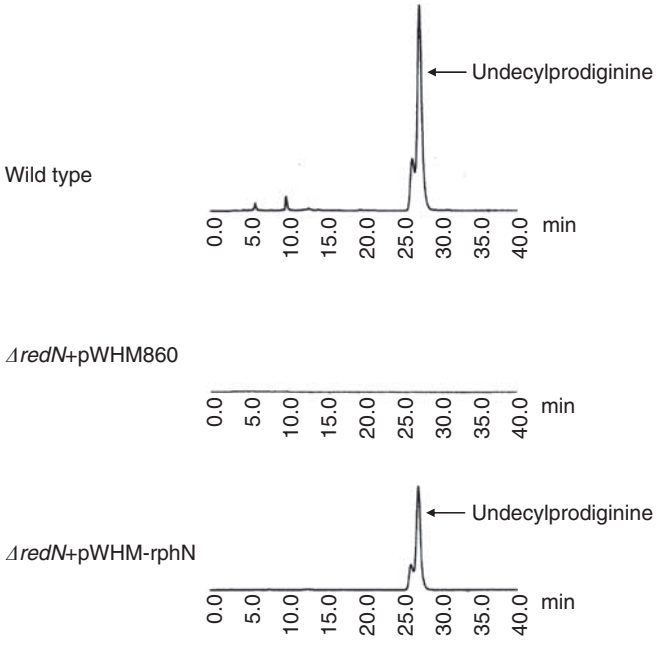

Figure 6 HPLC analysis of prodigiosins produced by the *redN* disruptant expressing *rphN*.

METHODS

Bacterial strains, plasmids and culture conditions

S. griseoviridis 2464-S5 and *S. coelicolor* A3(2) were used as sources of total DNA for the cloning experiment. Media and growth conditions for *S. griseoviridis* were described earlier.[6] Prodigiosin production by *S. coelicolor* was assessed on R2YE plates.[15] Yeast extract malt extract (YEME) liquid culture was used for genomic DNA isolation and for making protoplasts from *S. coelicolor*.[15] *Escherichia coli* XL1-blue MRF' and the plasmids, pGEM-5Z, pGEM-7Z, pGEM-11Z, pUC118 and pUC119 were used for sequencing analyses.

DNA isolation and manipulation

All restriction enzymes, T4 DNA ligase and calf intestinal alkaline phosphatase were obtained from Nippon Gene (Toyama, Japan). Transformation of *E. coli*

with plasmid DNA by electroporation was carried out under standard conditions using a Gene Pulser II electroporation system (Bio-Rad, Hercules, CA, USA). Other general procedures were carried out as described by Sambrook *et al.*[16]

Amplification and cloning of prodigiosin biosynthesis genes

A *redN*-like gene fragment was amplified using *S. griseoviridis* genomic DNA and a pair of primers (5′-GAYGGSGTSTTYWSSATGCAYGG-3′ and 5′-SGGRWASACSACSGTYTGRCA-3′). The reaction mixture consisted of 1× GC buffer I (TaKaRa, Kyoto, Japan), 0.4 mM dNTP (deoxyribonucleotide triphosphate) mixture, 2 μM of each primer, 0.5 ng μl^{-1} genomic DNA and 0.05 U μl^{-1} *LA Taq* DNA polymerase (TaKaRa). After heating at 95 °C for 4 min, PCR was carried out for 30 cycles (95 °C 1 min, 50 °C 30 s, 72 °C 45 s). After purification with QIAquick Gel Extraction Kit (Qiagen, Hilden, Germany), the PCR products were linked with pGEM-T Easy Vector (Promega, Madison, WI, USA) using a T4 DNA ligase. *E. coli* was transformed with the plasmid DNA and selected clones were used for sequencing analysis.

Three sets of primers (N1: 5′-CTSTACACSTCSGGSWSSACSGG-3′; C1: 5′-GTGCASACGTTSGTCTCSGTSGG-3′, C2: 5′-AGSRCSGASGGSACSGARTACCA-3′, C3: 5′-AGSRCGCTSGGSACSGARTACCA-3′) were used to amplify L-prolyl-AMP ligase gene fragments. Various pairs of primers (N1: 5′-TGGGAGMGSRCSTGCCT-3′, N2: 5′-CAGGCSRTSTCSCACMGSMT-3′, N3: 5′-CAGGCSRTSAGCCACMGSMT-3′; C1: 5′-ATSTCSSWSGTSCCSGAGAADAT-3′, C2: 5′-ATSTCSSWSGTSCCGCTGAADAT-3′, C3: 5′-ATSTCSKTSGTSCCSGAGAADAT-3′, C4: 5′-ATSTCSKTSGTSCCGCTGAADAT-3′) were used for the amplification of L-prolyl-PCP dehydrogenase gene fragments. PCR and cloning were carried out as described above.

Southern blot analysis of genomic DNA

Gene fragments homologous to *redH*, *redM* and *redW* have been amplified earlier by PCR from the roseophilin producer.[5] DNA fragments used as probes were labeled using the AlkPhos Direct labeling kit (GE Healthcare, Piscataway, NJ, USA). *S. griseoviridis* genomic DNA was digested with *Bam*HI and run on a 0.7% agarose gel. The DNA was transferred to nylon membranes and fixed. After the membranes were incubated with probes at 65 °C for 16 h, they were washed and then developed using the ECF detection kit (GE Healthcare). Images were obtained with an FLA2000 image reader (Fujifilm, Tokyo, Japan).

Cloning of a prodigiosin biosynthesis gene cluster

A cosmid library was constructed from the roseophilin producer. Genomic DNA of *S. griseoviridis* 2464-S5 was partially digested with *Sau*3AI and ligated to the pWE15 cosmid vector (Stratagene, La Jolla, CA, USA). The ligated DNAs were packaged using Gigapack III XL Packaging Extract (Stratagene) and used to infect *E. coli* XL1-blue MRF′. *E. coli* colonies obtained by transfection with the cosmids were then screened for the presence of a *redW*-like gene by colony hybridization, using the PCR product labeled with the AlkPhos Direct labeling kit (GE Healthcare) as a probe. Selected positive clones were subsequently analyzed by Southern hybridization with the same probe, and cosmid 31 was unambiguously found to contain the *redW*-like sequence. A *Sac*I 6.0-kbp fragment of the cosmid was sequenced to identify genes homologous to *redD*, *redX*, *redW* and *redY*. To isolate the biosynthesis gene cluster, cosmids were selected using *redM*-, *redH*- and *redN*-like genes as probes, and DNA sequencing was carried out using a *Sac*I 21.0-kbp fragment of cosmid16, a *Sal*I 5.0-kbp fragment of cosmid4, a *Sac*I 8.0-kbp fragment of cosmid10 and a *Nco*I 7.0-kbp fragment of cosmid11 (Figure 4).

Gene disruption in *S. coelicolor*

The disruption plasmid, pWHM3-DIS, was based on pWHM3, an *E. coli*/*Streptomyces* shuttle vector (7.2 kbp) containing a thiostrepton-resistant gene.[15] pWHM3 was digested with *Bcl*I and a 1.4-kbp fragment containing a part of the replication region in *Streptomyces* was removed. The remaining two *Bcl*I fragments (4.7 kbp and 1.1 kbp) were ligated to construct pWHM3-DIS.

The *redN* gene was disrupted by a double crossover event (Figure 5). A 2.7 kbp *Xba*I/*Hind*III fragment of *redN* contained both the upstream and downstream regions. The *redN* gene fragment was amplified by PCR with *S. coelicolor* genomic DNA and one set of primers with an additional restriction site (5′-TGCTCTAGATTCGACCTCGTCCACTACCTGCAG-3′ and 5′-ACCAAGCTTGTCGCCGGGGGTGAGGGAGGGCAG-3′). The PCR product and *Xba*I/*Hind*III-digested pGEM-11Z were ligated and introduced into *E. coli*. A plasmid carrying the appropriate DNA fragment was selected. After sequence confirmation, the plasmid was digested with *Bgl*II. A 0.7 kbp *Bgl*II DNA fragment in the *redN* gene was removed and the remaining 5.0-kbp fragment containing pGEM-11Z was self-ligated. A 2.0 kbp *Xba*I/*Hind*III fragment obtained from the plasmid was subcloned into the same site of pWHM3-DIS to give pRedN-DIS.

The disruption plasmid, pRedN-DIS, was introduced into *S. coelicolor*, and thiostrepton-resistant colonies were selected. After the selected colonies were cultivated for 3 days, an aliquot of the culture was plated on ATCC medium #5 plates to obtain spores. Diluted spores were plated on ATCC medium #5 plates and thiostrepton-sensitive colonies were selected. Genomic DNA was prepared from the transformant and subjected to PCR analysis with the same primers that were used to amplify a 2.7 kbp DNA fragment of the *redN* gene.

Expression of *rphN* in the *redN* disruptant

To express the *rphN* gene in the *redN* disruptant, *S. coelicolor* Δ*redN*, the *rphN*-carrying plasmid, pWHM-rphN, was constructed. To obtain the entire *rphN* gene, PCR amplification was carried out under a standard condition with KOD-DNA polymerase (Toyobo, Osaka, Japan) using a pair of primers with an additional restriction site (5′-TGCTCTAGAATGACCCACATCATGACCGACCGT-3′ and 5′-ACCAAGCTTTCAGGCCGGATCGAGGGGGACGCC-3′). After sequence confirmation, the *Xba*I/*Hind*III DNA fragment was inserted into the same sites of pWHM860[17] to give pWHM-rphN, in which the *rphN* gene was expressed under the control of the *ermE** promoter.

pWHM-rphN was introduced into *S. coelicolor* Δ*redN*, and the transformants were cultivated at 27 °C for 6 days on a rotary shaker in 500-ml Erlenmeyer flasks containing 100 ml of production medium. The medium

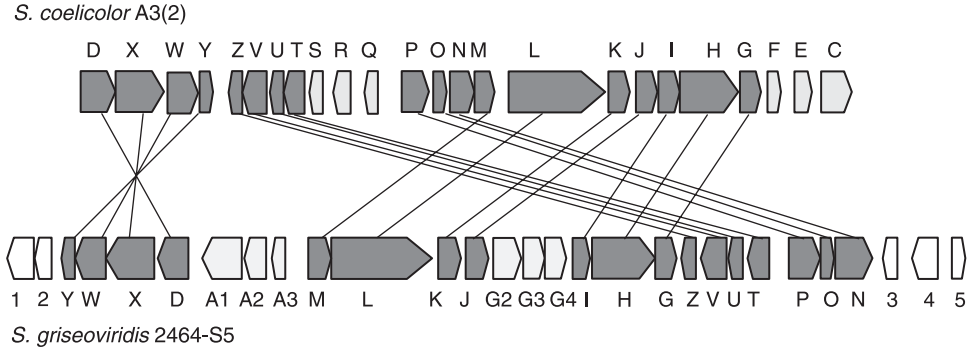

Figure 7 Comparison of the prodigiosin biosynthesis gene clusters between *S. coelicolor* (*red*) and *S. griseoviridis* (*rph*).

contained sucrose 103 g, glucose 10 g, yeast extract (Difco, Detroit, MI, USA) 5 g, Casamino acids (Difco) 0.1 g, sodium hydrogen L-glutamate monohydrate 3 g, K_2SO_4 0.25 g, $MgCl_2.6H_2O$ 10.12 g, $NaNO_3$ 0.06 g, TES (*N*-tris(hydroxymethyl)methyl-2-aminoethanesulfonic acid) buffer 5.73 g, 0.5 % KH_2PO_4 10 ml, 5 M $CaCl_2$ 4 ml, 1 M NaOH 7 ml and a trace element solution of 2 ml in 1000 ml distilled water (pH 7.2). The trace element solution consisted of $ZnCl_2$ 0.004%, $FeCl_2.6H_2O$ 0.02%, $CuCl_2.2H_2O$ 0.001%, $MnCl_2.4H_2O$ 0.001%, $Na_2B_4O_7.10H_2O$ 0.001% and $(NH_4)_6Mo_7O_{24}.4H_2O$ 0.001%. The fermentation broth (100 ml) was centrifuged and mycelium was extracted with acetone. After evaporation, an aqueous concentrate was extracted with ethyl acetate. The extract was dissolved in methanol and the productivity of prodigiosins was examined by reversed-phase HPLC (Senshu Pak PEGASIL ODS 4.6 i.d.×250 mm, Senshu Scientific, Tokyo, Japan) with methanol–acetonitrile–trifluoroacetic acid–water (80:3:0.15:17) at a flow rate of 1.0 ml min^{-1}. The corresponding peak was detected at 530 nm.

Nucleotide sequence and accession number

DNA sequencing was carried out with an automatic DNA sequencer (3100 Genetic Analyzer, Applied Biosystems, Foster City, CA, USA). Nucleotide sequences reported here have been deposited in the GenBank, DDBJ and EMBL databases under accession number AB469822 (*rph* gene cluster).

ACKNOWLEDGEMENTS

We thank Dr T Dairi of the Toyama Prefectural University for the generous gift of plasmids, *E. coli* strains and *S. coelicolor* A3(2). This work was supported in part by a Grant-in-Aid for Scientific Research, The Ministry of Education, Science, Sports and Culture, Japan.

1 Rapoport, H. & Holden, K. G. The synthesis of prodigiosin. *J. Am. Chem. Soc.* **84,** 635–642 (1962).
2 Gerber, N. N. & Stahly, P. D. Prodiginine (prodigiosin-like) pigments from *Streptoverticillium rubrireticuli*, an organism that causes pink staining of polyvinyl chloride. *Appl. Microbiol.* **30,** 807–810 (1975).
3 Tsao, S-W., Rudd, B. A. M., He, X-G., Chang, C-J. & Floss, H. G. Identification of a red pigment from *Streptomyces coelicolor* A3(2) as a mixture of prodigiosin derivatives. *J. Antibiot.* **38,** 128–131 (1985).
4 Song, J-M. *et al*. Purification and characterization of prodigiosin produced by integrated bioreactor from *Serratia* sp. KH-95. *J. Biotechnol. Bioeng.* **101,** 157–161 (2006).
5 Kawasaki, T., Sakurai, F. & Hayakawa, Y. A prodigiosin from the roseophilin producer *Streptomyces griseoviridis*. *J. Nat. Prod.* **71,** 1265–1267 (2008).
6 Hayakawa, Y., Kawakami, K., Seto, H. & Furihata, K. Structure of a new antibiotic, roseophilin. *Tetrahedron Lett.* **33,** 2701–2704 (1992).
7 Harris, A. K. P. *et al*. The *Serratia* gene cluster encoding biosynthesis of red antibiotic, prodigiosin, shows species- and strain-dependent genome context variation. *Microbiology* **150,** 3547–3560 (2004).
8 Cerdeno, A. M., Bibb, M. J. & Challis, G. L. Analysis of the prodiginine biosynthesis gene cluster of *Streptomyces coelicolor* A3(2): new mechanisms for chain initiation and termination in modular multienzymes. *Chem. Biol.* **8,** 817–829 (2001).
9 Kim, D. *et al*. Analysis of a prodigiosin biosynthetic gene cluster from the marine bacterium *Hahella chejuensis* KCTC 2396. *J. Microbiol. Biotechnol.* **16,** 1912–1918 (2006).
10 Thomas, M. G., Burkart, M. D. & Walsh, C. T. Conversion of L-proline to pyrrolyl-2-carboxyl-S-PCP during undecylprodigiosin and pyoluteorin biosynthesis. *Chem. Biol.* **9,** 171–184 (2002).
11 Wang, Z. X., Li, S. M. & Heide, L. Identification of the coumermycin A_1 biosynthetic gene cluster of *Streptomyces rishiriensis* DSM 40489. *Antimicrob. Agents Chemother.* **44,** 3040–3048 (2000).
12 Zhang, X. & Parry, R. J. Cloning and characterization of the pyrrolomycin biosynthesis gene clusters from *Actinosporangium vitaminophilum* ATCC 31673 and *Streptomyces* sp. strain UC 11065. *Antimicrob. Agents Chemother.* **51,** 946–957 (2007).
13 Mo, S. *et al*. Elucidation of the *Streptomyces coelicolor* pathway to 2-undecylpyrrole, a key intermediate in undecylprodiginine and streptorubin B biosynthesis. *Chem. Biol.* **15,** 137–148 (2008).
14 Williamson, N. R. *et al*. Biosynthesis of the red antibiotic, prodigiosin, in *Serratia*: identification of a novel 2-methyl-3-n-amyl-pyrrol (MAP) assembly pathway, definition of the terminal condensing enzyme, and implications for undecylprodiginine in biosynthesis in *Streptomyces*. *Mol. Microbiol.* **56,** 971–989 (2005).
15 Kieser, T., Bibb, M. J., Buttner, M. J., Chater, K. F. & Hopwood, D. A. *Practical Streptomyces Genetics* 405–420 (The John Innes Foundation, Norwich, 2000).
16 Sambrook, J. & Russell, D. W. *Molecular Cloning: A Laboratory Manual* 1.1–1.162 (Cold Spring Harbor Laboratory, Cold Spring Harbor, New York, 2001).
17 Meurer, G. & Hutchinson, R. Functional analysis of putative β-ketoacyl: acyl carrier protein synthase and acyltransferase active site motifs in a type II polyketide synthase of *Streptomyces glaucescens*. *J. Bacteriol.* **177,** 477–481 (1995).

The Journal of Antibiotics (2009) 62, 277–282
© 2009 Japan Antibiotics Research Association All rights reserved 0021-8820/09 $32.00
www.nature.com/ja

ORIGINAL ARTICLE

Chitinase inhibitors: extraction of the active framework from natural argifin and use of *in situ* click chemistry

Tomoyasu Hirose[1], Toshiaki Sunazuka[1], Akihiro Sugawara[1], Ayako Endo[1], Kanami Iguchi[1], Tsuyoshi Yamamoto[1], Hideaki Ui[1], Kazuro Shiomi[1], Takeshi Watanabe[2], K Barry Sharpless[3] and Satoshi Ōmura[1]

In situ **click chemistry is a target-guided synthesis technique for discovering potent protein ligands by assembling azides and alkynes into triazoles inside the affinity site of a target protein. We report the rapid discovery of a new and potent inhibitor of bacterial chitinases by the use of *in situ* click chemistry. We observed a target-templated formation of a potent triazole inhibitor of the chitinase-catalyzed chitin hydrolysis, through *in situ* click chemistry between a biologically active azide-containing scaffold and structurally unrelated alkyne fragments. Chitinase inhibitors have chemotherapeutic potential as fungicides, pesticides and antiasthmatics. Argifin, which has been isolated and characterized as a cyclopentapeptide natural product by our research group, shows strong inhibitory activity against chitinases. As a result of our efforts at developing a chitinase inhibitor from an azide-bearing argifin fragment and the application of the chitinase template and a library of alkynes, we rapidly obtained a very potent and new 1,5-disubstituted triazole inhibitor against *Serratia marcescens* chitinase (*Sm*Chi) B. The new inhibitor expressed 300-fold increase in the inhibitory activity against *Sm*ChiB compared with that of argifin. To the best of our knowledge, our finding of an enzyme-made 1,5-disubstituted triazole, using *in situ* click chemistry is the second example reported in the literature.**

The Journal of Antibiotics (2009) **62,** 277–282; doi:10.1038/ja.2009.28; published online 27 March 2009

Keywords: argifin; chitinase; *in situ* click chemistry; target-guided synthesis; triazole

INTRODUCTION

Chitin, the second most abundant polysaccharide in nature, is a constituent of fungal cell walls, the exoskeletons of crustaceans and insects, and the microfilarial sheaths of parasitic nematodes.[1–3] Accumulation of chitin by organisms is modulated by chitin synthase-mediated biosynthesis and by chitinase-mediated hydrolytic degradation. Thus, chitinases are expected to be specific targets for antifungal, insecticidal and antiparasitic agents (for a review, see Andersen *et al.*[4]). They also offer significant potential for the treatment of asthma and other diseases in humans.[5] Argifin (**1**) (Figure 1),[6–8] a member of a family of natural cyclic peptides produced by microorganisms, was isolated in our laboratory from the cultured broth of the fungal strain (*Gliocladium* sp. FTD-0668), and was found to be a potent inhibitor of blowfly[6] and *Serratia marcescens* chitinases (*Sm*Chi).[9–12] Recently, argifin complexes with fungal (*Aspergillus fumigatus*), human and bacterial chitinases have been resolved by X-ray crystallography.[11,12] These studies revealed that there are at least four conserved hydrogen-bond interactions between the N^{ω}-methylcarbamoyl-L-arginine moiety and the polar groups arrayed in the hydrolytic pocket of the family 18 chitinases examined to date. The remarkable fidelity of the hydrogen-bonding network between the chitinases and the argifin ligand implicates its critical role in revealing the micro- to nanomolar range of inhibition. In fact, van Aalten and co-workers revealed through X-ray analysis that the ability of the N^{ω}-methylcarbamoyl group to penetrate fully into the active-site pocket of chitinases strongly correlated with the inhibition of chitin hydrolysis.[13] Hence, we concluded that the N^{ω}-methylcarbamoyl-L-arginine core represents an ideal anchor to derivatize and elaborate better chitinase inhibitors.

Herein we report our early results of the design and simplification of azide-bearing N^{ω}-methylcarbamoyl-L-arginine substrate as a smaller analog of macrocyclic peptide natural product **1** and the use of target-guided synthesis (TGS) (for reports of TGS, see Rideout,[14] Rideout,[15] Ingelese and Benkovic,[16] Boger *et al.*,[17] Maly *et al.*,[18] Nicolaou *et al*,[19] Greasley *et al.*,[20] Nguyen and Huc,[21] Nicolaou *et al.*,[22] Kehoe *et al.*,[23] Poulin-Kerstein and Dervan,[24] and Hu *et al.*[25]) for the screening of new and more potent chitinase inhibitors, using the 1,3-dipolar cycloaddition[26] between an azide ligand and a library of acetylenes. The *in situ* click chemistry for drug discovery is

[1]The Kitasato Institute and Kitasato Institute for Life Science and Graduate School of Infection Control Sciences, Kitasato University, Minato-ku, Tokyo, Japan; [2]Department of Applied Biological Chemistry, Faculty of Agriculture, Niigata University, Niigata, Japan and [3]The Department of Chemistry and The Skaggs Institute for Chemical Biology, The Scripps Research Institute, La Jolla, CA, USA
Correspondence: Professor T Sunazuka or Professor S Ōmura, The Kitasato Institute and Kitasato Institute for Life Science and Graduate School of Infection Control Sciences, Kitasato University, 5-9-1 Shirokane, Minato-ku, Tokyo 108-8641, Japan.
E-mail: sunazuka@lisci.kitasato-u.ac.jp or omuras@insti.kitasato-u.ac.jp
Received 27 February 2009; revised 11 March 2009; accepted 11 March 2009; published online 27 March 2009

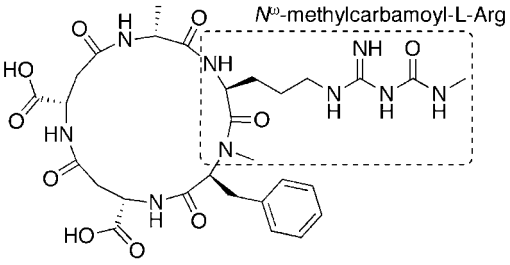

Argifin (1)

		IC_{50} values (μM)
Serratia marcescens chitinase	A (*Sm*ChiA)	0.025 ± 0.0024
	B (*Sm*ChiB)	6.4 ± 1.0
	C_1(*Sm*ChiC_1)	>30

Figure 1 Argifin (**1**) and the IC_{50} values against *Serratia marcescens* chitinases A, B and C_1.

dependent on irreversibly reacting reagents that are inert under physiological conditions,[27] as shown earlier by the discovery of highly potent inhibitors of acetylcholine esterase,[28–31] carbonic anhydrase II[32] and HIV-1 protease.[33]

RESULTS AND DISCUSSION

Preparation of the azide-bearing inhibitors

Initially, we investigated the appropriate inhibitors to develop *in situ* click chemistry from the N^{ω}-methylcarbamoyl-L-arginine scaffold. Although a simple arginine-derived inhibitor **2** discovered by van Aalten and co-workers had been reported independently,[13] it showed low inhibitory activity against *Sm*Chi in contrast to argifin **1**, which was examined by our group (Figure 2). We synthesized the azide-bearing inhibitor **3** as a reactive scaffold for capturing complementary acetylenic reagents to form triazole-linked inhibitors by TGS. Competition assay with 4-methylumberiferyl diacetylchitobiose (4-MU-$(GluNAc)_2$)[34,35] showed that this azide-bearing inhibitor **3** expressed a low inhibitory activity similar to that of the azide-lacking inhibitor **2**, which are in striking contrast to the potency of the natural product **1**. Hence, amide derivatives of azide **3** with amines other than methylamine were made and tested to see whether the binding could be restored to a level that would make azide **3** a sufficiently good anchor at the active site, to be used for the capture of alkyne-bearing candidates through *in situ* triazole formation. Fortunately, the dibenzylamide analog **5** of azide **3** emerged as a potent inhibitor (0.045 and 0.58 μM IC_{50} values against *Sm*ChiA and B, respectively). Interestingly, the IC_{50} value against *Sm*ChiB of **5** was 10-fold stronger than that of parent **1**. The monobenzylamide **4** was also active, but less than **5**. As seen in Figure 2, compounds **2**–**5** can be ranked by inhibition constants as **5** > **4** > **3** ≈ **2**. We therefore used potent azide analog **5** as a target 'anchor' molecule for *in situ* click chemistry.

Screening for enzyme-templated reaction

The *in situ* click chemistry experiments were carried out in parallel in 96-well microtiter plates to explore the chitinase-accelerated reaction using a mixture of *Sm*Chi A, B and C_1 (Sigma Co., Tokyo, Japan). Utilization of the mixed *Sm*Chi has the advantage of accelerating the identification of new inhibitors against each isozyme of chitinase through a one-off screening. Although a single isozyme or multiple isozymes of chitinase may participate in the formation of triazoles under this particular screening condition, the identification of the actual templating isozyme or isozymes can be determined in a follow-up assay using separate isozymes. Consequently, azide **5** (100 μM) and 71 structurally diverse alkynes (300 μM) were incubated in the presence

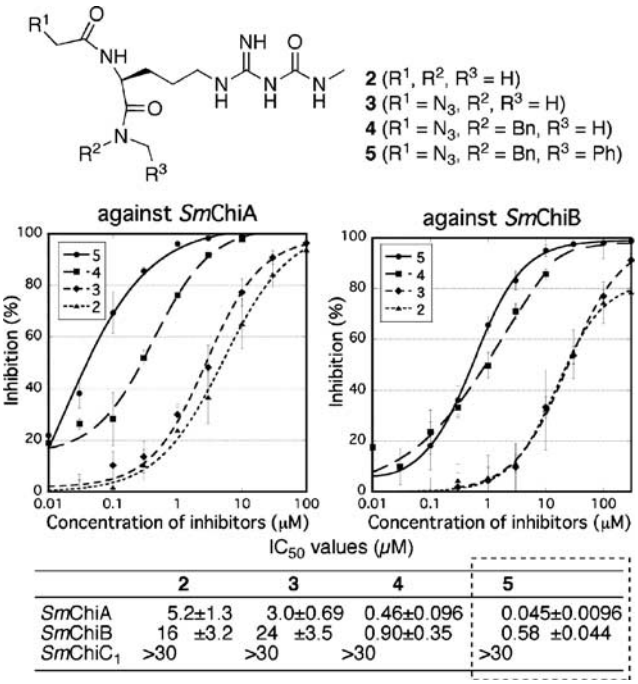

IC_{50} values (μM)

	2	3	4	5
*Sm*ChiA	5.2±1.3	3.0±0.69	0.46±0.096	0.045±0.0096
*Sm*ChiB	16 ±3.2	24 ±3.5	0.90±0.35	0.58 ±0.044
*Sm*ChiC_1	>30	>30	>30	>30

Figure 2 Structures and IC_{50} values of N^{ω}-methylcarbamoyl-L-arginine-derived inhibitors.

of *Sm*Chi A, B and C_1 (9.6 mUnit ml^{-1}) in 10% methanol containing phosphate buffer solution at pH 7.0 (Scheme 1). The formation of the triazole products was monitored by HPLC and mass spectrometry by selected ion recording detection (LCMS-SIR, also known as HPLC and mass spectrometry in selected ion monitoring (LCMS-SIM)) after 20 h at 37 °C. After analysis of each reaction mixture, only alkyne **6** (IC_{50} > 30 μM) was sufficiently accelerated in its cycloaddition with azide **5** in the presence of the enzymes to yield a detectable amount of triazole **7** (at this point not distinguished as to whether a *syn*- or *anti*-substituted triazole) in the background with great reproducibility by LCMS-SIR measurement (Figure 3). In effect, the chitinases had performed as a reaction vessel of molecular scale to create its own better inhibitor.

Preparations and inhibitory activities of triazole 7

Subsequently, azide **5** and alkyne **6** were subjected to copper(I)-catalyzed azide–alkyne cycloaddition conditions (CuAAC)[36–38] along with the ruthenium-catalyzed azide-alkyne cycloaddition reaction conditions (RuAAC),[39,40] to prepare pure regioisomers of **7** allowing the identification of the regiochemistry of the triazole formed by the enzymes. As expected, pure 1,4- and 1,5-disubstituted triazole products (***anti*-7** and ***syn*-7**) were obtained (Scheme 2). Having both pure triazoles in hand, we turned our attention to the identification of the generated triazole analog by TGS and the participating isozymes of the enzyme for this *in situ* click chemistry. For the determination of IC_{50} values against each *Sm*Chi isozyme, ***anti*-** and ***syn*-7** were assessed in a competition assay with 4-MU-$(GluNAc)_2$. As shown in Figure 4, the inhibitory activities of both regioisomers of **7** against *Sm*Chi A and C_1 were almost the same as those of **5**. On the other hand, ***syn*-7** displayed high inhibitory activity against *Sm*Chi B (IC_{50} value of 0.022 μM), which is approximately 30-fold stronger than that of **5** (approximately 300-fold improved potency as compared with the natural product **1**). These results strongly indicate that ***syn*-7** is most likely formed *in situ* by the *Sm*Chi B isozyme in the enzyme mixture.

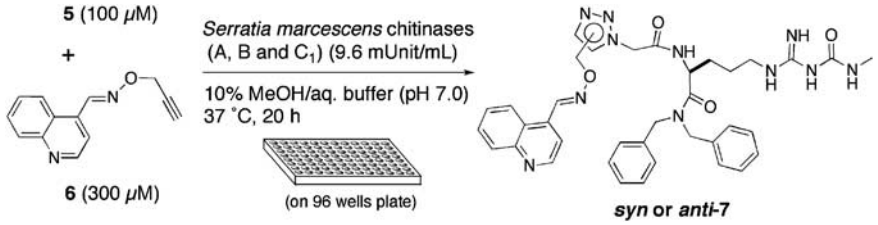

Scheme 1 *Sm*Chi templated *in situ* click chemistry protocol and the guided triazole analog.

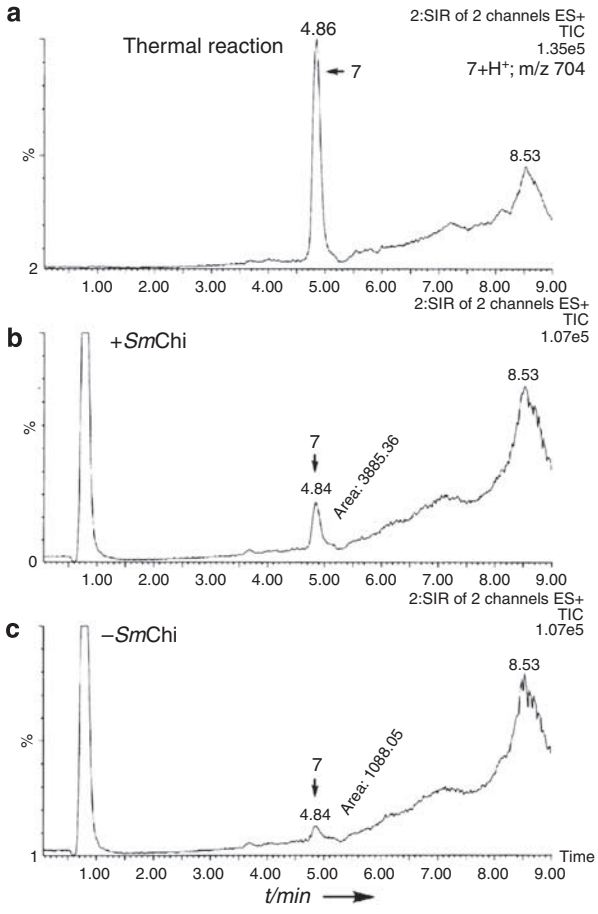

Figure 3 Results of *in situ* click chemistry between **5** and **6**, monitored by LCMS-SIR. (**a**) Authentic sample of **7** from thermal reaction (100 °C, 12 h), apparently single peak (4.9 min) of **7** (*anti*: *syn*=3: 2) was observed; (**b**) reaction (37 °C, 20 h) between **5** (100 μM) and **6** (300 μM) in the presence of *Sm*Chi (9.6 mUnit ml^{-1}); (**c**) without *Sm*Chi (background reaction).

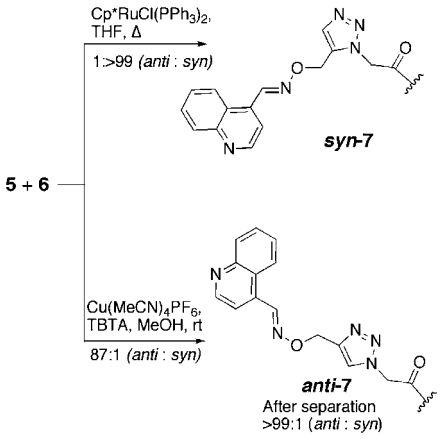

Scheme 2 Preparation of ***anti*** and ***syn*-7**. TBTA=*tris*-(benzyltriazolylmethyl) amine, THF=tetrahydrofuran.

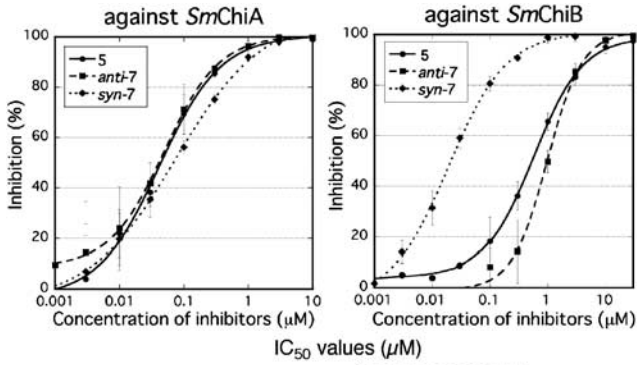

IC_{50} values (μM)

	anti-7	*syn*-7
*Sm*ChiA	0.050±0.0021	0.061±0.010
*Sm*ChiB	1.0 ±0.094	***0.022±0.0015***
*Sm*ChiC$_1$	>30	>30

Figure 4 IC_{50} values of ***anti*** and ***syn*-7** against *Sm*ChiA, B and C_1.

Acceleration effect of *syn*-triazole formation through *Sm*ChiB

Analysis of *syn-anti* selection for the *in situ* screening by LCMS-SIR revealed that a combination of azide **5** and alkyne **6** had led to the accelerated formation of ***syn*-7** in the presence of pure $(His)_6$-*Sm*ChiB in an enzyme-dose-dependent manner (Figure 5). Moreover, no *syn*-triazole formation was observed in the control incubation containing *Sm*Chi B and the same azide and alkyne in the presence of a natural product argadin acting as a potent inhibitor (see Supplementary Information for structure)[41] (IC_{50} values against *Sm*ChiB, 33 ± 2.8 nM), thereby validating ***syn*-7** as an *in situ* hit and confirming that its formation required the enzyme active site to be accessible. Interestingly, the regioisomer ***anti*-7**, which is predominantly formed under pure thermal Huisgen conditions, is less active against *Sm*ChiB than the 'anchor' molecule **5**, which probably presents the $–CH_2–N_3$ group in a unique position when **5** and the protein form their complex. At this point, the chitinase–**5** complex is most likely a single entity presenting the azide properly to the 'well-suited' alkyne ligand and correctly binding to the complex so that a *syn*-triazole selectively clicks into its existence. Now the two small molecules have become one, and this enzyme-templated molecule invariably binds more strongly than either component alone. The high kinetic barrier would effectively lower **5** and **6** until they are attracted to each other to form the thermodynamically unfavorable *syn*-isomer.

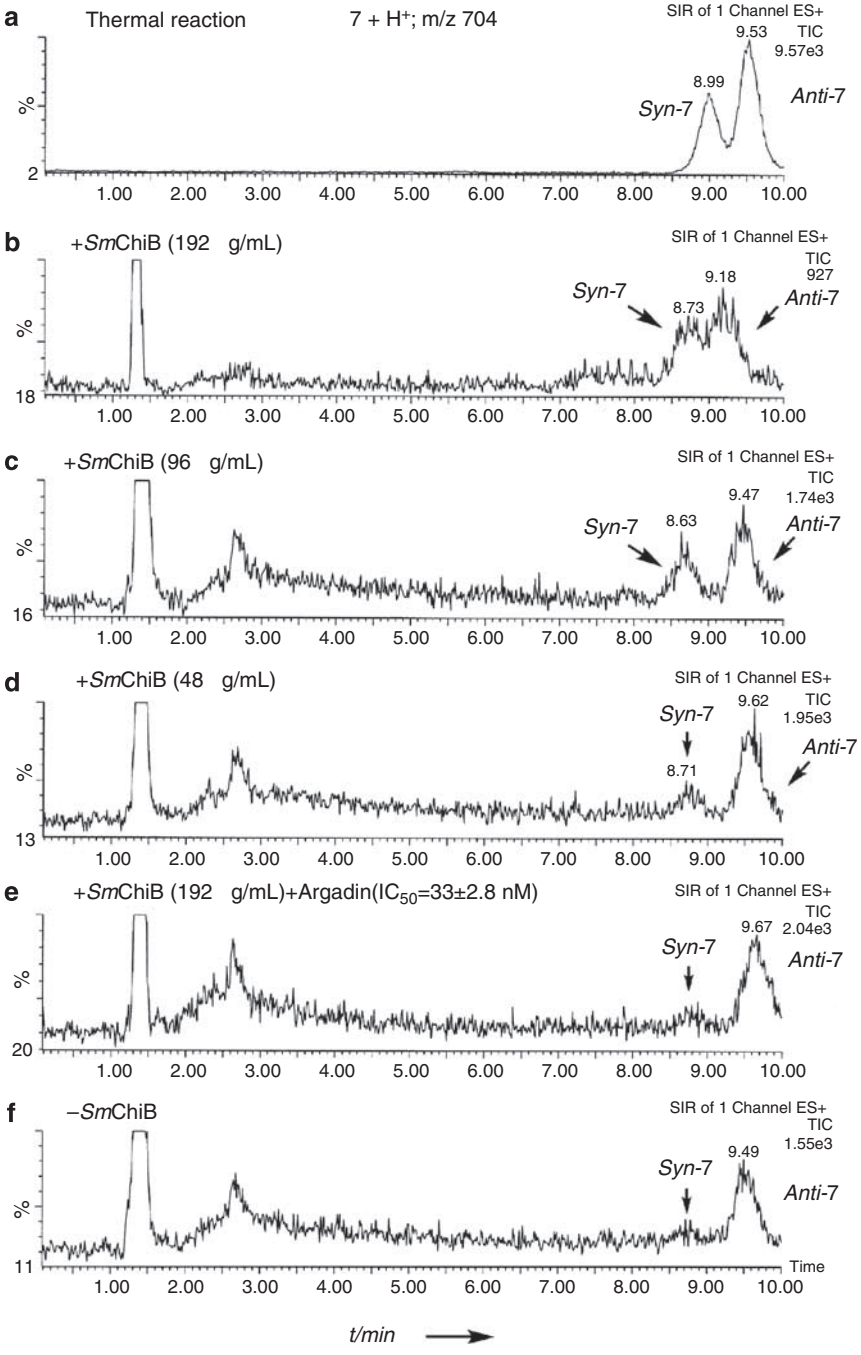

Figure 5 Identification of *syn-anti* selection for *in situ* click chemistry between **5** (100 μM) and **6** (300 μM), monitored by LCMS-SIR under different conditions from Figure 3. (**a**) Authentic sample of **7** from thermal reaction (100 °C, 12 h): ***syn*-7** (9.0 min) and ***anti*-7** (9.5 min) (2:3 ratio); (**b**) reaction with pure $(His)_6$-*Sm*ChiB (192 μg ml^{-1}; 37 °C, 20 h); (**c**) $(His)_6$-*Sm*ChiB (96 μg ml^{-1}; 37 °C, 20 h); (**d**) $(His)_6$-*Sm*ChiB (48 μg ml^{-1}; 37 °C, 20 h); (**e**) $(His)_6$-*Sm*ChiB (192 μg ml^{-1}), argadin (100 μM; 37 °C, 20 h); and (**f**) without enzyme (background reaction).

Conclusion and remarks

We discovered a highly active inhibitor of chitinase through *in situ* click chemistry. The strategy used an azide substituent appended to an active domain excised, as it were, from the more complex natural macrocyclic peptide **1**. The *Sm*Chi, which in this case was specifically *Sm*ChiB, acts as both mold and template for triazole formation between a unique pair of azide and alkyne fragments. Indeed, a number of analogs, based on bioactive molecules, would have to be synthesized to reveal the SAR for the affinity of a specific target molecule (e.g. enzymes) and to identify superior materials for traditional lead discovery. In the process of *in situ* click chemistry, the highly exergonic nature of triazole formation makes the process completely irreversible and thereby locks in unique information, a kind of embedded message of the encounter. More practically, it allowed us to discover a lead template for the discovery of a selective chitinase inhibitor directed toward the functions of *Sm*Chi, without the need for long and costly analog syntheses. Ongoing studies are focused on optimizing the structure and further evaluating

bioactivities against various types of chitinases, as well as promoting efforts to seek entirely new inhibitors, not only for chitinases but also for thorough application and refinement of the basic *in situ* methodology.

METHODS

Details of the experimental procedures and characterization of the new compounds, list of the acetylenes library, the expression of each *Serratia marcescens* chitinases and IC_{50} determination can be found in the Supplementary Information.

In situ click chemistry experiment using a mixture of *Sm*ChiA, B and C_1

Azide **5** (5 μl; 2.0 mM in MeOH) was diluted in 0.1 M phosphate buffer (pH 7.0) (60 μl). Subsequently, the required alkynes (5 μl; 6.0 mM in MeOH) were added to the azide solution, followed immediately by the addition of a solution of *Sm*Chi A, B and C_1, which was purchased from Sigma Co. (C-7809-1UN) (for the ratio of the *Sm*Chi isozymes, see Supplementary Figure 10 in the Supplementary Information), in 0.1 M phosphate buffer (30 μl; 32 mUnit ml^{-1}) to give final concentrations of 9.6 mUnit ml^{-1} *Sm*Chi, 100 μM azide **5** and 300 μM of each alkyne (Supplementary Figure 7) in 10% MeOH/phosphate buffer (100 μl). After mixing thoroughly, the reaction mixtures were incubated at 37 °C for 20 h, then diluted with 100 μl MeOH to restrain the enzyme activity and injected directly into the LC/UV-MS instrument to perform LCMS-SIR analysis (Column: Senshu Pak Pegasil (Senshu Scientific Co., Tokyo, Japan) ODS 2ø×50 mm; conditions for HPLC: gradient 10% MeCN (0.05% TFA)/H_2O (0.1% TFA) to 100% MeCN (0.05% TFA) over 8 min, flow 0.3 ml min^{-1}, detect 200–400 nm, temp 20 °C; MS-SIR: cone voltage 60 V, source temp 110 °C, desolvation temp 350 °C, selected mass 704 $[M+H]^+$). The triazole products were identified by their retention times and molecular weights. Control experiments without chitinases (azide **5** (5 μl; 2.0 mM in MeOH) and alkynes (5 μl; 6.0 mM in MeOH) in 0.1 M phosphate buffer (pH 7.0) (90 μl) at 37 °C for 20 h) were run consecutively.

One unit of chitinases can liberate 1.0 mg of *N*-acetyl-D-glucosamine from chitin per hour at pH 6.0 at in a 2-h assay.

Expression and purification of $(His)_6$-*Sm*ChiB

*Sm*ChiB gene was amplified by PCR and cloned *in frame* to pTrcHis B vector (Invitrogen, Tokyo, Japan) to give pTrcHis*Sm*ChiB. *E. coli* strain DH5α harboring plasmid pTrcHis*Sm*ChiB was harvested and disrupted by the same procedure used for expression of crude *Sm*ChiB. After centrifugation, the supernatant was applied to HisTrap Chelating HP column (Amersham Biosciences, Tokyo, Japan), and the bound proteins were eluted by a stepwise gradient of imidazole in 100 mM phosphate buffer. $(His)_6$-*Sm*ChiB was eluted at a concentration of over 150 mM imidazole and showed a molecular mass of 53 kDa on SDS-PAGE (Supplementary Figure 10). The combined fraction was concentrated and imidazole was removed using HiTrap Desalting column (Amersham BioSciences). The protein concentration (320 μg ml^{-1}) was determined by Bradford method using protein quantification kit-rapid (Dojindo, Kumamoto, Japan) with BSA as a standard protein (0.80 absorbance at 595 nm for diluted protein solution (×10)) (Supplementary Figure 10). The chitinolytic activity of purified $(His)_6$-*Sm*ChiB was assayed by the procedure in the Supplementary Information (Supplementary Figure 10).

In situ formation of *syn*-7 by *Sm*ChiB template reaction

A chromatographic and analytical method different from *in situ* click screening was used for determining the *syn-anti* selection of the *in situ* click chemistry product **7** by $(His)_6$-*Sm*ChiB. The assignment was accomplished by comparing the retention times of the *in situ* products with authentic samples prepared by the thermal reaction of triazole formation.

Azide **5** (5 μl; 2.0 mM in MeOH) was diluted in 0.1 M phosphate buffer (pH 7.0) (60 μl). Subsequently, the alkyne **6** (5 μl; 6.0 mM in MeOH) was added to the azide solution, followed immediately by the additon of a solution of $(His)_6$-*Sm*ChiB (320 μg ml^{-1}) in 0.1 M phosphate buffer (30 μl) to give a final concentration of 96 μg $ml^{-1}$$(His)_6$-*Sm*ChiB, 100 μM azide **5** and 300 μM alkyne **6** in 10% MeOH/phosphate buffer (100 μl). After mixing thoroughly, the reaction mixtures were kept at 37 °C for 20 h, then cooled to 20 °C and diluted with 100 μl MeCN to restrain the enzyme activity and injected directly into the LC/UV-MS instrument to perform LCMS-SIR analysis (Column: Develosil (Nomura Chemical Co., Aichi, Japan) C30-UG-5, 2ø×150 mm; conditions for HPLC: isocratic 29% MeCN(0.05% TFA)/H_2O(0.1%TFA), flow 0.3 ml min^{-1}, detect 200–400 nm, temp 20 °C; MS-SIR: cone voltage 95 V, source temp 110 °C, desolvation temp 350 °C, selected mass 704 $[M+H]^+$). The triazole products were identified by their retention times and molecular weights. In concurrence, experiments to investigate the dose dependency of the enzyme for production of ***syn*-7** were carried out under the same condition by using different concentrations of $(His)_6$-*Sm*ChiB (final concentrations 192 and 48 μg ml^{-1} $(His)_6$-*Sm*ChiB, respectively, 100 μM azide **5** and 300 μM of alkyne **6** in 10% MeOH/phosphate buffer). From these comparisons, dose-dependent production of ***syn*-7** was clearly observed (Figure 5). LCMS-SIR peaks of ***syn***- and ***anti*-7** were confirmed by co-injection of authentic sample **7** (from thermal reaction) and a crude mixture of enzyme template reaction ($(His)_6$-*Sm*ChiB 192 μg ml^{-1}, 100 μM azide and 300 μM alkyne at 37 °C, 20 h) (Supplementary Figure 11). Control experiments in the presence of the known *Sm*ChiB inhibitor Argadin[41] (IC_{50} 33 ± 2.8 nM) (final concentration: 192 μg ml^{-1} *Sm*ChiB, 100 μM argadin, 100 μM azide **5** and 300 μM alkyne **6**) and in the absence of enzyme (100 μM azide **5** and 300 μM alkyne **6**) were run consecutively.

ACKNOWLEDGEMENTS

This work was supported by the Grant of the 21st Century COE Program, Ministry of Education Culture, Sports, Science and Technology. We also thank Ms A Nakagawa, Ms N Sato and Dr K Nagai for various instrumental analyses.

1 Boot, R. G. *et al.* Identification of a novel acidic mammalian chitinase distinct from chitotriosidase. *J. Biol. Chem.* **276,** 6770–6778 (2001).
2 Shahabuddin, M., Toyoshima, T., Aikawa, M. & Kaslow, D. C. Transmission-blocking activity of a chitinase inhibitor and activation of malarial parasite chitinase by mosquito protease. *Proc. Natl Acad. Sci. USA* **90,** 4266–4270 (1993).
3 Shibata, Y., Foster, L. A., Bradfield, J. F. & Myrvik, Q. N. Oral administration of chitin down-regulates serum IgE levels and lung eosinophilia in the allergic mouse. *J. Immunol.* **164,** 1314–1321 (2000).
4 Andersen, O. A., Dixon, M. J., Eggleston, I. M. & van Aalten, D. M. F. Natural product family 18 chitinase inhibitors. *Nat. Prod. Rep.* **22,** 563–579 (2005).
5 Zhu, Z. *et al.* Acidic mammalian chitinase in asthmatic Th2 inflammation and IL-13 pathway activation. *Science* **304,** 1678–1682 (2004).
6 Ōmura, S. *et al.* Argifin, a new chitinase inhibitor, produced by *Gliodadium sp.* FTD-0668. I. Taxonomy, fermentation, and biological activities. *J. Antibiot.* **53,** 603–608 (2000).
7 Arai, N., Shiomi, K., Iwai, Y. & Ōmura, S. Argifin, a new chitinase inhibitor, produced by *Gliodadium sp.* FTD-0668. II. Isolation, physico-chemical properties, and structure elucidation. *J. Antibiot.* **53,** 609–614 (2000).
8 Shiomi, K. *et al.* Structure of argifin, a new chitinase inhibitor produced by *Gliocladium sp. Tetrahedron Lett.* **41,** 2141–2143 (2000).
9 Suzuki, K. *et al.* Chitinases A, B, and C1 of *Serratia marcescens* 2170 produced by recombinant *Escherichia coli*: enzymatic properties and synergism on chitin degradation. *Biosci. Biotechnol. Biochem.* **66,** 1075–1083 (2002).
10 Horn, S. J. *et al.* Comparative studies of chitinases A, B and C from *Serratia marcescens*. *Biocatal. Biotransform.* **24,** 39–53 (2006).
11 Rao, F. V. *et al.* Specificity and affinity of natural product cyclopentapeptide inhibitors against A. fumigatus, human, and bacterial chitinases. *Chem. Biol.* **12,** 65–76 (2005).
12 Houston, D. R. *et al.* High-resolution structures of a chitinase complexed with natural product cyclopentapeptide inhibitors: mimicry of carbohydrate substrate. *Proc. Natl Acad. Sci. USA* **99,** 9127–9132 (2002).
13 Andersen, O. A. *et al.* Structure-based dissection of the natural product cyclopentapeptide chitinase inhibitor argifin. *Chem. Biol.* **15,** 295–301 (2008).
14 Rideout, D. Self-assembling cytotoxins. *Science* **233,** 561–563 (1986).
15 Rideout, D., Calogeropoulu, T., Jaworski, J. & McCarthy, M. Synergism through direct covalent bonding between agents: a strategy for rational design of chemotherapeutic combinations. *Biopolymers* **29,** 247–262 (1990).
16 Inglese, J. & Benkovic, S. J. Multisubstrate adduct inhibitors of glycinamide ribonucleotide transformylase: synthetic and enzyme-assembled. *Tetrahedron* **47,** 2351–2364 (1991).
17 Boger, D. L. *et al.* 10-formyl-5,8,10-trideazafolic acid (10-formyl-TDAF): a potent inhibitor of glycinamide ribonucleotide transformylase. *Bioorg. Med. Chem.* **5,** 1817–1830 (1997).

18 Maly, D. J., Choong, I. C. & Ellman, J. A. Combinatorial target-guided ligand assembly: identification of potent subtype-selective c-Src inhibitors. *Proc. Natl Acad. Sci. USA* **97,** 2419–2424 (2000).
19 Nicolaou, K. C. *et al.* Target-accelerated combinatorial synthesis and discovery of highly potent antibiotics effective against vancomycin-resistant bacteria. *Angew. Chem. Int. Ed.*. **39,** 3823–3828 (2000).
20 Greasley, S. E. *et al.* Unexpected formation of an epoxide-derived multisubstrate adduct inhibitor on the active site of GAR transformylase. *Biochemistry* **40,** 13538–13547 (2001).
21 Nguyen, R. & Huc, I. Using an enzyme's active site to template inhibitors. *Angew. Chem. Int. Ed.* **40,** 1774–1776 (2001).
22 Nicolaou, K. C. *et al.* Synthesis and biological evaluation of vancomycin dimers with potent activity against vancomycin-resistant bacteria: target-accelerated combinatorial synthesis. *Chem. Eur. J.* **7,** 3824–3843 (2001).
23 Kehoe, J. W. *et al.* Tyrosylprotein sulfotransferase inhibitors generated by combinatorial target-guided ligand assembly. *Bioorg. Med. Chem. Lett.* **12,** 329–332 (2002).
24 Poulin-Kerstien, A. T. & Dervan, P. B. DNA-templated dimerization of hairpin polyamides. *J. Am. Chem. Soc.* **125,** 15811–15821 (2003).
25 Hu, X., Sun, J., Wang, H.-G. & Manetsch, R. Bcl-X_L-templated assembly of its own protein-protein interaction modulator from fragments decorated with thio acids and sulfonyl azides. *J. Am. Chem. Soc.* **130,** 13820–13821 (2008).
26 Huisgen, R. in *1,3-Dipolar Cycloaddition Chemistry*, Vol. 1 (ed. Padwa, A.) 1–176 (Wiley, New York, 1984).
27 Sharpless, K. B. & Manetsch, R. *In situ* click chemistry: a powerful means for lead discovery. *Expert Opin. Drug Discov.* **1,** 525–538 (2006).
28 Lewis, W. G. *et al.* Click chemistry *in situ*: acetylcholinesterase as a reaction vessel for the selective assembly of a femtomolar inhibitor from an array of building blocks. *Angew. Chem. Int. Ed.* **41,** 1053–1057 (2002).
29 Manetsch, R. *et al. In situ* click chemistry: enzyme inhibitors made to their own specifications. *J. Am. Chem. Soc.* **126,** 12809–12818 (2004).
30 Bourne, Y. *et al.* Freeze-frame inhibitor captures acetylcholinesterase in a unique conformation. *Proc. Natl Acad. Sci. USA* **101,** 1449–1454 (2004).
31 Krasiéski, A. *et al. In situ* selection of lead compounds by click chemistry: target-guided optimization of acetylcholinesterase inhibitors. *J. Am. Chem. Soc.* **127,** 6686–6692 (2005).
32 Mocharla, V. P. *et al. In situ* click chemistry: enzyme-generated inhibitors of carbonic anhydrase II. *Angew. Chem. Int. Ed.* **44,** 116–120 (2005).
33 Whiting, M. *et al.* Inhibitors of HIV-1 protease by using *in situ* click chemistry. *Angew. Chem. Int. Ed.* **45,** 1435–1439 (2006).
34 Brurberg, M. B. *et al.* Chitinase B from *Serratia marcescens* BJL200 is exported to the periplasm without processing. *Microbiology* **141,** 123–131 (1995).
35 Hodge, A., Gooday, G. W. & Alexander, I. J. Inhibition of chitinolytic activities from tree species and associated fungi. *Phytochemistry* **41,** 77–84 (1996).
36 Rostovtsev, V. V., Green, L. G., Fokin, V. V. & Sharpless, K. B. A stepwise Huisgen cycloaddition process: copper(I)-catalyzed regioselective ligation of azides and terminal alkynes. *Angew. Chem. Int. Ed.* **41,** 2596–2599 (2002).
37 Tornøe, C. W., Christensen, C. & Meldal, M. Peptidotriazoles on solid phase: [1,2,3]-triazoles by regiospecific copper(I)-catalyzed 1,3-dipolar cycloadditions of terminal alkynes to azides. *J. Org. Chem.* **67,** 3057–3064 (2002).
38 Chan, T. R., Hilgraf, R., Sharpless, K. B. & Fokin, V. V. Polytriazoles as copper(I)-stabilizing ligands in catalysis. *Org. Lett.* **6,** 2853–2885 (2004).
39 Zhang, L. *et al.* Ruthenium-catalyzed cycloaddition of alkynes and organic azides. *J. Am. Chem. Soc.* **127,** 15998–15999 (2005).
40 Boren, B. C. *et al.* Ruthenium-catalyzed azide-alkyne cycloaddition: scope and mechanism. *J. Am. Chem. Soc.* **130,** 8923–8930 (2008).
41 Arai, N. *et al.* Argadin, a new chitinase inhibitor, produced by *Clonostachys sp.* FO-7314. *Chem. Pharm. Bull.* **48,** 1442–1446 (2000).

Supplementary Information accompanies the paper on The Journal of Antibiotics website (http://www.nature.com/ja)

The Journal of Antibiotics (2009) 62, 283–285
© 2009 Japan Antibiotics Research Association All rights reserved 0021-8820/09 $32.00
www.nature.com/ja

NOTE

JBIR-17, a novel trichostatin analog from *Streptomyces* sp. 26634

Jun-ya Ueda[1], Ji-Hwan Hwang[2], Satoko Maeda[3], Taira Kato[4], Atsushi Ochiai[4], Kunio Isshiki[4], Minoru Yoshida[3], Motoki Takagi[1] and Kazuo Shin-ya[2]

The Journal of Antibiotics (2009) **62,** 283–285; doi:10.1038/ja.2009.22; published online 20 March 2009

Keywords: histone deacetylase; histone deacetylase inhibitor; *Streptomyces*; trichostatin

Histone deacetylases (HDACs) play an important role in the epigenetic regulation of gene expression by catalyzing the removal of acetyl groups from lysine residue of histone protein, stimulating chromatin condensation and promoting transcriptional repression.[1,2] HDACs are divided into four classes on the basis of their homology to yeast HDACs: class I (HDAC1, 2, 3 and 8), class IIa (HDAC4, 5, 7 and 9), class IIb (HDAC6 and 10), class III (SIRT1, 2, 3, 4, 5, 6 and 7) and class IV (HDAC11). As aberrant epigenetic changes are a hallmark of cancer, HDACs are a promising target for an anticancer drug. The inhibitors of HDACs can induce cell-cycle arrest, promote differentiation and stimulate tumor cell death. In fact, several HDAC inhibitors are currently in clinical trials both for solid and hematological malignancies.[1,2] Therefore, we attempted to search new HDAC inhibitors. As a result, we isolated a novel compound designated as JBIR-17 (**1**) from *Streptomyces* sp. 26634 (Figure 1). We report herein the isolation, structure elucidation and biological activity of **1**.

Streptomyces sp. 26634 was isolated from a leaf of *Kerria japonica* collected in Iwata, Shizuoka Prefecture, Japan, and cultured on a rotary shaker (220 r.p.m.) at 28°C for 4 days in a 500-ml Erlenmeyer flask containing 60 ml of a medium consisting of 4% β-cyclodextrin, 0.5% glycerol, 2% Pharmamedia (Traders Protein, Lubbock, TX, USA), 0.0005% $CuSO_4{\cdot}5H_2O$, 0.0005% $MnCl_2{\cdot}4H_2O$ and 0.0005% $ZnSO_4{\cdot}7H_2O$.

n-BuOH (37.5 ml) was added to the fermentation broth (60 ml) and shaken for 15 min. After centrifugation, the organic layer was evaporated *in vacuo*. The dried residue (107 mg) was subjected to reversed-phase medium-pressure liquid chromatography (Purif-Pack ODS 100, Moritex, Tokyo, Japan) and eluted with a MeOH–H_2O (5-100% MeOH) linear gradient system. The 70–90% MeOH eluate (3.7 mg) was further purified by reversed-phase HPLC using an XBridge Prep C_{18} column (5 μm optimum bed density (OBD), 4.6 i.d.×250 mm, Waters, Milford, MA, USA) with 35% aqueous CH_3CN containing 0.2% formic acid (flow rate, 1 ml min^{-1}) to yield JBIR-17 (**1**, 0.9 mg; retention time (Rt) 9.7 min) and trichostatin A (**2**, 0.7 mg; Rt 10.3 min).[3]

The physicochemical properties of **1** are summarized in Table 1. Compound **1** was obtained as a colorless amorphous solid, and its molecular formula was determined to be $C_{20}H_{26}N_2O_5$ by HR-electrospray ionization (ESI)-MS. The IR spectrum revealed the characteristic absorptions of the aroyl and/or amide carbonyl (ν_{max} 1652 cm^{-1}) and amide N-H (ν_{max} 1597 cm^{-1}) groups. The structure of **1** was mainly determined by NMR spectral analyses as follows.

The direct connectivity between each proton and carbon was established by the heteronuclear single quantum coherence spectrum, and the ^{13}C and ^{1}H NMR spectral data for **1** are shown in Table 2. A total of 20 signals were observed in the ^{13}C NMR spectrum, consistent with the HR-MS data. These signals included three carbonyl (C-1, C-7, C-1′), four olefinic (C-2 to C-5) and six aromatic (C-8 to C-13) carbons. The proton spin couplings between two olefinic protons 2-H (δ_H 5.91) and 3-H (δ_H 7.28), between an olefinic proton 5-H (δ_H 6.04) and a methyl proton 6-Me (δ_H 1.28) through a methine proton 6-H (δ_H 4.36), and between two equivalent aromatic protons 9,13-H (δ_H 7.84) and 10,12-H (δ_H 6.69) on a *p*-disubstituted benzene ring were observed in a double-quantum filtered (DQF)-COSY spectrum as shown in Figure 2 (bold line). The constant time heteronuclear multibond correlation (CT-HMBC) experiment revealed the presence of ^{1}H-^{13}C long-range couplings from an *N*,*N*-dimethyl proton (δ_H 3.05) to an aromatic carbon C-11 (δ_C 155.2), from 9,13-H to C-11 and a carbonyl carbon C-7 (δ_C 198.7), from 10,12-H to an aromatic carbon C-8 (δ_C 127.0), from 6-Me, 6-H and 5-H to C-7, from the

[1]Biomedicinal Information Research Center (BIRC), Japan Biological Informatics Consortium (JBIC), Koto-ku, Tokyo, Japan; [2]Biomedicinal Information Research Center (BIRC), National Institute of Advanced Industrial Science and Technology (AIST), Koto-ku, Tokyo, Japan; [3]Chemical Genomics Research Group/Chemical Genetics Laboratory, RIKEN Advanced Science Institute, Wako, Saitama, Japan and [4]Bioresource Laboratories, Mercian Corporation, Iwata, Shizuoka, Japan
Correspondence: Dr M Takagi, Biomedicinal Information Research Center (BIRC), Japan Biological Informatics Consortium (JBIC), 2-42 Aomi, Koto-ku, Tokyo 135-0064, Japan.
E-mail: motoki-takagi@aist.go.jp or
Dr K Shin-ya, Biomedicinal Information Research Center (BIRC), National Institute of Advanced Industrial Science and Technology (AIST), 2-42 Aomi, Koto-ku, Tokyo 135-0064, Japan.
E-mail: k-shinya@aist.go.jp
Received 4 February 2009; revised 26 February 2009; accepted 27 February 2009; published online 20 March 2009

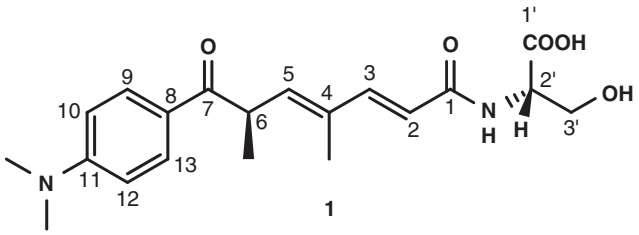

1

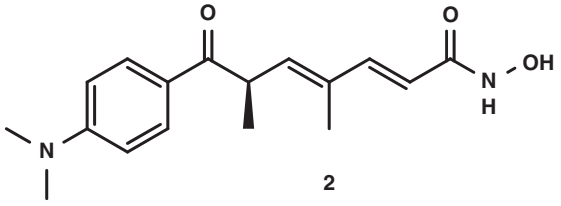

2

Figure 1 Structures of JBIR-17 (**1**) and trichostatin A (**2**).

Table 1 Physicochemical properties of 1

Appearance	Colorless amorphous solid
Optical rotation[a]	$[\alpha]_D^{25} -18.0^\circ$ (*c* 0.1, MeOH)
HR-ESI-MS[b] (m/z)	
Found	375.1880 $(M+H)^+$
Calculated	375.1920 ($C_{20}H_{27}N_2O_5$)
UV[c] λ_{max} nm (ε)	264 (24 700), 336 (23 500)
IR[d] (KBr) ν_{max} cm^{-1}	3415, 1653, 1597

Abbreviation: ESI, electrospray ionization.
[a]Optical rotation was measured on a SEPA-300 polarimeter (Horiba, Kyoto, Japan).
[b]HR-ESI-MS measurement was carried out on a LCT Premier XE mass spectrometer (Waters).
[c]UV spectrum was measured on a COULTER DU730 UV/Vis Spectrophotometer (Beckman, Fullerton, CA, USA).
[d]IR spectra was obtained on a FT-720 Fourier transform infrared spectrometer (Horiba).

Table 2 ^{13}C and ^{1}H NMR data for 1

Position	δ_C	δ_H
1	168.6	
2	117.5	5.91 (d, 15.4)
3	147.5	7.28 (d, 15.4)
4	132.5	
5	141.9	6.04 (d, 9.5)
6	40.9	4.36 (dq, 9.5, 6.9)
7	198.7	
8	127.0	
9, 13	130.7	7.84 (d, 8.8)
10, 12	111.2	6.69 (d, 8.8)
11	155.2	
1′	172.0	
2′	54.8	4.60 (br s)
3′	62.1	4.18 (br d, 10.5); 3.85 (br d, 10.5)
4-methyl	12.6	1.89 (s)
6-methyl	17.8	1.28 (d, 6.9)
11*N*,*N*-dimethyl	40.3	3.05 (s)

^{13}C (125 MHz) and ^{1}H (500 MHz) NMR spectra were taken on a NMR System 500 NB CL (Varian, Palo Alto, CA, USA) in $CDCl_3$, and the solvent peak was used as an internal standard (δ_C 77.0, δ_H 7.26).

vinyl methyl proton 4-Me (δ_H 1.89) to three olefinic carbons C-3 (δ_C 147.5), C-4 (δ_C 132.5) and C-5 (δ_C 141.9), and from 2-H and 3-H to an amide carbonyl carbon C-1 (δ_C 168.6). The stereochemistries of

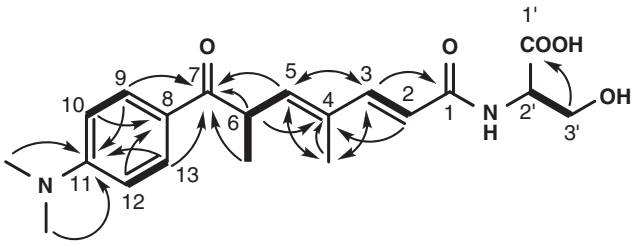

Figure 2 Key correlations in DQF-COSY (bold line) and CT-HMBC (arrow) spectra of **1**.

two olefins were determined as 2*E* and 4*E* according to the coupling constant ($J_{2,3}$=15.4 Hz) and the high-field-shifted ^{13}C chemical shift at 4-Me (δ_C 12.6). Thus, the partial structure was elucidated as a trichostatic acid (**3**) moiety, and their ^{13}C and ^{1}H NMR signals are superimposable with those of **2**[3] and **3**[4].

Additional substructure was elucidated as follows. A proton spin coupling between an α-methine proton 2′-H (δ_H 4.60; δ_C 54.8) and oxymethylene protons 3′-H (δ_H 4.18, 3.85; δ_C 62.1) was observed. A long-range coupling from 3′-H to a carboxylic carbonyl carbon C-1′ deduced that the remaining structure was a serine moiety, and the serine was assumed to attach to C-1 of trichostatin through an amide bond.

The linkage position and the absolute configuration of the serine moiety of **1** were confirmed as follows. To determine the absolute configuration of the serine moiety, Marfey's method was adopted. Compound **1** (0.8 mg) was hydrolyzed with 6 N HCl (0.2 ml) at 120°C overnight to obtain the serine residue. After acid hydrolysis, the reaction solution was adjusted to neutral pH and evaporated *in vacuo*. The residue was dissolved in an aqueous solution of 0.1 M $NaHCO_3$ (0.6 ml), and 10 mM N^{α}-(5-fluoro-2,4-dinitrophenyl)-L-alaninamide (FDAA) in Me_2CO (0.6 ml) was successively added. The mixture was kept at 70°C for 10 min with frequent shaking. After work-up with the addition of 0.2 N HCl, the filtered reaction mixture was subjected to ultra performance liquid chromatography (UPLC) analysis (Acquity UPLC BEH C_{18} 1.7 µm, 2.1×50 mm, Waters; 10% aqueous CH_3CN containing 0.1% formic acid; flow rate, 0.3 ml min^{-1}). The authentic D- and L-serine were reacted with FDAA in the same manner as described above. The serine residue obtained from the hydrolysate was determined to be L-serine (Rt 8.6 min; L-Ser, 8.5 min; D-Ser, 9.8 min). To confirm the linkage position of serine moiety, **1** was semi-synthesized from **2** as shown in Figure 3. Briefly, **2** (7.5 mg) was converted to **3** (3.4 mg) by $HClO_4$. Compound **3** was coupled with an *O*-*t*-butyl-L-serine *t*-butyl ester in the presence of PyBOP and *N*,*N*-diisopropylethylamine followed by deprotection in acidic condition to yield an L-serine adduct of **3** (0.9 mg). This synthetic compound showed an identical ^{1}H NMR spectrum to that of naturally isolated **1** from *Streptomyces* sp. 26634.

To evaluate inhibitory activity for HDACs of **1**, we used the reporter gene assay system using a luciferase gene as described earlier.[5,6] The human embryonic kidney 293T cells, transformed with the luciferase reporter gene driven by the cytomegalovirus promoter, produced 2.5 times more luciferase compared with the untreated control, when they were treated with **1** at a concentration of 30 µM. Furthermore, to clarify the selectivity against HDAC subtypes, **1** was tested in the HDAC inhibitory activity using HDAC1 (class I), 4 (class IIa) and 6 (class IIb) enzymes of 293T cell origin, which are usually used as the representative HDACs among each HDAC subtype.[7] Compound **1** showed inhibitory activity against HDAC4 and 6 with IC_{50} values of 69 and 4.7 µM, respectively, but no activity against HDAC1 at a

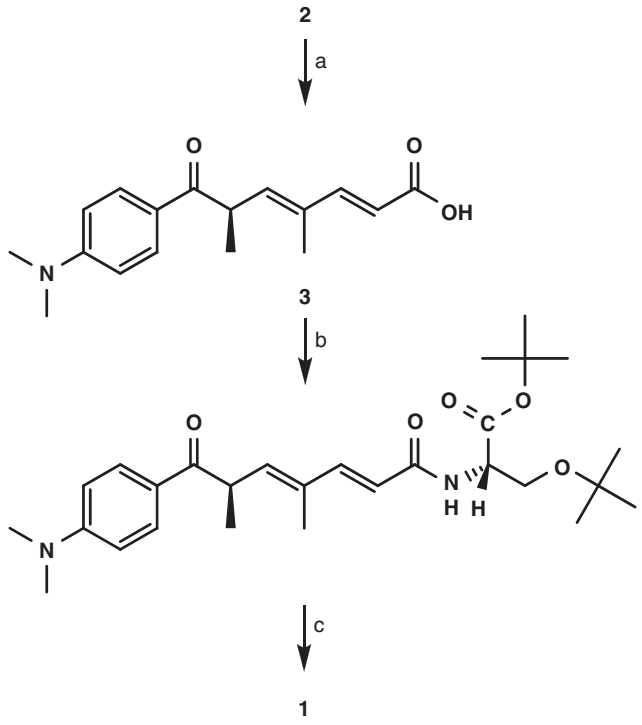

Figure 3 Scheme of chemical conversion from **2** to **1**. (**a**) 1.5 N $HClO_4$ aq, 50°C, overnight. (**b**) *O*-*t*-butyl-L-serine *t*-butyl ester, PyBOP, *N*,*N*-diisopropylethylamine in CH_2Cl_2/DMF (*N*,*N*-dimethylformamide), room temperature, 2 h. (**c**) 90% aqueous trifluoroacetic acid, room temperature, 1.5 h.

concentration of 100 μM. In contrast, **2** showed strong, but not selective, inhibitory effects against these HDACs (IC_{50} values, 18, 30 and 92 nM against HDAC1, 4 and 6, respectively) as reported earlier.[8,9] These results indicated that **1** selectively inhibited HDAC6 compared with HDAC1 and 4. HDAC6 is a cytoplasmic enzyme that regulates many important biological processes, including cell migration, immune synapse formation, viral infection and the degradation of misfolded proteins. Furthermore, HDAC6 deacetylates tubulin, Hsp90 and cortactin.[10–12] The diverse functions of HDAC6 suggest that it is a potential therapeutic target for a wide range of diseases. Thus, JBIR-17 could be a valuable tool for the studies of HDAC6 and enzymatic property among HDAC subtypes.

ACKNOWLEDGEMENTS

This work was supported in part by the New Energy and Industrial Technology Development Organization of Japan (NEDO), and a Grant-in-Aid for Scientific Research (20380070 to KS) from the Japan Society for the Promotion of Science (JSPS).

1 Carew, J. S., Giles, F. J. & Nawrocki, S. T. Histone deacetylase inhibitors: mechanisms of cell death and promise in combination cancer therapy. *Cancer Lett.* **269,** 7–17 (2008).
2 Shankar, S. & Srivastava, R. K. Histone deacetylase inhibitors: mechanisms and clinical significance in cancer: HDAC inhibitor-induced apoptosis. *Adv. Exp. Med. Biol.* **615,** 261–298 (2008).
3 Tsuji, N., Kobayashi, M., Nagashima, K., Wakisaka, Y. & Koizumi, K. A new antifungal antibiotic, trichostatin. *J. Antibiot.* **29,** 1–6 (1976).
4 Tsuji, N. & Kobayashi, M. Trichostatin C, a glucopyranosyl hydroxamate. *J. Antibiot.* **31,** 939–944 (1978).
5 Numajiri, Y., Takahashi, T., Takagi, M., Shin-ya, K. & Doi, T. Total synthesis of largazole and its biological evaluation. *Synlett.* **16,** 2483–2486 (2008).
6 Dressel, U., Renkawitz, R. & Baniahmad, A. Promoter specific sensitivity to inhibition of histone deacetylases: implications for hormonal gene control, cellular differentiation and cancer. *Anticancer Res.* **20,** 1017–1022 (2000).
7 Shivashimpi, G. M. *et al.* Molecular design of histone deacetylase inhibitors by aromatic ring shifting in chlamydocin framework. *Bioorg. Med. Chem.* **15,** 7830–7839 (2007).
8 Yoshida, M., Kijima, M., Akita, M. & Beppu, T. Potent and specific inhibition of mammalian histone deacetylase both *in vivo* and *in vitro* by trichostatin A. *J. Biol. Chem.* **265,** 17174–17179 (1990).
9 Furumai, R., Komatsu, Y., Nishino, N., Khochbin, S., Yoshida, M. & Horinouchi, S. Potent histone deacetylase inhibitors built from trichostatin A and cyclic tetrapeptide antibiotics including trapoxin. *Proc. Natl Acad. Sci. USA* **98,** 87–92 (2001).
10 Valenzuela-Fernández, A., Cabrero, J. R., Serrador, J. M. & Sánchez-Madrid, F. HDAC6: a key regulator of cytoskeleton, cell migration and cell-cell interactions. *Trends Cell Biol.* **18,** 291–297 (2008).
11 Rodriguez-Gonzalez, A. *et al.* Role of the aggresome pathway in cancer: targeting histone deacetylase 6-dependent protein degradation. *Cancer Res.* **68,** 2557–2560 (2008).
12 Matthias, P., Yoshida, M. & Khochbin, S. HDAC6 a new cellular stress surveillance factor. *Cell Cycle* **7,** 7–10 (2008).

The Journal of Antibiotics (2009) 62, 287–288
© 2009 Japan Antibiotics Research Association All rights reserved 0021-8820/09 $32.00
www.nature.com/ja

OBITUARY

Hans Zähner (7 June 1929–18 December 2008)

The Journal of Antibiotics (2009) **62,** 287–288; doi:10.1038/ja.2009.36

Professor Hans Zähner passed away on 18 December 2008 at the age of 79 after a prolonged illness.

Hans Zähner was born on 7 June 1929 in Zürich, Switzerland. He studied agricultural science at the Eidgenössische Technische Hochschule (ETH) in Zürich from 1949 to 1953 and worked with Professor Ernst Gäumann at the Institut für Spezielle Botanik at ETH, finishing his doctoral thesis on phytopathology in 1954. From 1954 to 1958, he collaborated with Professor Leopold Ettlinger and Roger Corbaz at the same institute. Their aim was to screen microorganisms for new biologically active compounds and extend the screening from fungi to include actinomycete strains. This period marked the beginning of a very successful collaboration with Professor Vlado Prelog and Walter Keller-Schierlein from the Institute of Organic Chemistry at ETH in the isolation and structure elucidation of new compounds. About 20 000 actinomycete strains were tested to see if they produced antibiotics. Besides the identification of 1100 producers of known antibiotics, 20 new compounds were isolated. The structures of 10 were determined and published in the series 'Stoffwechselprodukte von Actinomyceten': narbomycin, angolamycin, nonactin, foromacidins, echinomycin, granaticin, megacidin, acetomycin, cinerubins and holomycin.

In 1958, Hans Zähner took responsibility for microbiological research in the group led by Professor Ettlinger, who was appointed to the professorship of bacteriology at ETH. Together with Ralph Hütter and Elisabeth Bachmann at the Institut für Spezielle Botanik and his colleagues Professor Prelog and Walter Keller-Schierlein from the Institute of Organic Chemistry, he intensified the search for new antibiotics. Although the number of strains tested in screening programs was reduced, new methods for isolating actinomycetes from soil samples were developed, new test organisms and cultivation methods for these strains were used, and new screening methods were devised. These methodological changes led to a change in the nature of the detected compounds and resulted in the isolation of numerous new substances; for example, actinomycin Z, actiphenol, acumycin, aranciamycin, boromycin, ferrichrysin, granaticin B, lankamycin, lankacidin, manumycin, naphthocyclinones, naphthomycin, scopamycins and venturicidin B. Hans Zähner's scientific success led to his habilitation in 1960.

During investigation into the optimization of ferrimycin production, it was observed that the antibiotic activity of ferrimycin could be reversed by cultures of other actinomycete strains. This antagonism was specific to ferrimycin; other antibiotics like streptomycin and the tetracyclines did not share this property, and this was the beginning of Hans Zähner's successful studies of iron-chelating metabolites—the siderophores—resulting in the industrial production of desferrioxamine B, which was introduced on the market as Desferal in 1962 by Ciba (Basel, Switzerland).

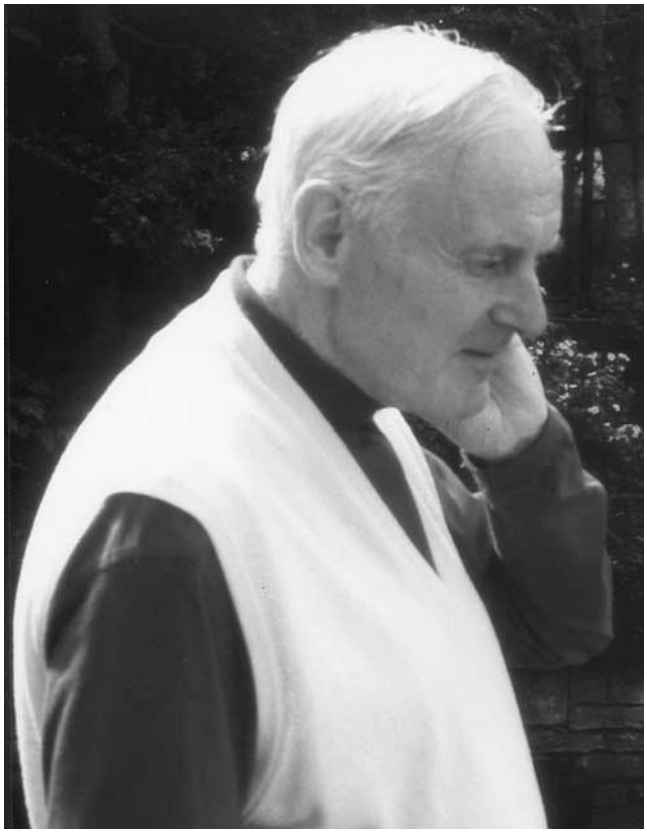

In 1964, he moved from ETH Zürich to the University of Tübingen in Germany to a newly created Chair in microbiology. There he founded the Institute of Microbiology and continued his work on screening for novel secondary metabolites. The screening for iron-chelating compounds, for antibiotics that act exclusively on chemically defined media and for antibiotics that cause morphological changes in fungi, was continued successfully and was completed by a chemical TLC-based screening program. Further remarkable compounds were detected by Hans Zähner and his group, including, among others, avilamycins, bafilomycins, the nikkomycins, phosphinothricin, tetracenomycins and urdamycins. At the beginning of his career, he started the communication series 'Microbial Products of Microorganisms',

which, in July 1994, the year of his retirement, reached Part No. 269. Under his supervision, 145 students obtained their doctoral degree in the Institute of Microbiology at the University of Tübingen.

Hans Zähner was a member of the Editorial Board of *The Journal of Antibiotics* from 1972 until 1995 and will sorely be missed by his friends and colleagues in the microbiological community.

He married his wife, Hedi, in 1954 and they have four children and three grandchildren. We all wish to express our deepest sympathy to Hedi and her family.

Hans-Peter Fiedler
Institute of Microbiology, University of Tübingen, Germany